UNIVERSITÀ DEGLI STUDI DI TRIESTE

UNIVERSITÀ DEGLI STUDI DI TRIESTE

XXXV CICLO DEL DOTTORATO DI RICERCA IN

BIOMEDICINA MOLECOLARE

Role of TRIM32, the ubiquitin ligase mutated in Limb Girdle Muscular Dystrophy R8

Settore scientifico-disciplinare: **BIO/18**

DOTTORANDO / A
XIONG LU Xiong Lu / 熊露

COORDINATORE
PROF. GERMANA MERONI

SUPERVISORE DI TESI
PROF. GERMANA MERONI

ANNO ACCADEMICO 2021/2022

ABSTRACT

Mutations in *TRIM32* result in the inherited disease Limb-girdle muscular dystrophy Recessive 8 (LGMDR8), a neuromuscular disorder manifesting in the proximal muscles around the hips and shoulders. TRIM32 is a RING E3 ligase belonging to the tripartite motif family (TRIM), which functions in the last step of ubiquitination, transferring the ubiquitin from E2 conjugating enzyme to specific substrates based on its ability to recognize different proteins. In literature, some studies report the critical role of TRIM32 in muscle physiology, muscle atrophy, muscle regeneration, as well as neuronal differentiation, however the exact LGMDR8 pathogenic mechanism is still unclear. Moreover, several possible substrates and interactors of TRIM32 have been found in these studies.

On the other hand, evidence support that the pathogenic mutations in *TRIM32* result in the loss function of TRIM32. Not only the full-length deletion of *TRIM32* has been discovered in LGMDR8 patients, but also the *Trim32* knock-out and *Trim32* pathogenic mutation knock-in mice share similar neuromuscular phenotypes. Therefore, the impaired myogenic process is very likely caused by the loss function of TRIM32 as the mechanism underlying LGMDR8.

In this project, we used an immortalized mouse myoblast cell line C2C12 to generate the *Trim32* knock-out and wild-type clones. Using the gene-edited C2C12 cells as the research tool, we determined the impairment of the myogenic program caused by the loss function of TRIM32, including low activity of myogenic-relative signaling pathways, the delayed and abnormal myotubes formation, and the down regulation of myogenesis marker myosin heavy chain (MHC). This deficient myogenesis is not caused by the malfunction of MyoD, a master myogenic regulatory factor (MRF), but likely due to the downregulation of Myogenin, which is a downstream target of MyoD predominately expressed at the late stage of differentiation. At last, we identify c-Myc, a proto-oncogene which was reported as an antagonist of MyoD activity on Myogenin expression, as likely regulated by TRIM32 at the beginning of differentiation.

Taken together, these results strongly indicate that TRIM32 functions is crucial in the myogenic differentiation program at its onset and provide new insight into LGMDR8 pathogenic mechanisms.

CATALOG

INTRODUCTION

1. Limb Girdle Muscular Dystrophy Recessive 8

1.1 The pathogenesis of Limb Girdle Muscular Dystrophy Recessive 8

Limb-Girdle Muscular Dystrophies (LGMDs) are a group of genetically inherited disorders affecting the neuromuscular system [1,2]. The different causative genes classify the LGMDs subtypes [3-5]. The updated nomenclature proposed to name the subtype based on the mode of inheritance (D, dominant; R, recessive), then its discovery order [6]. Limb-Girdle Muscular Dystrophy Recessive 8 (LGMDR8; OMIM #254110), one subtype of LGMDs, is a degenerative neuromuscular disease, mainly manifesting as pelvic and shoulder area muscle weakness and wasting [6-8] (**Figure 1**). In most cases, the age of onset varies from childhood to adulthood, progressing slowly [9]. The phenotypical symptoms include difficulties in running, walking, and climbing at the beginning, and loss of ambulation may occur in the late course of the disease [10-13]. In addition, facial muscles and cardiac and respiratory involvement are also reported in some of the most severe cases [7]. LGMDs are rare diseases globally. The prevalence is estimated to be in a range of from one in 14,500 to one in 123,000, showing geographical variance (https://rarediseases.org/rare-diseases/limb-girdle-muscular-dystrophies/). In an epidemiological study of LGMDs in Netherland in 2021, LGMDR8 accounts for a 1% rate of all LGMD subtypes [14]. However, considering the slow development of this disease, and diagnosis challenges, the prevalence of LGMDR8 may skews lower in many countries [15]. At present, the most efficient diagnosis method for LGMDR8 is direct mutation detection in the responsible gene, either through Sanger sequencing or via next-generation sequencing (NGS) with gene panel analysis and whole-exome sequencing [16-19], ancillary with examinations of muscle biopsy, electromyography (EMG), magnetic resonance imaging (MRI) and analysis of serum creatine kinase (CK) level in blood [13,20,21]. Even with substantial improvements in the diagnostic process, patients living with LGMDR8 continue to face the reality that there is no effective disease-specific therapy [19]. Although several non-disease-specific treatments, such as steroids and physical therapy, are used to slower disease progression, most patients are under the burden of healthy, social, and economic pressure [15,22]. Therefore, revealing the pathological mechanism of LGMDR8 is a pressing issue for developing disease-specific therapy.

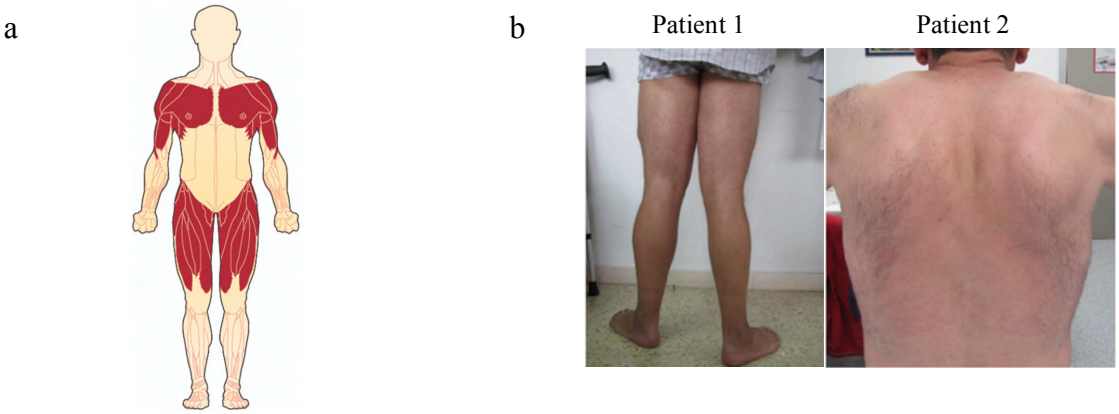

Figure 1 Muscular impairment in LGMDR8. a. The muscles highlighted by the red color are the main affected muscle (https://www.mda.org/disease/limb-girdle-muscular-dystrophy 2019). b. Patient 1 showed that distal muscle involvement led to distal atrophy and ankle contractions. Patient 2 showed mild paravertebral muscle atrophy with no scapular winging (Servián-Morilla, E. et al., 2019).

1.2 Mutations in *TRIM32* cause LGMDR8

LGMDR8 was first described in Manitoba Hutterite population in 1976 and further studies identified the mutation c.1459G>A (p.Asp487Asn) in the tripartite motif-containing protein gene 32 (*TRIM32*) as responsible for LGMDR8 patients in this population [7,9,23]. In recent years, more LGMDR8 patients were reported, also in non-Hutterite people, revealing many new pathological variants in *TRIM32* [24]. On the other hand, mutations in *TRIM32* can also cause Sarcotubular myopathy (STM; OMIM#268950) showing faster progression and severe phenotypes (**Figure 2**) [8]. To date, it is believed that LGMDR8 and STM represent different severities of the same disease as often the same mutation has been detected in patients presenting with either of the two clinical conditions [25]. Until now, 27 *TRIM32* related pathological mutations have been identified, including nonsense, missense, frameshift, full deletion variants; mutation c.1459G>A (p.Asp487Asn) is the most frequently reported [24,26]. An exception is a missense mutation (p.Pro130Ser), the only one reported to date, causing Bardet-Biedl syndrome type 11 (BBS11), a multi-systemic disorder including retinal dystrophy, obesity, kidney abnormalities, and polydactyly, with no skeletal muscle involvement [27] (**Figure 3**).

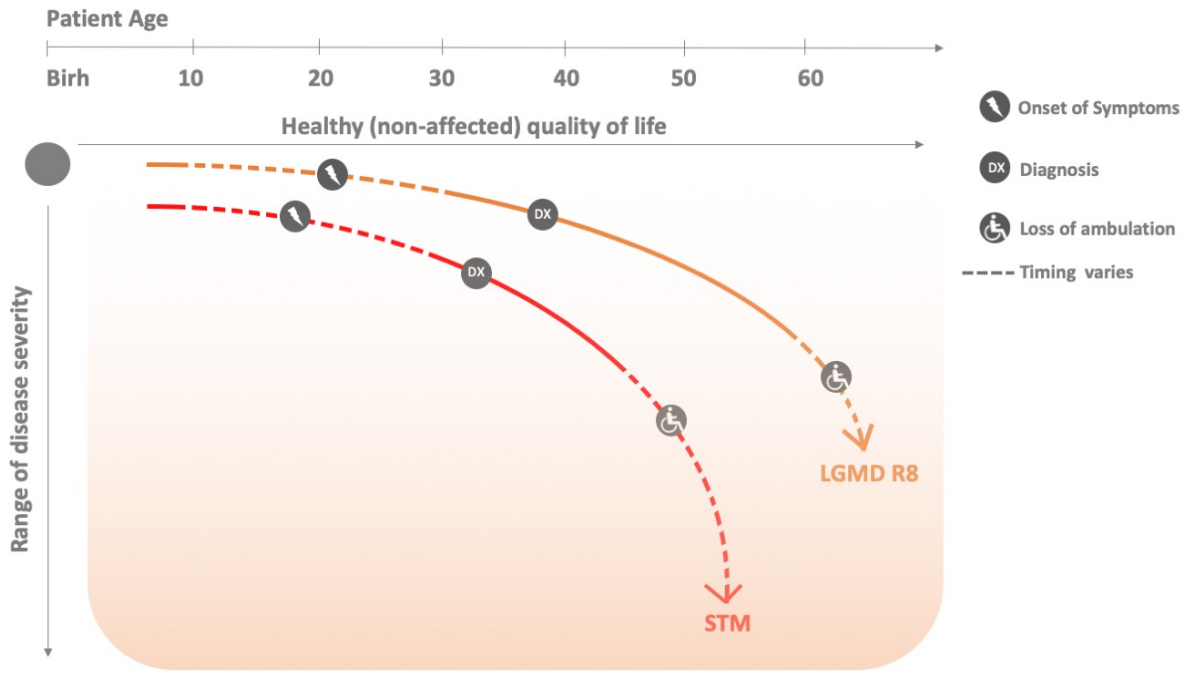

Figure 2 The disease progression of LGMDR8 and Sarcotubular myopathy (Modified from Dimitra G. et al., 2021).

1.3 Tripartite Motif 32, TRIM32

TRIM32 gene is located on human chromosome 9 - NC_000009.12; it is composed of two exons with the entire open reading frame contained in exon 2, which encodes the TRIM32 protein [5,28]. TRIM32 is a member of tripartite Motif (TRIM) family, one of the major of E3 ligases groups containing a RING domain which plays a catalytic role binding a ubiquitin-charged E2 enzyme to transfer ubiquitin (Ub) to the proper target (see below) [29]. Over 70 TRIM members were identified and involved in many cellular pathways [30]. TRIM32 contains a conserved N-terminal module including a RING domain, a single type 2 B-box domain, and a Coiled-Coil region while its C-terminal portion presents a 6-bladed β-propeller NHL domain [31]. TRIM32 is able to process self-ubiquitination and mediate ubiquitination on various substrates [10,32]. The RING domain carries out E3 ligase catalytic function [33,34]. The role of the B-box domain is not yet clear, while some data indicated that the B-box domain modulates ubiquitin chain assembly rate [35]. The Coiled-Coil domain regulates TRIM32 ability to form homo-oligomers, which serve as the active form [36]. The NHL repeat domain mediates protein–protein interactions likely providing substrate specificity (**Figure 3**) [37].

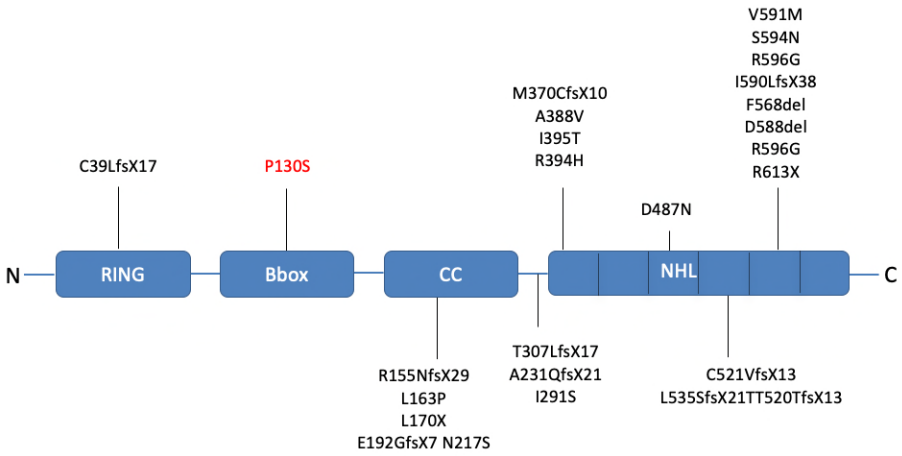

Figure 3 Graphical summary of the pathological mutations occurring in TRIM32. Domain names are indicated and the mutations within the NHL domains are grouped according to single NHL repeats. Most LGMDR8-causing mutations cluster within the C-terminal NHL domain of TRIM32 and may be in common with the allelic disease Sarcotubular myopathy (STM), while the P130S mutation in the B-box (red) is associated with Bardet-Biedl syndrome type 11 (Kumarasinghe. et al., 2021).

Previous studies suggested that the NHL motif is the focal region of LGMDR8 pathogenic missense variants, which indicated a perturbation in substrate recognition [26,37,38]. However, more pathological mutations out of NHL motif were described, including the mutation leading TRIM32 full length deletion [12,39,40]. Furthermore, several reports point out that some LGMDR8 pathogenic mutations in *TRIM32* lead to remarkable downregulation of TRIM32 protein. For example, TRIM32 shows a very low level in fibroblast isolated from LGMDR8 patients with the homozygous c.1459G>A (p.Asp487Asn) mutation in the NHL domain [41]. Reduced TRIM32 level has also been found in muscle samples from LGMDR8 patients carrying c177G>A (p.Val591Met) involving the NHL domain [40]. In addition to mutations clustered in NHL domain, in the LGMDR8 patient harboring the c.1560delC (p.Cys521ValfsX13) truncating mutation in the coiled-coil domain, no short TRIM32 form was observed in muscle lysates [39]. A frame-shift mutation c.115_116insT (p.Cys39LeufsX17) identified in LGMDR8 patients in the RING domain results in a premature stop codon, which in turn results in undetectable TRIM32 protein in the muscle sample [40]. This phenomenon is also observed in LGMDR8 mouse model. Analysis of a *Trim32* knock-in mouse myoblasts carrying the c.1459G>A (p.Asp489Asn) mutation, corresponding to the human LGMDR8/STM pathogenic mutation c.1459G>A (p. Asp487Asn), revealed an almost undetectable

TRIM32 protein compared to the wild-type mouse myoblasts. However, the mRNA level of *Trim32* did not show difference in *Trim32* mutated and wild-type myoblasts [42]. In this scenario, LGMDR8 is likely due to the total loss of function of TRIM32. The mechanism regulating TRIM32 degradation is unclear. One interesting study indicates that mutant p.Val591Met in myoblasts isolated from a LGMDR8 patient is degraded via the autophagy pathway [43].

2. Ubiquitination

As an E3 ligase enzyme, TRIM32 participates in the ubiquitination process. Ubiquitination is a vital post-translational modification (PTM) existing in eukaryotic cells. This process occurs through a tightly regulated enzymatic cascade which is carried on through the cooperation of three key enzymes, E1, E2, and E3, delivering and conjugating ubiquitin (Ub) as single peptide or as an Ub chain on target substrates as result (**Figure 4**). Depending on the topology of the Ub chain built on the substrate, the target protein turnover, subcellular localization, and activity can be regulated [44-46].

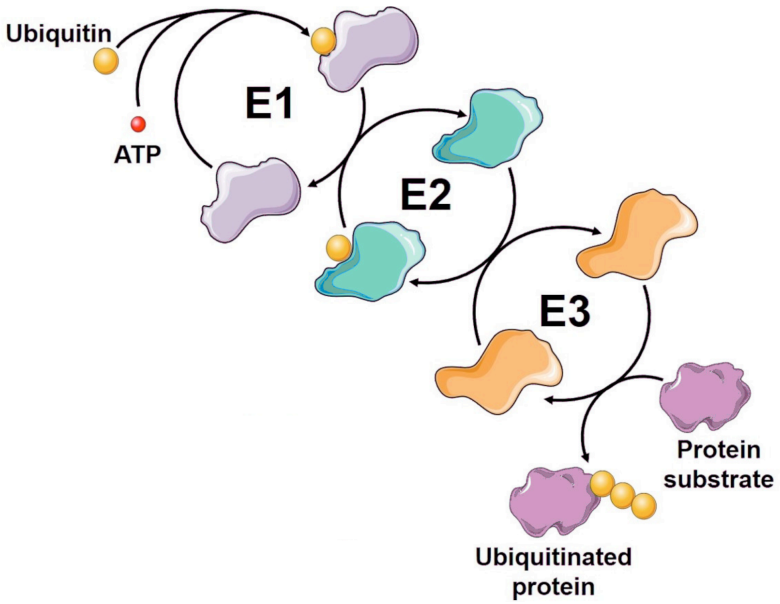

Figure 4 The cascade of ubiquitination. E1 activates ubiquitin and begins a cascade of enzymatic/substrate activity. E2 grabs the ubiquitin molecule from E1 and creates an E2-Ubiquitin conjugate intermediate. E3 recognizes substrate and transfers the ubiquitin molecule from the Ub-E2 intermediate to the target substrate (https://lifesensors.com/ubiquitinproteasomesystem/).

2.1 Ubiquitin

Ubiquitin (Ub) is a small regulatory protein consisting of 76 amino acids (8.6 kDa) whose C-terminal

glycine residue can be covalently attached to one amino group, of lysine residues most commonly (mono-ubiquitination), or to multiple lysine amino groups (multi-mono-ubiquitination) of substrate proteins, and which can be further extended by linkage of additional Ub to form Ub chains [47-49]. Mono-ubiquitination has many regulatory functions, for example, protein auto-inhibition, intracellular localization and trafficking, and regulation of protein complex formation, to name some [50-53]. The extension of Ub chain significantly expands its effects on a target protein. After the first Ub linking to the target substrate, the following Ub can bind the existing Ub to lysine residues as well as to the N-terminal methionine residue. There are seven lysine residues and an N-terminus in the Ub peptide: K6, K11, K27, K29, K33, K48, K63, and M1; each of them can participate in further ubiquitination, generating linkage-specific poly-Ub chains (**Figure 5**) [54-57]. The linkage pattern through different residues determines the versatility of this system in regulating a variety of cellular processes.

Lysine (K)48-linked poly-Ub chains were the first identified and best-characterized Ub chains. It triggers a well-known process called proteolysis [58]. The proteins tagged with K48 Ub-chains, representing "to be degraded protein," can be recognized and trafficked to 26S proteasome, which is a recycling station in cells. The 26S proteasome is a barrel-shaped structure comprising a central proteolytic core made of four ring structures flanked by two cylinders that selectively allow entry of ubiquitin-modified proteins. The ubiquitin-modified proteins in 26S proteasome will be quickly degraded into small peptide fragments, which can be used for new protein synthesis, and the cleaved Ub will be recycled in the pool available for other rounds of ubiquitination. This Ub-proteasome mediated degradation is termed ubiquitin-proteasome system (UPS) [59-61]. This process is essential for cell metabolisms such as cell cycle, cell apoptosis, gene expression, and to degrade the damaged, and unfolded proteins, or those that are no more needed in given times and spaces [61,62]. In muscle atrophy, UPS shows a high level of activity to induce a large amount of muscle protein degradation, resulting in a loss of muscle mass [63-67].

Another well-studied non-proteolytic form of ubiquitination is Lysine (K)63-linked chains. Unlike K48-induced target protein degradation, K63-Ub chains are suggested to adjust target protein activity and location, involved with processes such as endocytic trafficking, inflammation, and DNA repair [68-70]. Proteins modified with K63-Ub chains can be recognized, and bind other proteins with Ubiquitin Binding Domain (UBD), this type of interactions are essential in NF-κB signaling pathway stimulated by IL-1 and TNF-α [71]. In DNA-damage response pathway, the K63-Ub chains modified receptor-associated protein 80 (RAP80) helps BRCA1 associated repairing complex to be recruited at the site of damage [72,73]. Regarding other types of chains assembled through K6, K11, K27, K29,

K33, and M1, the function is poorly understood. Besides, mass spectrum data indicate that not only homo-type but also mixed and branched chains exist, although their role is still not known (**Figure 5**).

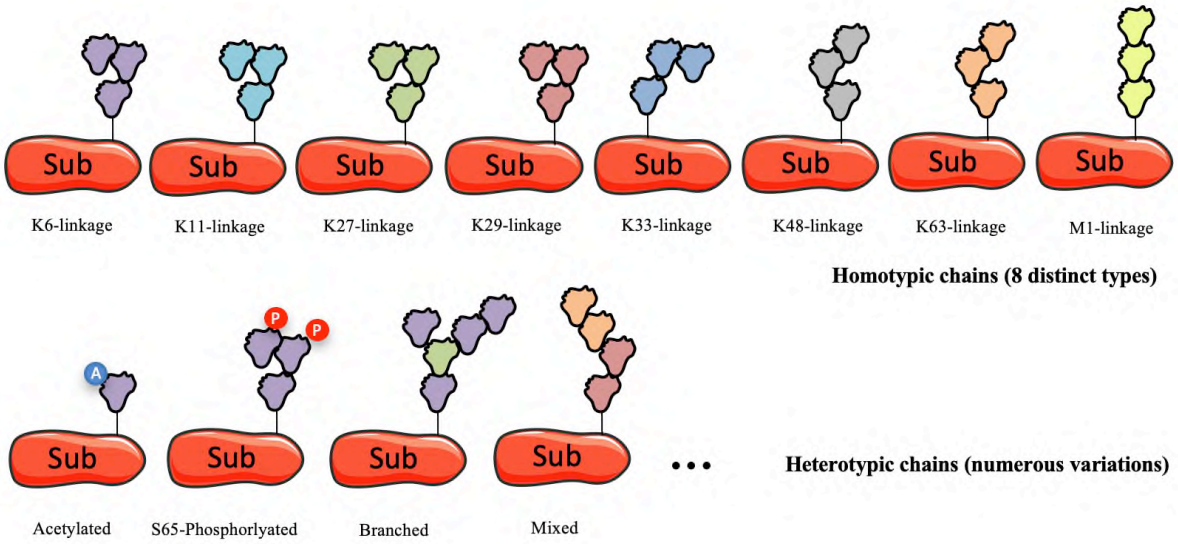

Figure 5 Targeting different lysine or Met1 of Ub for chain formation allows the generation of a great variety of distinct Ub modifications, including different homotypic chains, mixed and branched chains.

2.2 Ubiquitin-activating (E1) enzymes

The first step of ubiquitination is catalyzed by the Ub-activating enzyme (E1) that activates Ub in an ATP-dependent manner through the formation of a thiol-ester bond between the C terminus of Ub and the E1 active site cysteine (Cys). The human genome encodes two E1s, Uba1 and Uba6. Uba6 conjugates less than 1% of Ub, while Uba1 is responsible for 99% of the cellular conjugations [74-76].

2.3 Ubiquitin-conjugating (E2) enzymes

The activated Ub is then transferred to the active-site Cys of a Ub-conjugating enzyme (E2). On the other hand, the Ub-charged E2 enzyme can bind one of the several ubiquitin ligases (E3 enzymes) via a structurally conserved binding region. More than 30 E2 enzymes in the human genome have been found. Each E2 enzyme can interact with several E3 ligases and, in many cases, an E3 ligase can perform Ub transfer interacting with different E2s [77,78].

2.4 Ubiquitin ligase (E3)

The ubiquitin ligase (E3) transfers Ub from E2 to the interacting specific substrate. The human genome encodes nearly 600 E3 Ub ligases which intervene in the last and critical step for the specificity of ubiquitination. E3 ligases are classified into three major groups based on the unique catalytic mechanisms that they employ: The Homologous to E6-associated protein C-terminus (HECT) family, the RING-in-between-RING (RBR) family, and the Really Interesting New Gene (RING) family (**Figure 6**) [79,80].

HECT ligases are characterized by the presence of a conserved HECT domain and a variable N-terminus that mediates the target substrate's specificity. HECT ligases transfer Ub from E2 to substrate through a two-step reaction. In the first step, HECT ligases accept Ub from E2 on the domain catalytic cysteine. Then Ub is further moved and bound to the target substrate. Based on their N-terminal structures, HECT ligase can be divided into three subfamilies: neuronal precursor cell-expressed developmentally downregulated 4 (NEDD4), RLD domain-containing HECT (HERC), and the others which cannot be categorized into these two groups [81]. HECT ligases are involved in the regulation of many cell signaling pathways, such as Wnt, PI3K-AKT, Hedgehog, and p53 [82-85].

RBR ligases show a similar two-step catalytic process as HECT. They contain two RING domains and one in-between-RING (IBR) domain. RING-1 interacts with E2 and transfers Ub from E2 to the RING-2 domain, and the RING-2 domain conjugates Ub to the binding substrate. In this process, the IBR domain serves as a scaffold for an optimal conformation [86].

RING ligases compose the largest E3 ligase class, including also the TRIM family. RING E3 ligases are actually induces two groups; presence of a zinc-binding RING domain or a U-box domain that lacks the eight-canonical zinc-chelating residues but assuming a similar RING 3D structure [87,88]. Unlike HECT and RBR E3 ligases, RING E3 ligases do not conjugate Ub in the transferring process and are actual catalytic enzymes that facilitate Ub moving from E2 to a substrate without directly participating in the reaction [29,34]. Ub-charged E2 and substrate are in close proximity when they both bind RING E3 ligases. Recent studies offered more profound insight into E2-Ub intermediates that exist in multiple conformations either "open" or "close." Binding of the RING E3 ligase promotes E2-Ub into "close" conformation, which enforces Ub drop from E2 and then attracted by the exposed hydrophobic residues of substrate [89]. RING E3 ligases can function as monomers, dimers, or oligomers [90]. Many TRIM E3 ligase dimers and oligomers are the active or highly efficient forms. For example, binding to Ub-conjugated E2 promotes TRIM25 homo-dimerization, improving TRIM25 catalytic activity. Further, some studies indicate that the homo-association of TRIM32 through the coiled-coil domain is necessary for its E3 ligase activity [36].

2.5 Deubiquitinating Enzymes (DUBs)

Ubiquitination is a dynamic process that the Deubiquitinating Enzymes (DUBs) can revert. DUBs are a group of Ub proteases cleaving Ub from substrates to reverse the effects of ubiquitination. The net balance of ubiquitination and deubiquitinating hence determines proteins' fate. The human genome encodes around 100 DUBs [91-93]. Ubiquitin-specific proteases (USPs) represent a large DUBs family, which is vital in cell signaling. Many TRIMs, including TRIM32, work together with USPs to control the balance of ubiquitination on substrates. Actually, some DUBs work on the proteasome for disassembly before complete degradation [94-96].

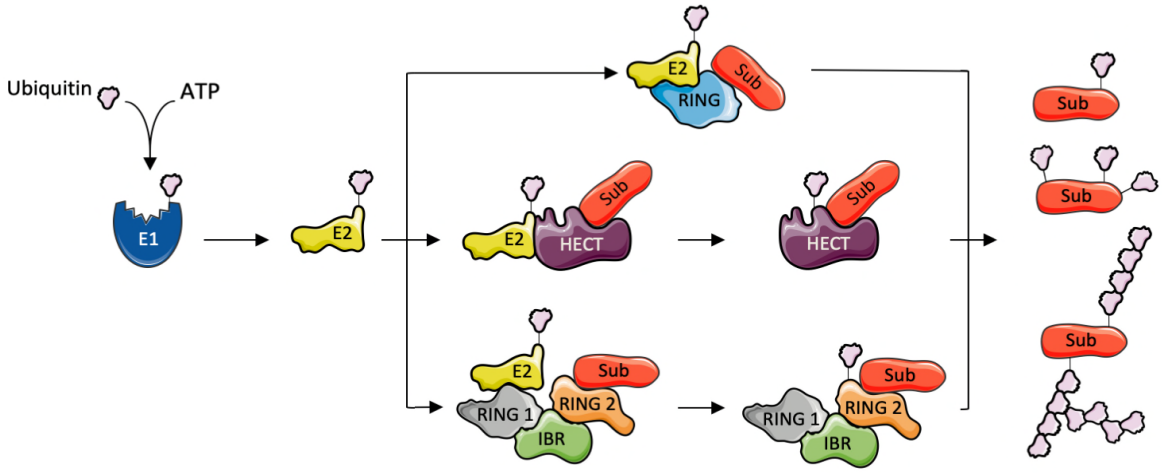

Figure 6 Protein ubiquitination is carried out by Ub-activating enzyme (E1), Ub-conjugating enzyme (E2), and Ub-ligating enzyme (E3). (1) The E1 activates Ub in an ATP-dependent manner through the formation of a thiol-ester bond. (2) The activated Ub is transferred to the active-site Cys of a E2. (3) The E3 facilitates ubiquitination of substrate and defines substrate specificity. The enzymatic HECT (homologous to the E6AP carboxyl terminus) domain E3s form a thioester with Ub, which is then transferred to the amino group of a substrate lysine, whereas non-HECT domain E3s contain a RING or RBR (RING-between RING-RING). They do not possess enzymatic activity but function as adaptors linking substrate and Ub-charged E2. Targeting different lysines or Met1 of Ub for chain formation allows the generation of a great variety of distinct Ub modifications, including different homotypic chains, mixed and branched chains (Kumarasinghe, et al., 2021).

3. Skeletal Muscle

3.1 Muscle Anatomy Structure

Striated skeletal muscle accounts for 35%-45% of our body mass. The skeletal muscle system is controlled by the somatic nervous system, and supports our body and performs powerful and precise movements, breathing, and locomotion [97,98]. The cellular unit of skeletal muscle is the muscle fiber, which is distinct from every other body cell type. The mature muscle fiber can reach 20-30 cm of length and display multiple nuclei supporting its high-level metabolism. Actin and myosin are two main functional proteins in the muscle fiber controlling its contraction and relaxation. Skeletal muscle fibers can be classified as type 1 (slow-twitch) and type 2 (fast-twitch). Type 1 fiber prefers aerobic metabolism; to that purpose it has more mitochondria and high myoglobin content. Conversely, type 2 fiber relies more on anaerobic respiration to produce ATP [99-101].

Each muscle fiber is surrounded by connective tissue called the endomysium, composed of collagen IV and V, interlaced with a nest network of blood vessels and nerves [102]. Thousands of muscle fibers bundle together into muscle fascicles enveloped in the connective tissue perimysium. Many muscle fascicles pack tightly with nerves and vessels to constitute a skeletal muscle [103,104] (**Figure 7**). The structure and amount of muscle tissue varies based on health condition and age [105]. A general loss of skeletal muscle mass is a characteristic, debilitating response to fasting. However, more dramatically, it can be a response to many severe diseases, including advanced cancer, renal failure, sepsis, and diabetes, and it is known as muscle atrophy. Importantly, the healthy skeletal muscle shows the regenerative ability to repair the damage [106].

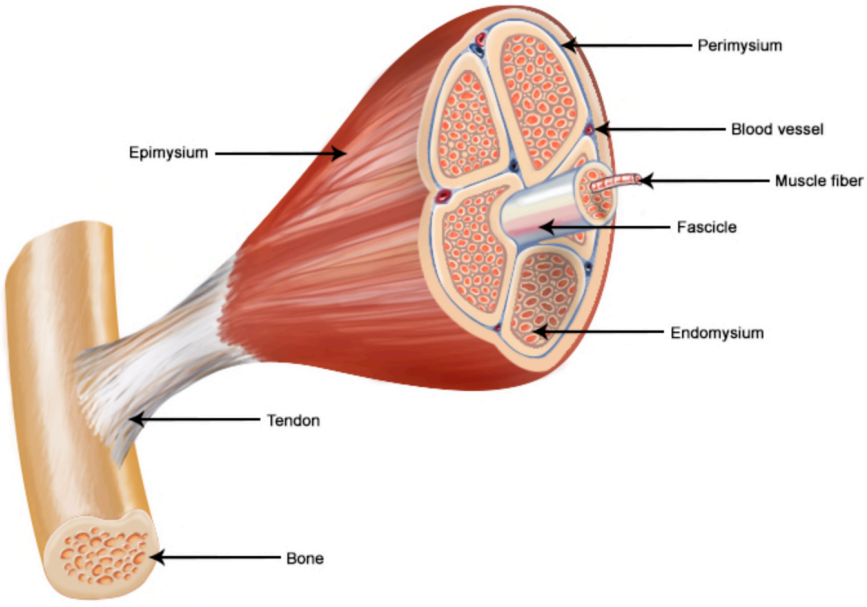

Figure 7 The structure of skeletal muscle. Each skeletal muscle fiber is a single cylindrical muscle cell. An individual skeletal muscle is made up of muscle fibers bundled together and wrapped in connective tissue. Each muscle is surrounded by a connective tissue sheath called the epimysium. Portions of the epimysium project inward to divide the muscle into compartments. Each compartment contains a bundle of muscle fibers. Each bundle of muscle fiber is called a fasciculus and is surrounded by a layer of connective tissue called the perimysium. Within the fasciculus, each individual muscle cell, called a muscle fiber, is surrounded by connective tissue called the endomysium. (https://training.seer.cancer.gov/anatomy/muscular/structure.html)

3.2 Structure and Function of Muscle Fiber

Sarcomere

The sarcomere is the smallest contractile unit in the skeletal muscle fiber cytoplasm. Each sarcomere is mainly composed of two well-organized proteins: myosin and actin, which serve for muscle contraction. Some other auxiliary proteins surround or bind myosin and actin. The structure in **Figure 8** represents a basic sarcomere [107,108]. The sarcomere is a symmetric structure where one end of actin anchors to the Z-disc, and the other connects myosin in the middle of the sarcomere. The sarcomeric Z-disc, the anchoring plane of actin filaments, links titin (also called connectin) and actin filaments from opposing sarcomere halves in a lattice connected by α-actinin [109-111]. A line in the centre of the sarcomere is termed an M line (**Figure 8**) [112].

The myosin filament contains numerous heads. These heads are attached to the actin filaments with the assistance of myosin-binding protein C (MyBP-C), forming actin-myosin cross bridges. The power stroke forcing muscle contraction exists in the numerous actin-myosin cross bridges. Another protein group consists of several isoforms of tropomodulin/leiomodin homology family, and it regulates actin filament formation. By consuming the chemical energy released by ATP hydrolysis, myosin heads slide actin filaments move toward the M line, forcing the contracting of each sarcomere [109,113,114].

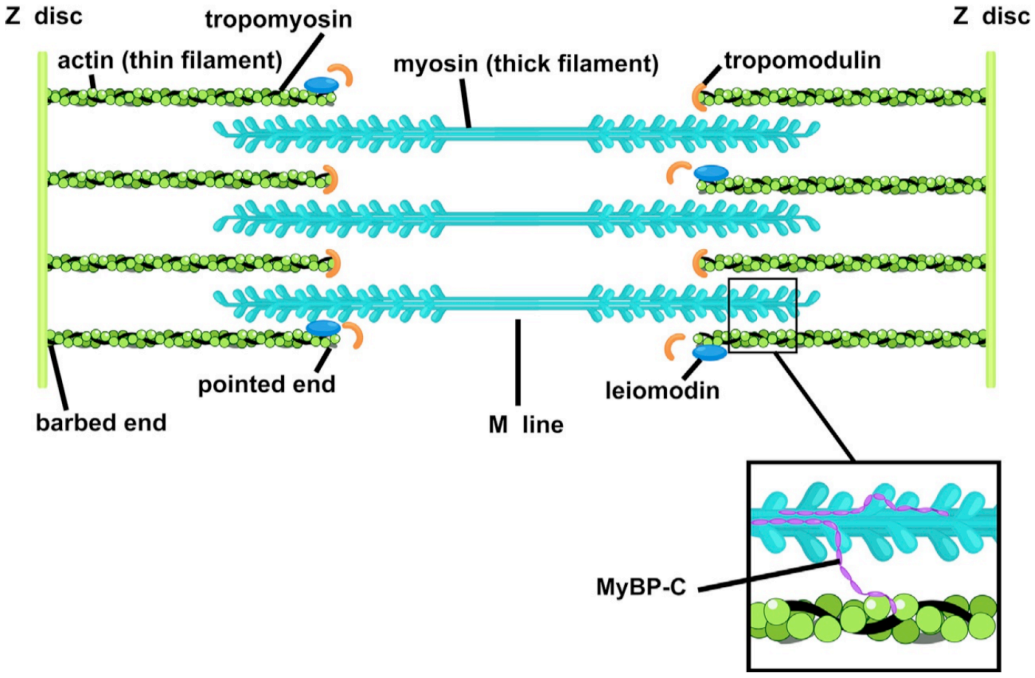

Figure 8 A schematic view of a sarcomere. Shown in the figure are schematic locations of actin and myosin as well as tropomodulin, leiomodin and myosin-binding protein C (MyBP-C). The inset shows two putative binding modes of MyBP-C. (P Young, et al., 1998)

Sarcolemma

Sarcolemma is the plasma membrane of muscle fiber. It is the site where neuromuscular junction form and contains ion channels, transporters, and pumps for calcium. Not only the calcium signal regulates the myogenic fusion during fiber formation, but also the change of calcium level in muscle fiber is the switch of muscle contraction and relaxation. The fast reaction of muscle fiber reacting to neuro stimulation is depending on the rapid release and recycle of calcium, which benefits from sarcoplasmic reticulum (SR), a cellular calcium store. Some sites of sarcolemma form invaginations into cytoplasm named T-tubules, and SR distributes in the cytoplasm and is closed to the walls of T-tubules. The receptors on sarcolemma receive the stimulation from extracellular matrix (ECM) and transmit the signal to SR, promoting calcium release immediately. The increased calcium level in cytoplasm stimulates myosin to bind actin filaments and force them to move. When the stimulation from ECM is removed, the calcium in cytoplasm is collected back into SR and myosin is inactivated [115-117]. In addition, sarcolemma physically connects to the sarcomere through dystrophin and other proteins (costamere, see below). This structure connecting sarcolemma and sarcomere provides supporting to sarcolemma, and transmits various signals between ECM and cytoplasm [118] (**Figure 9**).

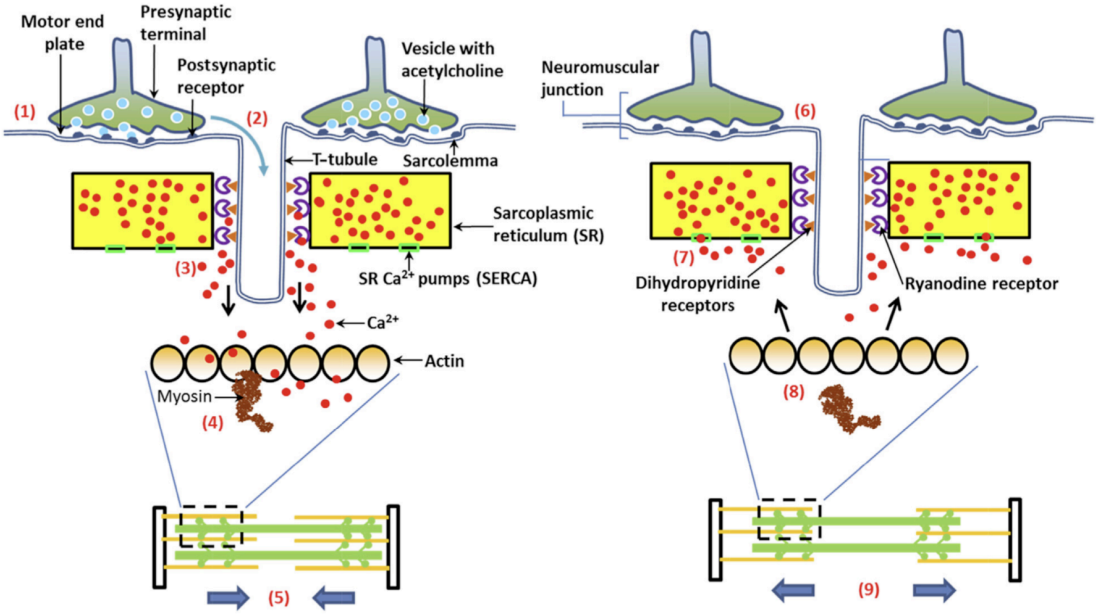

Figure 9 Sarcolemma and Excitation–contraction and relaxation of skeletal muscle. Electrical stimulation of the cell membrane by acetylcholine, the spread of action potential to the junction between sarcoplasmic reticulum (SR) and T-tubule, release of Ca^{2+} from the SR, binding of Ca^{2+} to Tn initiates actin–myosin interactions leading to muscle contraction (Steps 1–5). The lack of electrical stimuli causes sequestration of Ca^{2+} back into the SR and prevents actin–myosin interactions, thereby allowing the muscle to relax completely (Steps 6-9) (S. K. Gollapudi, et al., 2014).

Costamere

A sarcomere is connected to the sarcolemma through another functional unit termed of the costamere [119-121]. The shape of the costamere is like a rib, with one end binding to the actin filament and the other contacting the ECM. Costamere are scattered in each sarcomere, aligned with Z-disc, passing the contractile force from the sarcomere to basal lamina and transmitting signaling between cytoskeleton and ECM in skeletal muscle [122,123]. Costamere mainly comprises two sub-units: the dystrophin-glycoprotein complex (DGC) and the vinculin–talin–integrin system [124-128] (**Figure 10**). The correct association of these two complexes is regulated by the transcription factors: myocyte enhancer factor-2 (MEF2), the serum response factor (SRF), and histone deacetylase [123,129,130]. The correct alignment of costameres with the Z-discs depends on intermediate filaments such as desmin and plectin. Many muscular dystrophies are caused by the mutations of costamere components, Duchenne muscular dystrophy (DMD) (total absence of dystrophin), Limb girdle muscular dystrophy (LGMD) 2C (mutations in γ-sarcoglycanopathy), 2D (mutations in α-sarcoglycan), 2E (mutations in β-sarcogycan), and 2F (mutations in δ-sarcoglycanopathy) for incidence [5,131,132].

The dystrophin-glycoprotein complex (DGC) is a group of well-organized proteins crossing sarcolemma. Dystrophin connects actin filaments in the cytoplasm to the subsarcolemmal protein syntrophin and α-dystrobrevin. Syntrophin is bound to two trans-sarcolemma proteins, sarcoglycans α−ε and dystroglycan α/β. One isoform of dystroglycan extends to ECM and links to the laminin α2. This complex string sarcomere, sarcolemma, and ECM, providing structural support to the sarcolemma. On the other hand, it mediates membrane targeting and stabilizes the sarcospan protein [133-135].

The vinculin-talin-integrin system is the other complex that links actin filament and sarcolemma. This complex mainly contains two cytoskeletal proteins, vinculin and talin, as well as very important transmembrane proteins, integrins. Vinculin and talin work as a physical connection between actin filaments and integrins. Integrins recruit signaling proteins to transduce mechanical stimuli from ECM to the cytoplasm through focal adhesion kinase (FAK), melusine, paxillin, src, cas and phosphatidylinositol (4) phosphate 5 kinase type I (PIPKI). This system is critical for signaling transmission between the ECM and cytoplasm and regulates cell reorganization and adhesion. Integrins mediated signaling is predominantly regulated by an integrin-linked kinase (ILK), which is essential for controlling shape and mobility in myogenic fusion [136-140].

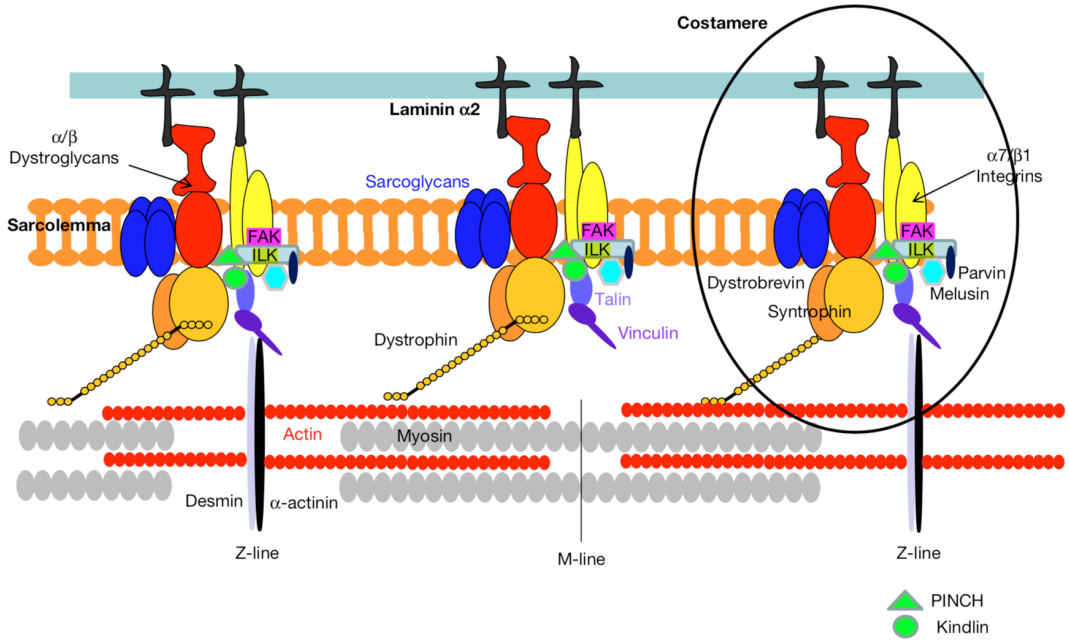

Figure 10 Schematic representation of proteins forming costamere in skeletal muscle as indicated. FAK, focal adhesion kinase; ILK, integrin-linked kinase; PINCH, particularly interesting cysteine- and histidine-rich protein. (Oihane Jaka, et al., 2015)

3.3 Muscle regeneration

The myogenic process occurs not only during embryonic development but also during adult muscle regeneration [141,142]. The regulation and molecular program of these two processes share common features, but some differences remain [143]. The patients with LGMDR8 have a normal embryonic development, hence we mainly focus on muscle regeneration here.

Satellite cells

The capacity for muscle regeneration lies in a unique adult stem cell type, the satellite cell [144,145]. Like other stem cell types, the muscle stem cells termed mononuclear satellite cells display a high nucleus-to-cytoplasm ratio. They wedge between the endomysium and the fiber membrane. Satellite cells account for 2–7% of the total muscle nuclei. However, this proportion depends on many factors, such as age, muscle type, and pathological condition [146,147]. For example, Duchenne Muscular Dystrophy patients show a reduced satellite cell population [148]. Specific markers are expressed in satellite cells, which can be used to distinguish satellite cells from other cells and define the satellite cell condition (**Table 1**) [149]. Among them, the most widely used is the paired box protein (PAX7), expressed in all satellite cells, whereas the expression of MyoD is a marker of proliferating satellite cells (**Figures 11 and 13**) [150-152]. In normal conditions, the satellite cells keep quiescent. Once activated, they will finally enter into the myogenic process and form new muscle fiber [153].

The muscle regeneration process upon muscle injury is a finely orchestrated set of cellular responses, resulting in the regeneration of a well-innervated, fully vascularized, and contractile muscle apparatus. Efficient muscle regeneration relies on specific myogenic pathway activation in satellite cells and some other cell types' contribution [154].

Table 1 Satellite Cell Markers

Molecular Markers	Satellite Cell Expression		Experimental Protocol
	Quiescent	Proliferating	
Cell surface			
M-cadherin	+/-	+	In vivo/ in vitro
Syndecan-3	+	+	In vivo/ in vitro
Syndecan-4	+	+	In vivo/ in vitro
c-met	+	+	In vivo/ in vitro
VCAM-1	+	+	In vivo
NCAM	+	+	In vivo
Glycoprotein Leu-19	+	+	In vivo/ in vitro
CD34	+/-	+/-	In vitro
Cytoskeletal			
Desmin	-	+	In vivo/ in vitro
Transcription factors			
Pax7	+	+	In vivo/ in vitro
Myf5	+/-	+	In vivo/ in vitro
MyoD	-	+	In vivo/ in vitro
MNF	+	+	In vivo/ in vitro
MSTN	+	+/-	In vivo/ in vitro
IRF-2	+	+	In vivo/ in vitro
Msx1	+	-	In vivo/ in vitro

MSTN, myostatin; VCAM-1, vascular cell adhesion molecule-1; NCAM, neural cell adhesion molecule; MNF, myocyte nuclear factor; IRF-2, interferon regulatory factor-2. Reference numbers are given in parentheses. (SOPHIE B. P. CHARGÉ, et al., 2004)

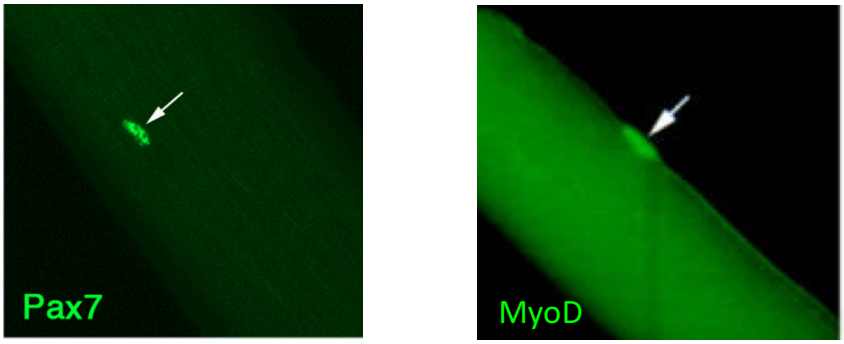

Figure 11 Satellite cells in their niche on the surface of freshly isolated Extensor Digitorum Longus (EDL) myofiber were co-immunoassayed for Pax7 (satellite cell) and MyoD (proliferating satellite cell) (Gnocchi, et al., 2009).

First stage of muscle regeneration

Muscle damage initially triggers a complex inflammatory reaction. In this process, the newly synthesized cytokines such as TNF-α, IL-1/4/10, and TGF- β are secreted, and these are known to stimulate the satellite cells. In addition, the damaged muscle debris release FGF-4 and FGF-6, regulating satellite cell proliferation and basement membrane formation [155-160]. Upon exposure to the activation signals, the satellite cells are quickly stimulated, migrate to the damaged site, and start proliferating. At this stage, the expression of PAX7 decreases and is replaced by the other two myogenic regulatory factors (MRFs), Myf5 and MyoD [161,162] (**Figure 12**). These committed satellite cells are termed myoblasts or myogenic progenitors. Myf5 and MyoD are highly and constantly expressed in the proliferative myoblasts and their function is likely to overlap. Substantial evidence describes MyoD as a critical factor in muscle regeneration. *MyoD* knock-out mice show reduced regenerative capacity characterized by increased myoblasts and decreased regenerated muscle fibers. *In vitro*, the knockout of *MyoD* completely blocks myoblasts' differentiation progression. The role of Myf5 is still elusive because of the lack of *Myf5* knock-out mouse model. Some studies report that Myf5 controls myoblasts proliferation while MyoD triggers myoblasts differentiation [163-167].

Second stage of muscle regeneration

Several rounds of proliferation provide enough myoblast pool for repairing the muscle damage. At this point, these myoblasts withdraw from the cell cycle and enter into differentiation. Starting differentiation, Myf5 and MyoD expression rapidly decrease, while Myogenin and MRF4 become

the main expressed MRFs in this stage. *Myogenin* is a downstream target of MyoD and Myf5, essential for advanced stage of differentiation [168,169] (**Figures 12 and 13**). Myogenin triggers the expression of a series of genes involving muscle contractility, such as myosin heavy chain, a prototype of molecular motor—a protein that converts chemical energy from ATP to mechanical energy, thus known as a marker for muscle fiber [170,171]. *Myogenin* knock-out mice die in perinatal due to a severe muscle malfunction [172]. The role of MRF4 is still not completely clear. MRF4 shows the highest level in adult muscle than any other MRF, indicating its role in muscle physiology [173-175]. In this stage, the shape of myoblasts changes from satellite to fusiform, adhering parallel with each other or with the existing muscle fiber. The cells at this stage are termed Myocytes [176].

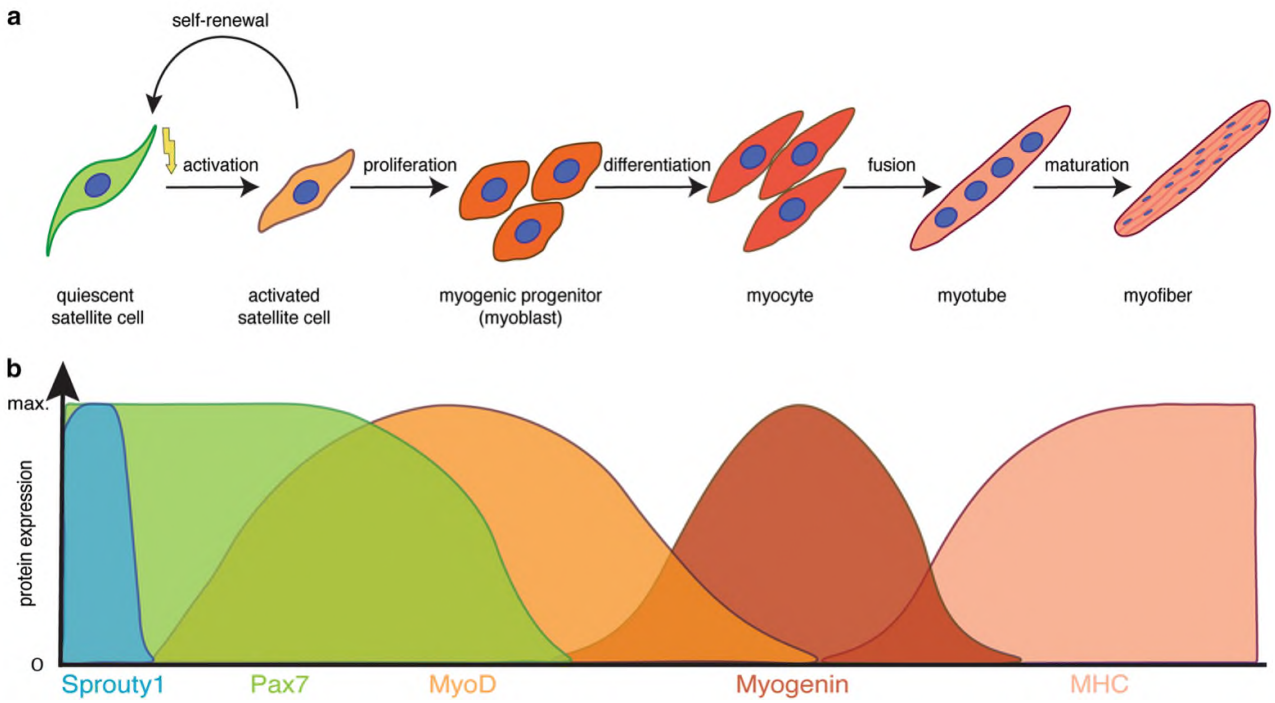

Figure 12 Myogenic lineage progression and expression profile of key myogenic regulators. a Schematic illustration of the myogenic lineage progression. Satellite cells are activated, e.g., due to injury, start to proliferate, thereby generating myogenic progenitor cells. Upon differentiation, myogenic progenitor cells differentiate into myocytes, which fuse to form myotubes and mature to become myofibers, the contractile unit of skeletal muscle. b Expression profile of key modulators of myogenic lineage progression. MHC, Myosin Heavy Chain. (Schmidt, M., et al., 2019)

Third stage of muscle regeneration

The third stage mainly refers to myocyte fusion. This process requires vast and complicated signal pathways, molecules, and cell morphology changes. Many molecules are involved in cell recognition, extracellular environment change, cell membrane topography, and cytoskeletal reorganization. [177,178] At the last step, myocytes secrete perfusion vesicles accumulating at the contact site of the two adherent cells. With more and more pores created in the contact membranes, the membranes finally dissolve to give rise to new multinucleated muscle fiber or integrate the myocyte into the existing muscle fiber. Because it is hard to establish a proper experimental system for visualizing and studying mammalian cell-cell fusion, we still do not know the master regulator in the fusion process. [179,180] Nevertheless, evidence indicates that both MyoD and Myogenin can regulate myoblast fusion by inducing the muscle-specific membrane protein Myomaker and Myomixer. [181]

Globally, MRFs are determination factors required to establish myogenic identity. They function as an orchestrated cascade with some overlapping actions. Besides, other cell signals can regulate MRFs expression, and the gene regulatory network involved in this process is complicated by cross-regulations, feed-back and feed-forward loops. In this scenario, the mechanism of muscle regeneration is a vast and tangled network, and more studies are required to fully reveal it.

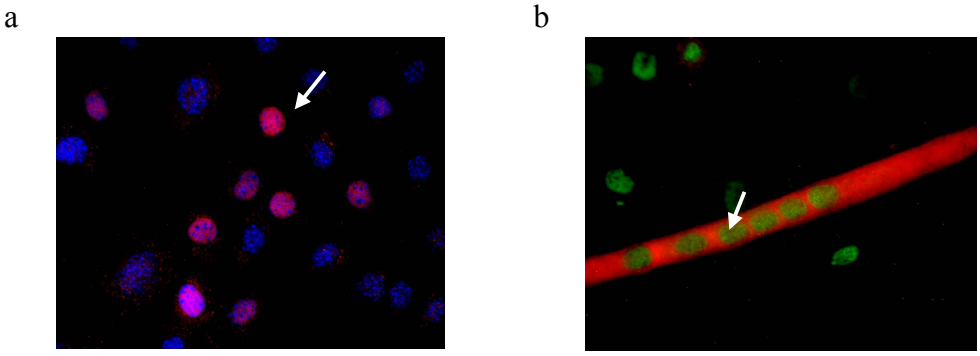

Figure 13 Culturing C2C12 cells for myogenic process *in vitro*. a. Co-immunostaining for MyoD (red) and DAPI (blue) in proliferating C2C12 cells (Day 0 of differentiation). b. Co-immunostaining for Myogenin (green) and Myosin Heavy Chain (red) in myotube (Day 6 of differentiation) (This work).

4. TRIM32 is a E3 Ubiquitin Ligase in muscle physiology

TRIM32 is involved in various signaling pathways by affecting many substrates' activity. TRIM32 widely distributes in different tissues, particularly in the nervous system, brain, muscle, and cancer cells. TRIM32 specifically mediates the ubiquitination of different substrates in various cells and

stages of development; the outcomes to cells can be very different. For example, TRIM32 promotes cancer cell proliferation by involving AKT, Wnt, and NF-κB pathways [182-184]. However, in muscle and neuron generation, TRIM32 is described as essential in inhibiting cell proliferation and enabling differentiation, although the exact mechanism is not precisely known.

On the other hand, the ability to interact with different E2 enzymes also expands TRIM32 possible effects on substrates. Recombinant TRIM32 can promote its auto-ubiquitination in the presence of E2 enzymes of the D subfamily (UbE2D, UbcH5), can form poly-ubiquitin chains with UbE2N (Ubc13)/UbE2V2 (Mms2), and can process self-ubiquitination with a single ubiquitin molecule with the priming E2s UbE2W (Ubc16), UbE2E1 (UbcH6), and UbE2E3 (UbcH9) [35]. Different E2 enzymes work on mono- or poly-ubiquitination of substrates and can determine linkage-specific poly-Ub chain (K6, K11, K27, K29, K33, K48, and K63). Therefore, the coupling of TRIM32 with different E2s results in various outcomes of physiological substrates *in vivo*. For example, TRIM32 promotes PB1 degradation by attaching K48-linked ubiquitination to it. In another case, TRIM32 mediates STING K63-linked ubiquitination influencing its activity [185,186]. Various TRIM32 and E2-conjugating enzyme combinations increase their specificity on substrates, which also partially explains their essential role in numerous physiological processes.

In addition to acting as E3 ligase, some reports indicate that TRIM32 can function binding to RNA (e.g., binding to the miRNA Let-7a) and interacting with other proteins without an ubiquitination outcome (e.g., Myosin). In this scenario, the leading site is represented by TRIM32 NHL repeats instead of the RING domain. What is the extent of this RNA binding activity still needs deep investigation.

Globally, TRIM32 participates in numerous physiological processes through its E3 ligase activity or possibly as an RNA regulator [187]. Although the multifaceted TRIM32 provides many possibilities to explain the pathological mechanism of LGMDR8, the fundamental critical molecular mechanisms can hide deeply behind this complicated action network.

5. TRIM32 and Muscle Atrophy

Skeletal muscle is in a dynamic balance between anabolic (or hypertrophic) and catabolic (atrophic) processes. Some external stresses and diseases can break this balance and incline to atrophic. In this situation, two E3 Ub ligases, MuRF1/TRIM63 and Atrogin-1, are upregulated, and mediate muscular protein degradation through the Ub-proteasome system, resulting in muscle mass loss and

malfunctioning. In various models of muscle atrophy, MuRF1 and Atrogin-1 are the major regulators of atrophic processes in muscle [188-190]. The role of TRIM32 in muscle atrophy is very controversial. Unlike MuRF1 and Atrogin-1, TRIM32 is not a key inducer for muscular protein degradation in muscle atrophy. However, many filament proteins, including actin, α-actinin, tropomyosin, and dysbindin, were identified as substrates of TRIM32 *in vitro* [191,192]. Considering the low level of TRIM32 and the localization of these tightly arranged muscular proteins *in vivo*, its E3 ligase activity on these putative targets *in vivo* can be complicated.

Besides, TRIM32 is probably essential for the integrity of costamere. TRIM32 has been found around Z-discs in the sarcomere, and desmin, the intermediate filament that regulate the costamere correct alignment to Z-discs, is a substrate of TRIM32 [192]. In addition, study on drosophila *thin/abba*, the orthologous gene of *Trim32*, found that thin mutation can significantly result in disorganization of the costameric orthologs β-integrin, Spectrin, Talin, and Vinculin [193].

Actin is a ubiquitous cytoskeletal protein, and its α-isoform is the major myofibrillar protein exclusively expressed in muscle [94]. α-actinin interacts with myosin in thick filaments to constitute the fundamental contractile module of muscle [95,96]. Actin can be mono-ubiquitinated by TRIM32 *in vitro* and reduced in HEK293 cells when TRIM32 is ectopically expressed. On the other hand, TRIM32 is a myosin-binding protein but does not mediate the ubiquitination of myosin, and its effect on myosin is unclear [191]. Desmin forms intermediate filaments that compose the primary cytoskeletal network in muscle and are important in maintaining myofibril stability and alignment. In support of the potential involvement of TRIM32 in promoting muscle atrophy, TRIM32 mediates the poly-ubiquitination of desmin *in vitro*, and blocking TRIM32 expression by shRNA can prevent desmin degradation in muscle atrophy [192] (**Figure 14**).

Some data demonstrate that TRIM32 induces autophagy as a protective mechanism to attenuate muscle damage during atrophy. TRIM32 downregulation does not affect the basal autophagy flux in undifferentiated and differentiated C2.7 cells (a murine myoblast cell line) but impairs autophagy induction in atrophic conditions *in vitro* and *in vivo*. The further analysis of mass spectrometry-based protein interaction screening and co-immunoprecipitation proved that TRIM32 induces K63-poly-ubiquitination of ULK1 (Unc-51 like autophagy activating kinase 1), and this process is regulated by AMBRA1 (the activating molecule in BECN1-regulated autophagy protein 1) since the formation of TRIM32-AMBRA1 intermediate can strongly enhance the efficiency of ULK1 ubiquitination [194,195]. In atrophic conditions, ULK1 is activated and promotes autophagy through its downstream targets, VPS34 and BECLIN1 (**Figure 14**) [196]. The study also confirms that the *Trim32* LGMDR8

pathogenic mutations p.Asp487Asn and p.Arg394His reduce its ability to promote ULK1 association with K63-linked poly-Ub, which impairs autophagy induction with atrophic stimuli [195]. However, by contrast, an increased autophagy flux is present in muscle biopsies from the LGMDR8 patients with p.Val591Met and p.Asn217Ser/Phe568del, which indicates that malfunction of TRIM32 induces autophagy *in vivo* [40].

Other studies point to the role of TRIM32 in maintaining glycolytic metabolism. AKT pathway is also probably involved in muscle atrophy and muscle hypertrophy through being regulated by TRIM32. When muscle atrophy is induced by fasting, TRIM32 reduces PI3K-Akt-FoxO signaling by promoting plakoglobin-PI3K dissociation, thus inhibiting glucose uptake and causing muscle atrophy (**Figure 14**) [197]. TRIM32 prevents pathological cardiac hypertrophy by inhibiting the Akt pathway as well [198].

The above discussion suggests a role of TRIM32 in muscle atrophy. On the other hand, many studies propose a key role of TRIM32 in muscle regeneration. There are two facts supporting TRIM32 contributing to the myogenic process: 1. the level of TRIM32 in normal muscle and muscle atrophy models did not show any difference. A significant increase of TRIM32 is instead present during muscle regeneration [41,199]. 2. When muscle atrophy is induced by fasting and cardiotoxins (CTX), *Trim32* knockout and *Trim32* wild-type mouse lines show the same atrophic level (body weight and muscle weight reduction). Some substrates of TRIM32, such as actin and desmin, which are essential for muscle cell function and structure, do not display differences in their levels [41]. Conversely, the loss of TRIM32 inhibits the differentiation and maturation of satellite cells, and a muscle regeneration defect is observed in *Trim32* knock-out and LGMDR8 pathogenic mutated *Trim32* knock-in mouse models [42,200].

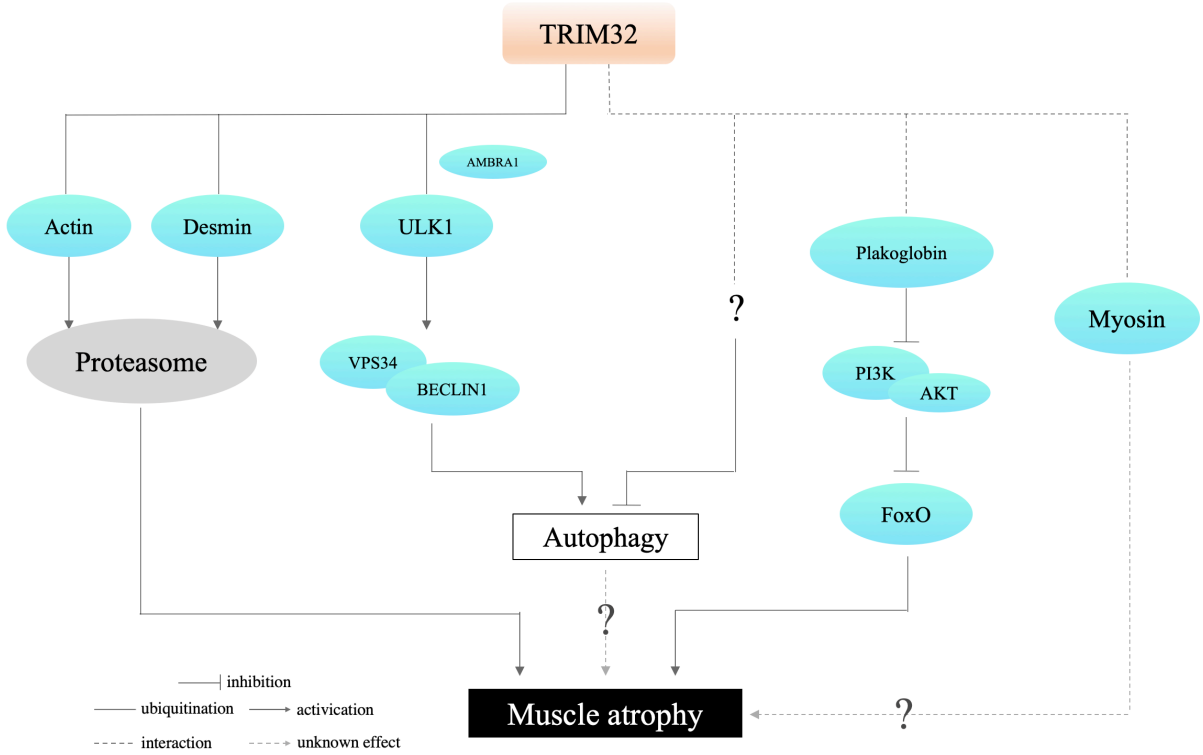

Figure 14 The signaling mechanisms contributing to muscle atrophy that are regulated by TRIM32. Emphasis is placed on substrates and interactors of TRIM32, and their target molecules.

6. TRIM32 and muscle regeneration

Studies on muscle samples from LDMGR8 patients suggest impaired myogenesis and possible involvement of pathogenic mechanisms. Myoblasts isolated from LGMDR8 proliferate slowly in culture, likely due to the increase of two substrates of TRIM32, NDRG2 and PIAS4. The myoblasts from LGMDR8 patients cannot generate normal myotubes in the proper medium, even though the defects of myogenesis observed are heterogeneous. For example, compared to the myotubes generated from healthy myoblast, the myoblasts harboring p.Val591Met mutation form thinner (small diameter) myotubes, but the mutation p.Asn271Ser/p.Phe568del results in short (small length) myotubes. On the other hand, the myoblasts with *TRIM32* mutations are larger in size and flatter than normal myoblasts, showing low cellular mobility. Further, senescence-associated β-galactosidase (SA-β-gal) assay proved the premature senescence in *TRIM32* mutant myoblast [40].

6.1 TRIM32 affect muscle regeneration in animal models

Trim32 knock-out (KO) mice show a similar pathological phenotype to muscle tissue of LGMDR8 patients. *Trim32* KO mice are born phenotypically indistinguishable from wild-type littermates, while

they start to show differences after 8 weeks. The muscle weight of *Trim32* KO mice is lower than wild-type and heterozygous *Trim32* and is accompanied by impaired muscle function, such as weak muscle strength. The morphological and histochemical examination reveals an increased number of internal myonuclei, variation in fiber size, atrophic fibers dispersed between slightly hypertrophied fibers, and a defect of generating myotubes which highlights the impaired muscle regeneration in *Trim32* KO mice [200]. In keeping with this, mice carrying the LGMDR8 pathogenic p.Asp489Asn mutation (c.1465G>A) at the *Trim32* locus presented a similar but milder myopathy phenotype. In the hind limb suspension model, TRIM32 expression significantly increased during muscle reloading (muscle regeneration) rather than unloading (muscle atrophy). Besides, real-time PCR of primary myoblasts versus skeletal muscle tissue revealed that the level of *Trim32* mRNA expression is 16 times higher in myoblasts than in skeletal muscle tissue [201]. On the other hand, the drosophila orthologue of TRIM32, thin/abba, promotes cell growth through stabilizing two glycolytic enzymes, Aldolase (Ald) and phosphoglycerate mutase 78 (Pglym). The loss of thin/abba causes reduced levels of glycolytic larval muscle and brain. All results indicate the crucial role of TRIM32 in muscle regeneration (**Figure 16**) [202].

6.2 TRIM32 induces NDRG2 degradation during myoblasts proliferation

The N-myc downstream-regulated gene (NDRG) family is involved in stress responses, cell proliferation, and differentiation. NDRG is a tumor suppressor gene with low expression in poorly differentiated, highly proliferating cancer cell lines [203-205]. According to this, NDRG2 expression levels increase in differentiated human and mouse myotubes compared with undifferentiated myoblasts [206-208]. Suppression of NDRG2 in differentiated mouse C2C12 myotubes inhibits the further growth of myotube. Proteomic profiling of these myotubes also determines significant downregulation of the myosin heavy chain 3 (MHC3) protein and vimentin. Both are contractile-type filaments associated with myoblast and muscle regeneration. Of note, in muscle tissue NDRG2 is a target of a peroxisome proliferator-activated receptor-gamma coactivator-1α (PGC-1α) and estrogen-related receptor alpha (ERRα) transcriptional program, which is enhanced in response to endurance exercise [209]. These results suggest a positive role of NDRG2 in myogenic differentiation. However, in the stage of myoblasts proliferation, overexpression of NDRG2 induces premature senescence, resulting in myoblasts losing the ability to proliferate and the potential to differentiate. The mechanisms mediating this effect are unknown [210].

NDRG2 is ubiquitinated by TRIM32 via both K48 and K63 in vitro. Ubiquitinated NDGR2 is decreased in *Trim32* KO myoblasts, resulting in an accumulation of NDRG2. However, no direct

evidence proves that ubiquitinated NDRG2 is degraded by the proteasome. Overexpression of NDRG2 in myoblasts slows cell proliferation and delays cell cycle withdrawal, which is a sign of cell premature senescence [210]. In line with this, the premature senescence of myoblast is observed in LGMDR8 patients [40]. Indeed, high NDRG2 protein level was found in senescent lens epithelial cells, contributing to reduced cell viability [211]. These data indicate that TRIM32 may mediate NDRG2 degradation through UPS in myoblasts, and loss of TRIM32 may induce NDRG2 accumulation in myoblasts, likely accelerating myoblasts premature senescence, and abolishing their potential to differentiate.

As an increased NDRG2 is observed in myotubes, either TRIM32 releases the effect on NDRG2 degradation in myogenic differentiation, or there may be other molecules engaged in limiting TRIM32's effect on NDRG2. More evidence is needed to support this hypothesis (**Figure 16**).

6.3 TRIM32 mediates PIAS4 degradation

PIAS4 belongs to the mammalian PIAS family, a group of E3-SUMO ligases characterized by an SP-RING domain [212]. The SUMOylation process is closely related to ubiquitination, resulting in the conjugation of the ubiquitin-like SUMO molecule to target substrates, mainly transcription factors, regulating their activity. The role of SUMOylation in cell physiology and pathology has not been well described. However, the increased level of SUMOylation is observed in senescent cells, indicating that it implements this process [213-215]. A study of PIAS4 in fibroblast is consistent with this speculation. The overexpression of PIAS4 leads to a senescence arrest through the activation of p53 and Rb pathways in keratinocytes [216,217]. TRIM32 induces PIAS4 degradation in myoblast as well. PIAS4 accumulates in *Trim32* knock-out myoblasts during proliferation and differentiation compared to the control *Trim32* wild-type myoblasts. Proteasome inhibitor MG132 blocks PIAS4 degradation in *Trim32* wild-type myoblasts but does not show any effect in *Trim32* knock-out myoblast. Interestingly, the accumulation of PIAS4 in *Trim32* knock-out myoblast is accompanied by the myoblasts premature senescence. Suppression of PIAS4 by siRNA decreases a cellular senescence marker, heterochromatin protein 1 (HP1g), in *Trim32* knock-out myoblast [41]. These data suggest that high PIAS4 level causes myoblast premature senescence in *Trim32* knock-out myoblast (**Figure 16**).

However, this study has two limitations: 1. It demonstrates that TRIM32 expression sharply increases in the myoblast differentiation compared to the proliferation in this study. If PIAS4 is a substrate of TRIM32, it is supposed to be downregulated in differentiation. However, similar to NDRG2, a slight increase in PIAS4 protein level has been observed in differentiation. Hence the interaction of TRIM32

and PIAS4 in myotubes needs to be further studied. 2. The study shows that an accumulation of PIAS4 inhibits the myogenic program. However, in hind limb suspension and reloading experiments on the mouse model, a lower level of PIAS4 is detected in the *Trim32* knock-out muscle sample compared to the *Trim32* wild-type sample during reloading (muscle regeneration stage). This conflicting result indicates that differences may exist between myoblast differentiation *in vitro* and muscle regeneration *in vivo* [217,218].

The two examples above demonstrate that the loss of TRIM32 function causes premature senescence through NDRG2 and PIAS4, manifesting cell premature senescence and blockage of differentiation. Interestingly, the ectopic overexpression of TRIM32 in NIH 3T3 mouse embryonic fibroblasts does not promote cell growth but inhibits cell proliferation, given that reduced Ki67 proliferation marker and phospho-histone-H3 mitosis marker are detected [219]. These results suggest that TRIM32 players, other than NDRG2 and PIAS4, are likely involved.

6.4 TRIM32 regulates muscle fiber types through neurofilaments regulation

The *Trim32* mutation knock-in mouse and *Trim32* knock-out mouse have been generated to get more insight into TRIM32 role in the pathogenesis of LGMDR8 *in vivo*. The knock-in mouse carrying the c.1465G>A (p.Asp489Asn) shows a remarkable decrease of TRIM32 at the protein level [42]. Indeed, the knock-in and knock-out mice have similar myogenic defects, as mentioned before. In addition, the *Trim32* knock-out mouse shows the decrease of three types of neurofilaments in the nervous system, including neurofilament light polypeptide (NEFL), neurofilament medium polypeptide (NEFM), and neurofilament heavy polypeptide (NEFH) [220,221]. Since NEFL and NEFM control axonal caliber, a further assessment confirmed a reduced average diameter of axons in the hind limbs, which originate from the motor axon in the lumbar spine segment L4 ventral roots. The switch of big axons to small axons corresponds to a switch from type II myofibril (fast myofibril) to type I myofibril (slow myofibril) in the hind limb muscle of *Trim32* knock-out mouse [200] (**Figure 16**).

Although a possible interplay of TRIM32, neurofilament, and myosin protein is proposed in this study, its relevance with LGMDR8 phenotypes is unclear. Probably, the loss function of TRIM32 affects the neurofilaments innervating muscle fiber. As a result, the myofibril shift from fast to slow type. These studies *in vivo* suggest a possible neuromuscular cause of LGMDR8 disease.

6.5 TRIM32 promotes neuronal differentiation by inhibiting Let-7a

Indeed, TRIM32 has been proven to regulate neuronal differentiation. At the beginning of neuronal differentiation, the neural stem cells (NSCs) go through an asymmetrical division to give one daughter cell which keeps stemness properties, while the other enters into the differentiation program. In this process, TRIM32 protein is preferentially 'inherited' by the daughter cell which initiates differentiation. Further experiments show that the overexpression of TRIM32 inhibits proliferation and induces differentiation in mouse neural progenitors. The interaction of TRIM32 and microRNAs mentioned above may regulate neural differentiation. TRIM32 exists in a complex with Argonaute 1 (Ago1) containing processed microRNAs in mouse brain lysates. Let-7a is one associated microRNA in the complex [219]. This microRNA is known to control proliferation in normal and malignant cells [222-224] and is upregulated during neuronal differentiation [225] (**Figure 16**). Inhibition of Let-7a suppresses neural stem cell (NSCs) differentiation, and conversely, cells overexpressing Let-7a express the neuronal differentiation marker TuJ1 after four days of transfection. These results indicate that Let-7a might be a downstream target of TRIM32, and likely that TRIM32 can regulate neural differentiation by controlling Let-7a activity.

6.6 Interacting with PKCζ regulates TRIM32 cellular location

TRIM32 is expressed in activated satellite cells and also in differentiating myoblasts. Freshly isolated quiescent satellite cells (Pax7+) are negative for TRIM32, suggesting that TRIM32 is unlikely to be expressed in quiescent satellite cells. These cells are activated and start to proliferate when cultured *in vitro*. TRIM32 level increases within 42 hours of culturing. Besides, TRIM32 is exclusively present in nuclei at 24 hours of culture but shows strong nuclear and cytoplasmic staining after 42 hours of culturing. However, the physiological relevance of this trafficking from the nucleus to the cytoplasm is currently unknown [199]. Interestingly, TRIM32 transports from the cytoplasm to the nucleus in neurogenic process, in the opposite direction compared to what reported in the myogenic process. The different cellular spatial and temporal expression patterns of TRIM32 in myoblasts and neural stem cells suggest various effects and substrates in different cell types and development stages [96].

TRIM32 trafficking is controlled by an apical membrane protein kinase C ζ (PKCζ) in neural stem cells. In conditions supporting proliferating of neural stem cells, PKCζ interacts with TRIM32 to retain TRIM32 in the cytoplasm (**Figure 16**). However, at the beginning of differentiation, this interaction is abrogated due to the downregulation of PKCζ. Without the containment, TRIM32 can translocate to the nucleus to initiate differentiation probably through regulating c-Myc level [226].

Another research in T helper 2 cells discusses TRIM32 can mediate PKCζ ubiquitination and target it to degradation, in the regulation of inflammation [227]. However, the interaction between TRIM32 and PKCζ is not detected in mouse embryonic stem cells (mESCs) [228], and this mechanism needs to be further investigated in myoblasts.

6.7 TRIM32 inhibits MEFs reprograming through reduction of Oct4

In addition to the positive role in cell differentiation, TRIM32 is suggested to inhibit cell reprogramming. In mouse embryonic fibroblasts (MEFs), TRIM32 inhibits the cellular transition towards induced pluripotent stem cells (iPSCs). The transcription factor Oct4 is critical for self-renewal and in sustaining the stemness of undifferentiated embryonic cells. A high level of Oct4 has been found in *Trim32* knock-out mouse embryonic fibroblasts (MEFs), enhancing MEFs reprogramming into induced pluripotent stem cells (iPSCs). In HEK293T cells, the overexpression of TRIM32 can ubiquitinate ectopic Oct4 and likely induce its degradation [228] (**Figure 16**). Two possible explanations are considered during differentiation; in the first one, at the initiation of differentiation, TRIM32 translocates from the cytoplasm to the nucleus and induces ubiquitination of Oct4 in the nucleus, then the ubiquitinated Oct4 transfers into the cytoplasm where it is degraded. In the second scenario, the induction of differentiation promotes Oct4 to translocate from the nucleus to the cytoplasm where TRIM32 targets it for degradation through proteasome (**Figure 16**).

6.8 TRIM32 and c-Myc

Those cells cannot be appropriately activated when culturing quiescent satellite cells isolated from *Trim32* knock-out mice. After the same time of culturing, much fewer cells can be stained by Myogenin, which indicates a defective myogenic process in *Trim32* knock-out satellite cells. This phenomenon could relate to the dysregulation of c-Myc. The interaction of c-Myc and TRIM32 was first studied during neurogenesis. Co-immunoprecipitation shows an interaction of c-Myc and TRIM32 from mouse brain lysates, indicating their interaction *in vivo*. Indeed, the c-Myc level is reduced upon TRIM32 co-expression in 293T cells, where proteasome inhibitors can prevent c-Myc degradation [219]. The *Trim32* p.Cys24Ala mutant with no ubiquitin ligase activity does not affect the c-Myc level [199,219]. Additional studies demonstrate that in the myogenic process, c-Myc levels are significantly reduced upon TRIM32 over-expression in C2C12 cells [96]. TRIM32 regulates c-Myc turnover but no directed evidence proves that c-Myc is a substrate of TRIM32 *in vivo*. Only one literature reported that c-Myc is a possible substrate of TRIM32 *in vitro* ubiquitination assay, but the

result is in doubt [96]. c-Myc is dramatically downregulated in myogenic differentiation, suggesting its critical role in regulating myogenesis. The mechanism of TRIM32 mediating c-Myc level is worth to be further investigated (**Figure 16**).

c-Myc is a well-known master transcriptional regulator in many cell types, controlling several target genes and noncoding RNA (lincRNA) [229]. To promote transcriptional activation at target genes, c-Myc forms heterodimers with its partner Max and recruit chromatin-modifying complexes to E-box-containing promoters [230-232]. A sustained high expression of c-Myc promotes cellular proliferating, growth, and cell renewal, which has been shown to contribute to the genesis of many types of human tumors [233]. c-Myc contains two conserved regions: Myc box I (MBI) and Myc box II (MBII) in N-terminal. MBI functions as a phosphorylation-dependent binding site for the ubiquitin ligase Fbw7, and MBII is one of the binding sites for the ligase SKP2. These two ligases induce rapid turnover of c-Myc protein [234,235]. The C-terminal of c-Myc harbors nuclear localization signals, and BHLH and LZ motifs mediating dimerization with Max and DNA binding [236] (**Figure 15**). c-Myc inhibiting differentiating has been discussed in some studies, but the detailed mechanism remains unknown [237-239].

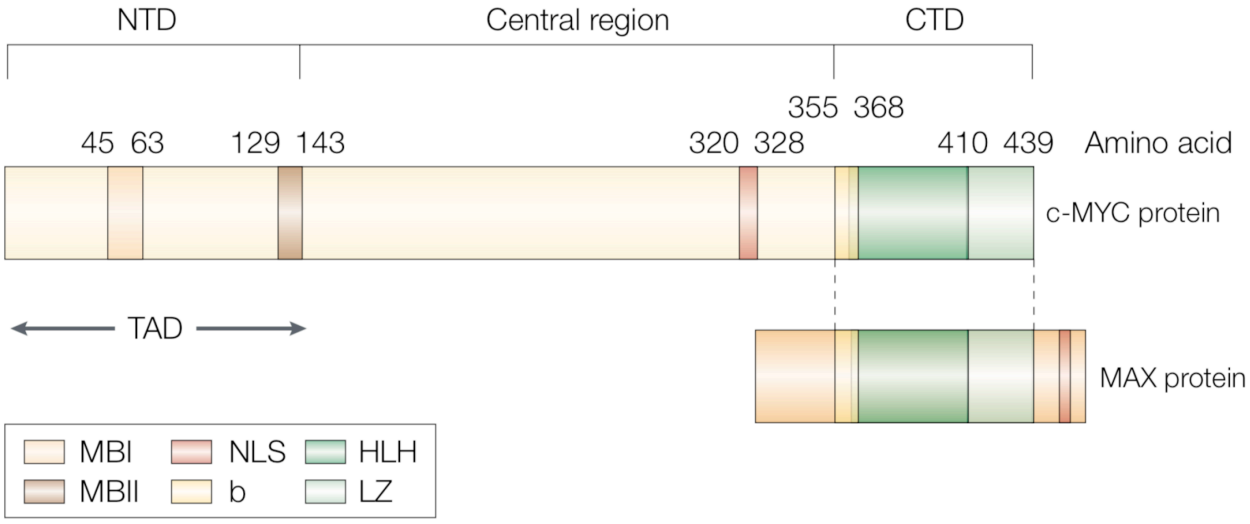

Figure 15 Functional domains of human c-MYC protein. The carboxy-terminal domain (CTD) of human c-MYC protein harbours the basic (b) helix–loop–helix (HLH) leucine zipper (LZ) motif for dimerization with its partner, MAX, and subsequent DNA binding of MYC–MAX heterodimers. The amino-terminal domain (NTD) harbours conserved 'MYC Boxes' I and II (MBI and MBII), which are essential for the transactivation of c-MYC target genes. (Pelengaris, et al., 2002)

Some studies point out that the loss of TRIM32 suppression on c-Myc in myoblasts increases the c-Myc level, thus inhibiting myoblasts' withdrawal from the cell cycle, resulting in a block of differentiation [240,241]. One piece of evidence arguing against this hypothesis. c-Myc controls a wide range of gene expression and further regulates the cell cycle by associating with its partner Max. However, a mutation in c-Myc with a partial deletion of leucine zipper (LZ) motif, which doesn't affect c-Myc and Max association and thus retains the capacity for the growth phenotype of myoblasts, abolishes c-Myc effect of blocking myoblasts differentiation. This result suggests that c-Myc inhibiting myogenic differentiation may be independent of its ability to sustain proliferation [242].

In addition, c-Myc blocks the myogenic process by downregulating myogenic regulatory factors (MRF), mainly Myogenin. The evidence supporting this hypothesis demonstrates inhibition of *Myogenin* gene expression level by c-Myc overexpression myoblasts and NIH3T3 cells [229,243]. Besides, the co-expression of MyoD and Myogenin can relieve c-Myc-induced inhibition of differentiation in NIH 3T3 cells [229]. However, some limitations exist in this study on NIH 3T3 cells. First, the co-expression of MyoD and Myogenin cannot bypass the inhibitory effects of c-Myc, indicating other critical molecules existing in this differentiation-blocking process. Second, although exogenous MyoD expression triggers the myogenic conversion of NIH 3T3 cells, it fails to form myotubes [244]. Therefore, the effect of c-Myc should be validated in myoblasts or C2C12 cells, which can process a full myogenic program.

Some miRNA and lincRNA regulated by c-Myc are involved in myoblast differentiation. The ChIP-seq screen of chicken primary myoblasts reveals five c-Myc-induced miRNAs (CI5s) and 5c-Myc-repressed miRNA (CR5s), which have been reported to involve muscle development. Further tests proved that the expression of CI5s promotes while CR5s repress the proliferation of chicken myoblasts. When inducing myoblast differentiation, the combined overexpression of CI5s inhibits MyoD, Myogenin, and MHC expression and represses differentiation. Conversely, the overexpression of CR5s shows the opposite effect in myoblast differentiation. These miRNAs are validated and likely to be involved in regulating the cell cycle, ERK-MAPK, and Akt pathway. On the other hand, c-Myc regulates noncoding RNA (lincRNA) linc-2949 and linc1369 expression, which are identified to interact with muscle-specific miRNAs. Therefore, c-Myc is also suggested to inhibit myoblast differentiation and promote myoblast proliferation through regulating miRNA and lincRNA [229].

c-Myc is also reported to be cleaved, producing an N-terminal fragment, including MBI and MBII, called Myc-nick. Calpain r, a calcium-activated Calpain, is one but not the major enzyme to cleave c-Myc into Myc-nick *in vivo* because Calpain inhibitors are incapable of blocking the accumulation

of Myc-nick in fibroblasts. Unlike the nuclear full-length c-Myc, Myc-nick is detected in the cytoplasm of confluent fibroblasts. With ectopically overexpressed Myc-nick, the fibroblasts form long protrusions, a necessary morphologic change for fibroblast fusion. Further investigation demonstrates that Myc-nick promotes protrusion formation by regulating α-tubulin acetylation. However, the production of Myc-nick has to be further confirmed with more evidence, especially in neural and muscle cells [245-247].

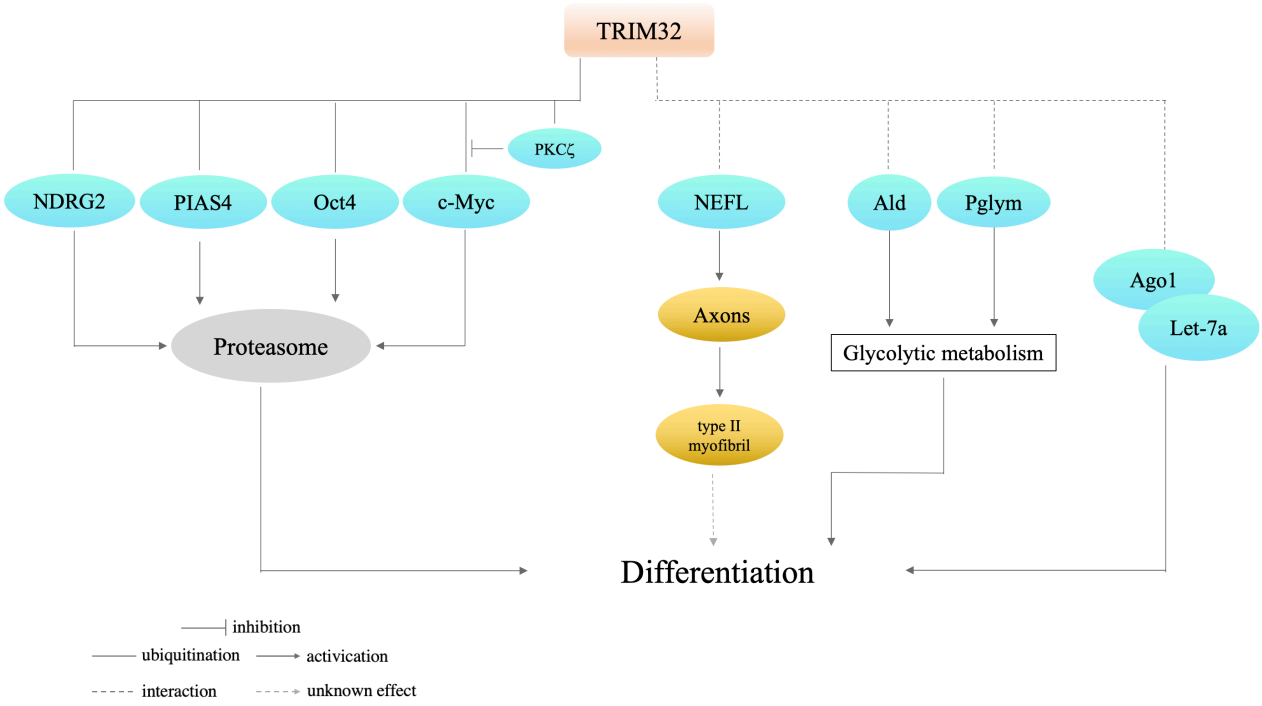

Figure 16 The signaling mechanisms contributing to cell differentiation that regulated by TRIM32. Emphasis is placed on substrates and interactors of TRIM32, and the affected cell physiological process.

There are much data indicating that TRIM32 is a vital factor for neuromuscular physiology through interacting with different molecules (**Figure 17**). However, for many of them, we do not know the exact molecular mechanism through which TRIM32 regulates their activity, or we cannot assure their role in the pathogenesis of LGMDR8. What makes the situation more complicated is that some data are still debated, as discussed above. In this project, we generated wild-type (WT) and knock-out (KO) *Trim32* C2C12 myoblasts to investigate its function in myoblast proliferation and differentiation, with the aim of discovering signaling pathway regulated by TRIM32 which are significant for myogenic process and paving the way for LGMDR8 drug discovery in the future.

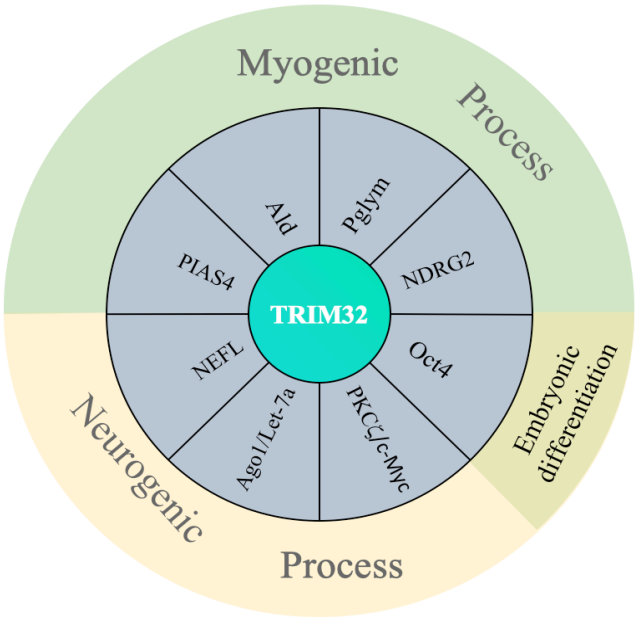

Figure 17 The molecules regulated by TRIM32 in myogenic process (Ald, Pglym, NDRG2 and PIAS4), neurogenic process (NEFL, Ago1/Let-7a, and PKCζ/c-Myc), and embryonic differentiation (Oct4).

AIM OF THE WORK

LGMDR8 is a genetic neuromuscular disorder characterized by progressive weakness of proximal muscles around the hips and shoulders. This disease is caused by mutations in the *TRIM32* gene, whose protein product is a member of the TRIM protein family of E3 ubiquitin ligases. These mutations in *TRIM32* likely lead to the complete loss of function of TRIM32. Several substrates and interactors of TRIM32 have been discovered. They are mainly involved in the process of muscle atrophy, muscle regeneration, and neurogenic differentiation. However, the pathogenic mechanisms underlying LGMDR8 have not been elucidated yet and to date there are no studies that systematically characterize the role of TRIM32 during myoblast differentiation in *Trim32* knock-out.

In this project, we generated *Trim32* knock-out C2C12 myoblasts and used them as model to study myoblasts differentiation upon loss function of TRIM32. Moreover, we investigated the potential critical molecules regulated by TRIM32 in the myogenic program, which complements and refines the pathogenic mechanism underlying LGMDR8. The work was structured addressing the following specific aims:

Aim 1. Generation of *Trim32* knock-out and wild-type C2C12 cell clones.
Aim 2. Characterization of the defects in the myogenic program in *Trim32* knock-out C2C12 cells.
Aim 3. Identification of critical molecules involved in the observed differentiation impairment of *Trim32* knock-out cells.

MATERIALS AND MEHODS

1. Generation of *Trim32* knock-out and wild-type C2C12 cells using the CRISPR/Cas9 system

CRISPR/Cas9 based genome editing has become a popular tool for targeted genome manipulation. This system requires a functional Cas9 protein and a guide RNA for effective double-stranded breakage at a desired site. We use an All-in-one vector (pCas) with a target sequence cloned (guide RNA) and *Cas9*. The target sequence is located at the 5' end of murine *Trim32* ORF. The system we used includes a donor vector (pDonor-vector) carrying GFP-LoxP-Puro-LoxP, and two homologous arms (left arm and right arm). The homologous arms are obtained from the sequences around the guide RNA of *Trim32* (**Figure 18**).

gRNA: CGGGAAGTGCTAGAATGT

Left Arm:

AGGCTTGGACCCCAAACTTACACAGTGTTCTTTGCGTACAGTTCCTGTATGTGTCATCG
CCTCTAAGATTTGTAAGACTTCTCTTACAAGGAGCACCATTTATGAGTAGCCTTACCCA
GTTGTCAGGCTCCATCCCTCTTCCCACTGTACCTCACAGTGTAGACCTTCATGTGACATT
CTCTGATCGGCAGGGTTATTCTCTGCTTTCCTGCTTGTATGTCATATTATTTAACCCTTC
CAGTAATGGTATAAGATAGGCAATTTAGGCTCTTCCCTGAATTCCTCCATAACATAATG
CATTAATCATTTGTGTGTGTGTGTGTGTGTGTGTGTGTGTGTGTATGTAAGGGGAGG
GGGGTGGGAGAGACACTATTTCCTAAGTCATAATCACTGCAATAAAATGCTTATAAAT
AAGTAAATGATTCAATGGATGATTATAGCTATTCTCTAAGTGTTTCTAGACTGAAATAA
CTTATATGGGAGTAGAAAAATGAATAATGGTTTGTTTTTTCTCTTTAGCAGGAATCTGA
CACTGGGGCATGAATATTAAGCTGTGTGGCTCTAAGCTGTGTTAGCAGGAACCTTCACT
GGAAGAGCA

Right Arm:

GCTGCCCCTTTTGCAGCAAGATTACTCGCATCACCAGCCTGACCCAGCTGACCGACAAC
CTGACGGTGCTGAAGATCATTGACACAGCTGGGCTCAGTGAGGCCGTCGGCCTGCTCA
TGTGCCGAGGCTGTGGCCGGCGGCTGCCTCGGCAGTTCTGCCGAAGCTGTGGTGTGGT
GTTGTGTGAACCCTGCCGGGAGGCAGATCACCAACCCCCTGGCCACTGCACACTTCCG
GTCAAGGAGGCAGCTGAGGAGCGGCGGAGGGACTTCGGGGAGAAGTTGACTCGTCTA
AGGGAACTTACTGGAGAGCTGCAGAGGAGGAAGGCAGCCTTGGAGGGCGTCTCCAGG
GATCTTCAGGCAAGGTATAAGGCTGTTCTTCAAGAATATGGCCATGAGGAACGCCGCA
TCCAGGAAGAGCTAGCCCGCTCTCGGAAGTTCTTCACAGGCTCCTTGGCTGAGGTTGA
GAAGTCCAACAGTCAAGTGGTAGAGGAGCAGAGCTACCTACTCAACATTGCTGAGGTG
CAGGCCGTGTCTCGCTGTGACTACTTTCTAGCGAAGATCAAGCAAGCTGATGTAGCCCT
CCTGGAGGAGACAGCGGATG

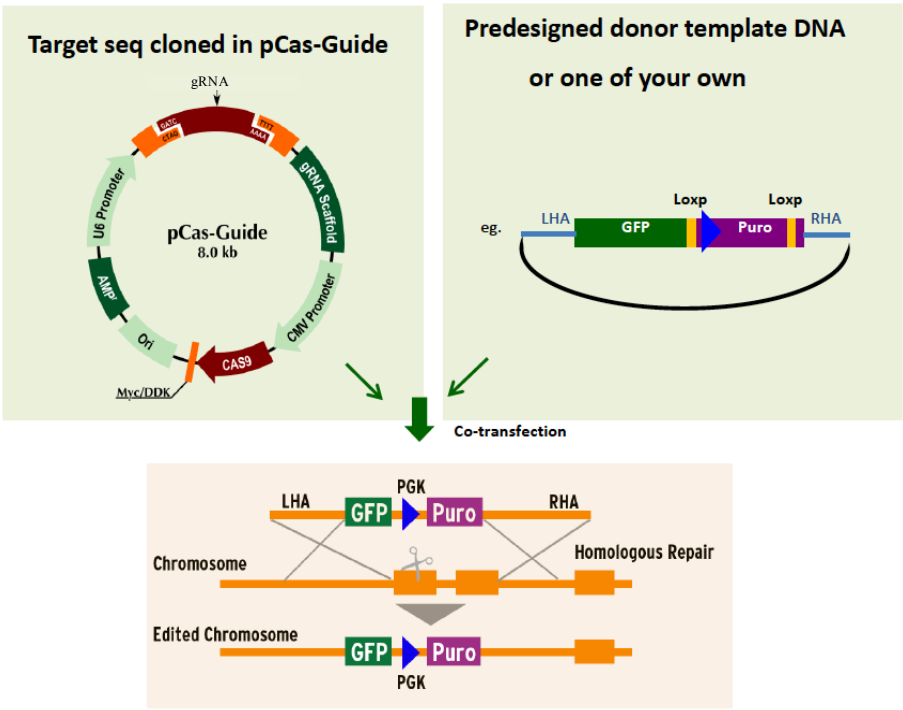

Figure 18 Flow chart of CRISPR genome editing

The pCas-Guide and the donor plasmids were obtained from Origene #SKU GE100003 and #KN318203. The pCas-Guide and pDonor-vector were co-transfected in proliferating C2C12 cells using either lipofectamine 3000 (L3000015, Invitrogen) or Mirus TransIT-X2® Dynamic Delivery System (MIR6004).

1. Approximately 18-24 hours before transfection, ~3x10^5 cells were seeded in 2mL culture medium into each well of a 6-well plate to obtain 50-70% confluence on the following day.
2. 1ug pCas-Guide and 1ug pDonor DNA were co-transfected into cells using two systems: either lipofectamine 3000 (L3000015, Invitrogen) or Mirus TransIT-X2® Dynamic Delivery System (MIR6004). The transfection steps are following the instructions for each system.
3. 48hr post transfection, cells were split for 1:10, grow additional 3 days; then were split again 1:10, for 7 times in total. Since puromycin resistant gene in the donor vector contains PGK promoter, the donor plasmid DNA before genomic integration will also provide puromycin resistance. The reason to grow cells for around 3 weeks before puromycin selection is to dilute out cells containing the donor in episomal form, avoiding as much as possible its random integration.
4. Then puromycin selection was applied to cells directly in the puromycin containing complete media in 10cm dishes. The dose of puromycin was determined before with a kill curve to find

out the lowest dose that kills the non-transfected cells completely 4-7 days' post selection; the range of puromycin is 1μg/ml to 10μg/ml). The media was changed every 2-3 days for 10 days and isolated individual cell colonies were picked and expanded.

2. Genomic DNA Extraction

All pipettes using in DNA extraction are sterilized under UV light for 30 minutes. All tips used in DNA extraction are DNAse-free. Cells are collected from 100 mm petri dish, washed with PBS (ECB4004L), and then re-suspended in 3 mL of solution B (5M NaCl, 1M Tris-HCl pH 7.5, 0.5 M EDTA pH 8) in 15mL polypropylene centrifuge tube. 200 uL of SDS 10% and 50 uL of Proteinase K (10mg/mL) were added and mixed well, and the tube was left in 55 °C water bath overnight. At second day, 1.8 mL saturated NaCl (6 M) was added to the tube, then was shook vigorously 15 seconds. The tube was centrifuged for 15 minutes at 2500 rpm, then transferred the supernatant to a new tube. Two volumes of ethanol (95%) were added, and the tube was gently inverted to precipitate genomic DNA. The precipitated DNA is spooled out with heat-sealed glass pipet, and washed with ethanol (80%). Genomic DNA was re-suspended in DNA-free water after air drying briefly. The quantity and quality of genomic DNA is assessed by NanoDrop 2000c (Thermo Fisher Scientific).

The identification of *Trim32* knock-out (KO) and wild-type (WT) clones was performed by Sanger sequence of PCR fragments performed with the following primers (40 cycles, annealing at 64°C), using genomic DNA of clones.

Fwd_T32ex2 GCAGGAATCTGACACTGG

Rev_T32_RA GTCAATGATCTTCAGCACCG

3. RNA Extraction

The RNA using in RT-PCR is extracted by TRIzol reagent (ambion 15596-026). All pipettes, tips and tubes using in RNA extraction are RNase-free. The culture medium was removed from petri dish (6cm or 10cm), then washed with PBS. TRIzol reagent was add directly to cells in petri dish (3 mL for 6cm dish; 8 mL for 10cm dish). The cells were pipetted up and down then lysed for 5 minutes at room temperature. The cells were moved to Eppendorf Tubes and 0,2 mL of chloroform was added per 1 mL TRIzol reagent. Cells were Incubated for 3 minutes after vigorously shaking. The sample was centrifuge at 12,000g for 15 minutes at 4 °C. The aqueous phase was carefully move to a new tube and 0,5 mL of isopropanol (100%) was added per 1 mL TRIzol reagent. After 10 minutes of incubation at room temperature, the tube was centrifuged at 12,000g for 10 minutes at 4 °C. The

supernatant was discarded and the RNA pellet was washed with 1 mL ethanol (75%) per 1mL TRIzol reagent. The sample was vortex briefly and centrifuged at 7500g for 5 minutes at 4 °C. The wash was discarded, and the RNA pellet was air dried for 5 minutes. The RNA is re-suspended in RNase-free water, and incubated at 60 °C for 15 minutes. The quantity and quality of RNA is assessed by NanoDrop 2000c (Thermo Fisher Scientific).

4. RNAseq Analysis

The RNA used in RNAseq analysis was extracted by RNeasy® Mini Kit (QIAGEN, 74104) following the instruction. The extracted RNA was quantitatively and qualitatively evaluated using NanoDrop 2000c (Thermo Fisher Scientific) and Agilent Bioanalyzer 2100 (Agilent, Santa Clara, CA, USA), respectively. RNA was then stored at – 80° C until use. For each sample 1ug of Total RNA with an RNA Integrity Number (RIN) higher of 8 was reserved for RNASeq analysis.

RNA sequencing and analysis described here below were performed by Danilo Licastro, Area Science Park, Trieste. For each sample libraries were generated starting from 500 ng of total RNA by Illumina Stranded mRNA Prep (Illumina Inc., San Diego, CA, USA) according to the manufacturer's protocol. Briefly, total RNA was incubated with oligo(dT) magnetic beads to capture messenger RNAs (mRNAs) with polyA tails. The mRNA was then purified before undertaking a fragmentation and denaturation step to be primed for cDNA synthesis. The obtained hexamer-primed RNA fragments were reverse transcribed with Actinomycin D, which allows RNA-dependent synthesis and improves strand specificity. The produced first strand complementary DNA (cDNA) was used as template while the original RNA template was removed and a second strand cDNA replacement synthesizes to generate blunt-ended, double-stranded cDNA fragments. In place of deoxythymidine triphosphate (dTTP), deoxyuridine triphosphate (dUTP) was incorporated to quench the second strand during amplification and achieve strand specificity. An extra adenine (A) nucleotide is added by ligation to the 3′ ends of the blunt fragments in order to prevent cDNA concatenation during adapter ligation. A corresponding thymine (T) nucleotide on the 3′ end of the adapter, provides a complementary overhang for ligating the adapter to the fragment. Pre-index anchors were ligated to the ends of the double-stranded cDNA fragments to prepare them for dual indexing. An anchors selective amplification added indexes and primer sequences for cluster generation producing the final dual-indexed library.

The libraries were quantified using Qubit dsDNA BR Assay Kit (Thermo Fisher Scientific, MA, USA) on Qubit 2.0 Fluorometer (Thermo Fisher Scientific, MA, USA) and checked for dimension with

DNA 1000 Chip on Bioanalyzer 2100 (Agilent Technologies) before pooling. The final sequencing pool was quantified by qPCR (KAPA) before sequencing. Sequencing was performed on Novaseq 6000 sequencer (Illumina Inc., San Diego, CA, USA) according to the manufacturer's protocol generating for each sample almost 50 million clusters of 2 x 150 bp paired-end reads. Illumina BCLFASTQ v2.20 software was used for de-multiplexing and production of FASTQ files. Raw files were subsequently quality checked with FASTQC software (http://www.bioinformatics.bbsrc.ac.uk/projects/fastqc) and sequences with low quality score or including adaptor dimers, were discarded from the analysis.

The resulting set of selected reads were aligned onto the Mouse genome using Spliced Transcripts Alignment to a Reference algorithm STAR version 2.7.3. using GRCm39 Genome Assembly and Gencode.v28 as gene definition [248]. The resulting Mapped reads were used as input for feature Counts functions of Rsubread packages and used as Genes counts for Differential expression analysis using Deseq2 package [249]. We used shrinkage estimator from the apeglm package for visualization and ranking [250]. Differentially expressed genes (DEGs) were selected for $|\log2(FC)| \leq -1$ or ≥ 1 and corrected P value ≤ 0.05 and used as input to perform pathway enrichment analysis by IPA system (Ingenuity® Systems, www.ingenuity.com).

Though IPA, all DEGs were categorized in canonical pathways. IPA also predicted possible master regulators and downstream disease and functions. Upstream and downstream predictions and DEGs were combined in functional networks.

5. Cell Culture

C2C12, an immortalized mouse myoblast cell line, is maintained in culture in growth medium with DMEM (Euroclone, ECM0101L), 20% fetal bovine serum (FBS, Gibco 10270), 4 mM L-glutamine (Euroclone, ECB3000D), 100 units penicillin/100 μg streptomycin (Gibco, 15104).

For myogenesis induction, cells are cultured in proliferating medium to reach 50-60% confluence, seeding these un-confluent cells at a density of 7.5×10^4 cells/mL in 6 cm (5 mL) or 10 cm (10 mL) petri dishes. Growth medium is then replaced by differentiation medium (DMEM (Euroclone, ECM0101L), 2% donor horse serum (biowest, S0900), 4 mM L-glutamine (Euroclone, ECB3000D), 100 units penicillin/100 μg streptomycin (Gibco, 15104)) at the second day (counting as Day0 of

differentiation). The differentiating medium was changed every day, for different time points before fixation or cell harvesting for protein extraction.

Time course experiments to check c-Myc stability has been analyzed by treating the cells with 50 ug/mL cycloheximide (Sigma Aldrich, #1810), 20 uM MG132 (Merck, #474790), and the combination of 50 ug/mL cycloheximide and 20 uM MG132. The time of treatment is indicated in the result and discussion.

Plasmid DNA harboring MycGFP-TRIM32 and MycGFP-TRIM32ΔRING, already available in the lab have been transfected in C2C12 cells through Lipofectamine 3000 vector (L3000015, Invitrogen) following manufacturer's instructions.

6. Immunofluorescence Experiments

C2C12 cells have been seeded on glass coverslips at a density of 7.5 x 10^4 cells/mL in 6cm (5mL). Coverslips were collected at different time points and washed twice in PBS 1X (137mM NaCl, 2.7 mM KCl, 10 mM Na_2HPO_4, 1.8 mM KH_2PO_4, pH 7.4) and fixed in 4% paraformaldehyde (PFA) for 15 minutes at room temperature, or fixed in methanol for 10 minutes on ice (for myosin heavy chain stain). Cells were then washed again in PBS 1X and blocked with 5% BSA in PBS-Triton (0.3%) for 1 hour at room temperature. Coverslips have been then incubated with primary antibodies, diluted in 1% BSA in PBS-Triton (0.3%), overnight at 4 ℃. Cells were then washed in PBS 1X. Staining was obtained after incubation for 1 hour at room temperature with a Cy3- conjugated anti-rabbit antibody (1:200 dilution, #AP132C, Millipore) or FITC-conjugated anti mouse antibody (1:200 dilution, #F0479, DAKO). Coverslips was mounted with Vectashield mounting medium plus DAPI (Vector Laboratories) and cells were observed with epifluorescence microscopy. 20x magnification images were used to calculate differentiation index, through ImageJ (NIH, Bethesda, USA), while high-resolution 63X magnification images was used to measure the myotube length and diameter, and identify the distribution of different proteins in the cells, through ImageJ software. The antibodies used in immunofluorescence experiments are Myosin Heavy Chain III (Santa cruz biotechnology, #sc-20641, 1:200), MyoD1 (Proteintech, #18943-1-AP, 1:100), Myogenin (Santa Cruz biotechnology, #sc-52903, 1:50), phosphor-Histone3-ser10 (Cell Signaling, #9701, 1:100).

7. SDS-PAGE and Western blot

C2C12 cells have been lysed in RIPA buffer (50 mM Tris-HCl pH 8, 0.3% SDS, 150 mM NaCl, 0.5% NaDOC, 1% NP-40, add 1mM PMSF and 100X α-P8340 before using) or Myosin extraction buffer (300 mM NaCl, 0.1M NaH_2PO_4, 0.05M Na_2HPO_4, 0.01M $Na_4P_2O_7$, 1mM $MgCl_2$, 10mM EDTA, add 1mM PMSF and 100X α-P8340, and 1mM DTT before using). Samples have been then sonicated 5 seconds x 3 pulses. The insoluble fraction has been removed by centrifugation at 14,000 rpm at 4°C for 10 minutes. Protein quantification has been measured through a Bradford assay (BioRad, Cat. #500-0006) following the manufacturer's instructions. Proteins have been boiled at 95°C for 5 minutes in sample buffer (250 mM Tris-HCl pH 6.8, 40% glycerol, 8% SDS, 5% β-mercaptoethanol, 0.04% bromophenol blue, 200mM DTT) and then loaded on 7.5%, 10%, or 12% acrylamide gels (PAGE), depending on the resolution required for each protein detected, and blotted on PVDF membranes (Immobilon-P, IPVH- 00010, Millipore) overnight at 4°C. Membranes have been then blocked in 5% Milk in TBS 1X (150 mM NaCl, 10 mM Tris, 0.065% HCl, pH 7.4) with 0.1% Tween (TBST), for 1 hour at room temperature. Primary antibodies have been diluted in 5% Milk in TBST or 5% BSA in TBST based on the indication of datasheet, and incubated for 2 hours at room temperature:

- Anti-TRIM32 (Proteintech, #10326-1-AP) 1:1500 dilution
- Anti-TRIM32 (GTX, #113937) 1:1000 dilution
- Anti-Myosin Heavy Chain III (Santa Cruz Biotechnology, #sc-20641) 1:2000 dilution
- Anti-MyoD1 (Proteintech, #18943-1-AP) 1:1500 dilution
- Anti-Myogenin (Santa Cruz Biotechnology, #sc-52903) 1:500 dilution
- Anti-c-Myc (Cell Signaling, #5605) 1:1000 dilution
- Anti-GAPDH (Sigma, #8795) 1:5000
- Anti- β-Tubulin (Sigma, #T4026) 1:5000

Secondary antibodies have been incubated for 1 hour at room temperature, diluted in 5% Milk in TBST:

- Anti-Mouse HRP (Millipore, #AP308P) 1:5000
- Anti-Rabbit HRP (Bethyl Laboratories, #A120-208P) 1:5000

For bands detection, membranes were incubated with HRP substrate (ECL Pierce, Invitrogen, 32106), for 1 minute, then at ChemiDOCTM Touch Imaging System. The band analyzed by Image Lab software (Bio-Rad).

8. Myotube measurement, Differentiation index, and pHH3 positive cells calculation

Myotube length and diameter were measured upon Myosin Heavy Chain III staining, through the ImageJ software relative to the resolution of the image (scale bar is indicated in Result and Discussion section for each immunofluorescence).

Differentiation index was calculated as the ratio of the number of nuclei in the Myosin Heavy Chain positive (+) cells to the total number of nuclei in each immunofluorescence filed. The numbers of nuclei are counted by the ImageJ software.

Percentage of pHH3 positive was calculated as the ratio of number of nuclei with Phospho-histone H3 Ser10 positive to the total number of nuclei in each immunofluorescence filed. The numbers of nuclei are measured by ImageJ software.

9. Statistical Analysis

All the experiments in C2C12 cells have been performed at least three times. Further experiments in C2C12 have been performed in biological triplicates (N = 3 WT and N = 3 KO C2C12). Statistical analysis performed to assess differences between samples was done using a two tail Student's t test (Prism7), as indicated in each experiment.

RESULTS AND DISCUSSION

1. Generation of *Trim32* knock-out (KO) C2C12 cells

An immortalized mouse myoblast cell line, C2C12, has been chosen for its ability to mimic muscular differentiation, from myoblasts to myotubes, under appropriate conditions. The myoblasts readily proliferate in high-serum conditions and differentiate and fuse in low-serum conditions. CRISPR/Cas9 (clustered regularly interspaced short palindromic repeat/CRISPR-associated) genome editing system has been chosen to generate *Trim32* KO C2C12 clones. We employed a two-plasmid-system: the guide RNA (gRNA) plasmid that encodes also for the Cas9 enzyme and the donor plasmid, designed for homologous-directed repair of *Trim32* gene carries GFP and PURO resistance as the selecting marker. These plasmids have been co-transfected into undifferentiated C2C12. After selection of the PURO-resistant clones, genomic DNA was extracted from 200 clones and *Trim32* sequence around the CRISPR guide employed was analyzed through PCR followed by Sanger

sequencing. According to the sequencing results, in many *Trim32*-targeted clones, a recurrent mutation was generated: c.49delG leading to a premature stop codon (p.E17Kfs*1) with the production of a very short N-terminal portion, if any (**Figure 19a**).

From six putative KO and five WT (clones in which mutations did not occur) most promising clones' total RNA was extracted, retro-transcribed and *Trim32* region amplified and Sanger sequenced to confirm the genomic mutations also at the transcript level. Further, high-quality RNA was extracted from a first selection of wild-type and mutated clones to perform Illumina RNAseq experiments. The first analysis of these RNAseq data was to assess the mutations generated in *Trim32* especially when different alleles were present and PCR and Sanger sequencing cannot discriminate easily. Based on the RNAseq results, other two mutations were identified in a compound heterozygous clone: c.22_61del and c.49_50insG, which also result in premature stop codons (p.S8Vfs*52 and p.E17Gfs*12) and short N-terminal fragments (**Figure 19a**). Furthermore, the absence of TRIM32 protein in *Trim32* KO clones was confirmed by western blotting analysis using two polyclonal antibodies that detects the N terminus (Proteintech) and the central region (GeneTex) of TRIM32 protein (**Figure 19b**). Three *Trim32* KO (Two homozygous and one compound heterozygous clones), and three *Trim32* WT clones were selected for the thesis work (**Table 2**). Unfortunately, even trying three different commercial TRIM32 antibodies in the immunofluorescent experiment, they all failed to specifically stain TRIM32 with this technique and thus are not suitable to reveal or not TRIM32 distribution in WT and KO clones, respectively.

The analysis of RNAseq did not show the expression of Cas9 in all clones, suggesting either the loss of gRNA plasmid or the silencing of gRNA plasmid in these myoblasts, which prevents other random gene edition by Cas9 in the selected clones. Together, the three *Trim32* KO and three WT clones have been clearly identified at DNA (Sanger sequence), RNA (RNAseq) and protein level (Immunoblotting).

Instead of using a gRNA with random sequence, we selected the *Trim32* WT C2C12 myoblasts from the pool of targeted cells. We expected to avoid the undesired editing of genomic DNA caused by random sequence. We selected those WT clones in which the proliferation process is reproducible and most comparable to the parental C2C12 myoblasts. Although the formation of myotubes in WT clones is a bit delayed (around 1 day later), their phenotypes are otherwise consistent with parental C2C12 myoblasts. Therefore, we assume that the mild difference between WT and parental C2C12 cells is due to the accumulation of experimental passages on the myoblasts during the gene editing

process that partly reduces their differentiation potential. Out of this initial characterization of C2C12 edited cells, we eventually selected three KO and three WT myoblast clones (**Table 2**), assuring that all results obtained in the subsequent experiments can be repeated and caused by the knock-out of TRIM32 in these selected clones.

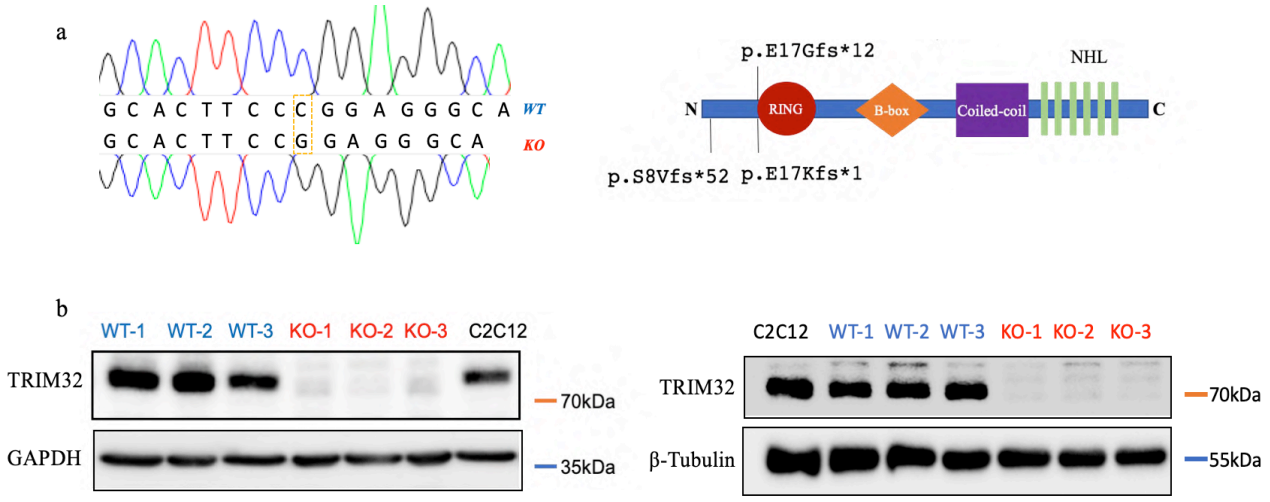

Figure 19 Generation and characterization of *Trim32* KO and WT C2C12 clones. a. Sanger sequence results of WT and the most recurrent mutation c.49delG in *Trim32* (Left). The three mutations of *Trim32* (c.49delG, c.22_61del, and c.49_50insG) result in three premature stop codons in TRIM32 protein (p.E17Kfs*1, p.S8Vfs*52, and p.E17Gfs*12), which probably produce short N-terminal fragments without function (Right). b. Representative Western Blot analysis for TRIM32 protein levels detection in parental C2C12, three KO, and three WT clones, using two different TRIM32 antibodies; 20 µg of protein extract was loaded. In the left panel, TRIM32 antibody from Proteintech (#10326-1-AP) was used, and GAPDH as loading control. In the right panel, TRIM32 antibody from GeneTex (#GTX113937) was used, and β-Tubulin as loading control.

Table 2 Features of the selected KO and WT clones.

	Clones	Trim32 Genotype	Mutation on TRIM32[a]	Cas9 expression
KO	KO-1	c.49delG	p.E17Kfs*1	-
	KO-2	c.49delG	p.E17Kfs*1	-
	KO-3	c.22_61del/c.49_50insG	p.S8Vfs*52/p.E17Gfs*12	-
WT	WT-1	WT	-	-
	WT-2	WT	-	-
	WT-3	WT	-	-

a. "-" not detected

2. RNAseq reveals that the knock-out of *Trim32* impairs C2C12 myogenic process

The three KO and three WT C2C12 clones were cultured in the proper condition (see Materials and Methods) for inducing differentiation. Total RNA was extracted from both proliferating cells (Day 0 of differentiation) and differentiating cells (Day 3 of differentiation), and Illumina RNAseq experiments was performed in collaboration with Danilo Licastro, Area Science Park, Trieste. In our preliminary experiments, we observed the appearance of myotubes at day 3/4 of differentiation in *Trim32* wild-type clones. We assumed that the main changes in signaling pathways and myogenic program occur before day 4, hence the RNAseq was performed before differentiation (Day 0) and in the initial phases of differentiation (Day 3).

Principal Component Analysis (PCA) showed that *Trim32* KO and WT cells show significant difference at transcriptional level (18% variance WT *vs* KO) (**Figure 20**). Similar homogeneity separates *Trim32* WT and KO myoblasts into two group at day 0 and day 3. At day3, *Trim32* WT and KO cells are transcriptionally more distant than at day 0 (short distance on PC2 axis at Day 0) (**Figure 20**). This may suggest that *Trim32* predominantly regulates myogenic differentiation rather than myoblasts proliferation, consisting with previous studies on TRIM32. On the other hand, as expected, a significant difference of genes expression is revealed from day 0 to day 3 (57% variance D0 vs D3) (**Figure 20**), indicating that likely WT and KO cells initiate a differentiation program under the proper

condition, but because of the absence of TRIM32 in the KO cells, they are unable to reach to the same degree of differentiation at day 3 as WT cells.

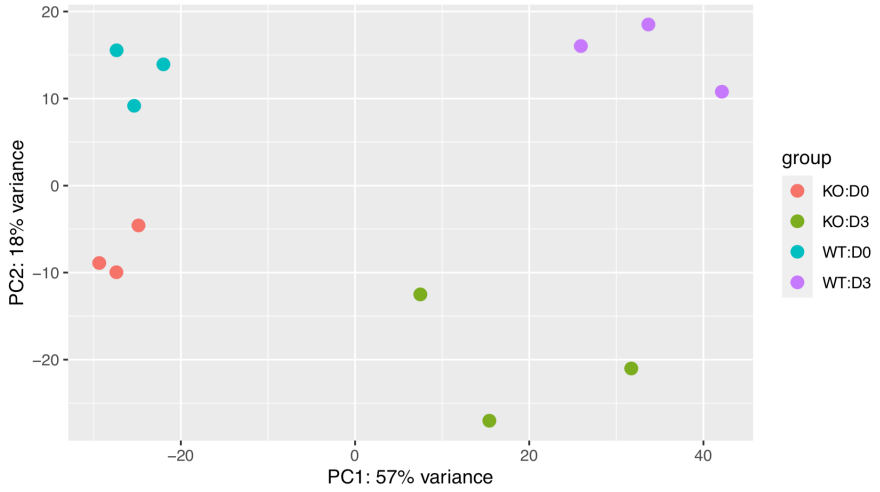

Figure 20 PCA analtsis of RNAseq data of *Trim32* KO and WT C2C12 cells in proliferation (Day 0) and differentiation (Day 3). The difference of total gene expression of WT and KO myoblasts at day 0 and day 3 is shown. The variance is a statistical measure of how much variation in the result can be attributed PC1: time from day 0 to day 3, PC2: different genotypes of *Trim32* WT and KO C2C12 cells.

Then, the differentially expressed genes (DEGs) obtained as described in M&M in different comparisons were employed to identify the most enriched canonical signaling pathways in *Trim32* WT *vs* KO cells. At day 0. enriched canonical pathway analysis through IPA identified 62 significant pathways (p-value < 0.05). Regarding the z-score of more than 2.0 for significant activation in WT compared with KO, or less than −2.0 for significant inhibition status in WT compared with KO in the pathway analysis, only 3 of the total 62 pathways had absolute z-score of more than 2.0. The few significant pathways with absolute z-score > 2.0 are consistent with the lower variance of DEGs between WT and KO cells at day 0 shown in PCA analysis. **Figure 21** shows the six most active (orange) and four most inhibited (blue) canonical pathways in WT compared with KO, ranked by –Log (p-value). The three most activated canonical signaling pathways in WT are CREB signaling in neurons (z = 2.8), breast cancer regulation by stathmin1 (z = 2.2), and phagosome formation (z = 2.1). CREB, also known as cAMP response element-binding protein, can regulate the transcription of numerous neuropeptides. No studies suggest CREB is directly engaged in the myogenic process, but cAMP has been reported to show a transient upregulation before myogenic fusion. The effect of cAMP on myogenesis is unknown. Stathmin1 is a positive factor for myotube formation and enhancing muscle strength. Phagosome formation is a process that mainly involves cell membrane change which is also active in myogenic fusion [251-253].

In addition, two other critical signaling pathways, calcium (z = 1.3) signaling and Focal adhesion kinase (FAK) signaling (z = 1.2), also contribute to myogenesis. Calcium level is the main switch that regulates muscle contraction and relaxation, and many studies revealed the critical role of calcium signaling in myogenic differentiation. Focal adhesion kinase signaling regulates the expression of Caveolin 3 and β1 Integrin, which are essential for myoblast fusion [254-256].

On the other hand, no significant inhibited canonical signaling pathway (z score < - 2.0) in WT compared with KO is revealed. **Figure 21** shows the four most significant inhibited pathways (Blue), and three of them show p-value > 0.05. WNT/ β-catenin signaling and wound healing signaling pathways are involved in the stimulation of myogenesis [257,258], and GP6 signaling pathway plays a crucial role in platelet procoagulant activity and subsequent thrombin and fibrin formation [259].

The analysis of enriched canonical pathways at day 0 shows the higher activity of several pathways in WT than KO. However, globally, the significant difference between WT and KO is relatively low.

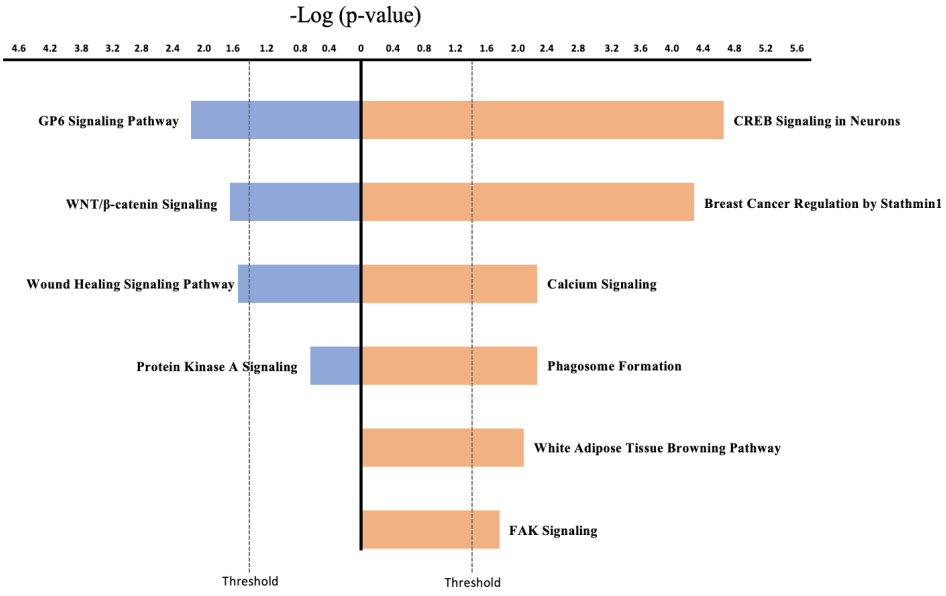

Figure 21 The most active and inhibited canonical signaling pathways in *Trim32* WT compared with KO C2C12 cells at Day 0, ranked by the value of –Log (p-value). Threshold p-value = 0.05. The canonical signaling pathways activated is marked by orange, and the canonical signaling pathways inhibited is marked by blue.

In the same way, we subsequently analyzed the canonical signaling pathways enriched in DEGs in WT *vs* KO clones at day 3. Compared with day 0, more significant different canonical signaling

pathways (p-value < 0.05) are revealed. Out of 123 significant canonical signaling pathways, 14 show the absolute z-score > 2.0, indicating an increased difference in cell physiology between WT and KO.

The six most significant active canonical signaling pathways in WT compared with KO are actin cytoskeleton signaling (z = 2.7), oxytocin signaling pathway (z = 3.0), Integrin-linked kinase (ILK) signaling (z = 2.5), phagosome formation (z = 2.8), SNARE signaling pathway (z = 3.0), and regulation of actin-based mobility by Rho (z = 2.7) (**Figure 22**). The regulation of actin is active in myogenic fusion; it controls the morphology and mobility of myocytes, promoting cell recognition and adhesion. Vesicle fusion mediated by SNARE is essential for myocyte fusion at the third stage of myogenesis. In addition, Integrin-linked kinase (ILK) signaling is the critical regulator in the the vinculin-talin-integrin system assembly, a fundamental costamere complex. (discussed in the introduction).

Only dilated cardiomyopathy signaling pathway is enriched with z score < - 2.0, which probably suggests the disorder and malfunction in KO cells. The three significant canonical pathways are RHOGDI (z = -1.6), pulmonary idiopathic (z = -1), and the role of CHK proteins in cell cycle checkpoint control (z = -1) pathways (**Figure 22**). CHK proteins initiate cell cycle checkpoints, regulating DNA repair and cell cycle arrest. In addition, a higher activated RHOGDI signaling suggests that Rho-GTPase activity is inhibited by RHOGDI signaling in KO clones. RHOGDI is a down-regulator signaling of Rho family GTPases typified by its ability to prevent nucleotide exchange and membrane association. Rho-GTPase-activating proteins, such as GRAF1, are transiently up-regulated during myogenesis. Studies in C2C12 cells revealed that Rho-GTPase is necessary and sufficient for mediating RhoA down-regulation and inducing muscle differentiation [260]. These pathways showing relatively higher activity in KO cells may disrupt the myogenic program.

Based on the preliminary analyse, *Trim32* WT cells appears to be in a more advanced stage of differentiation than KO cells.

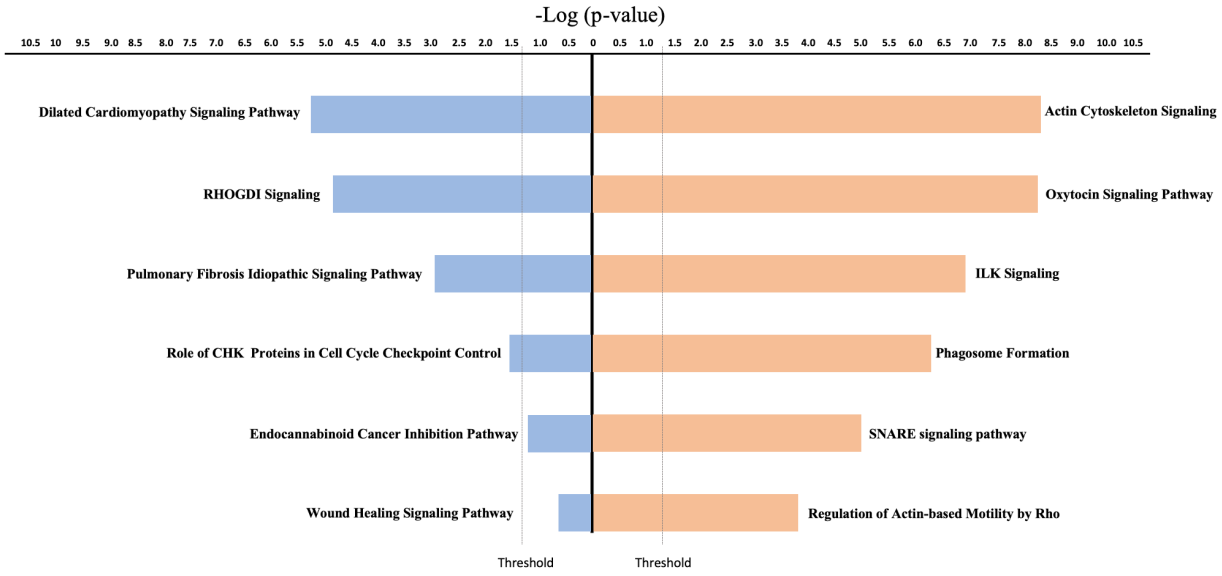

Figure 22 The most active and inhibited canonical signaling pathways in *Trim32* WT compared with KO C2C12 cells at Day 3, ranked by the value of –Log (p-value). Threshold p-value = 0.05. The canonical signaling pathways activated is marked by orange, and the canonical signaling pathways inhibited is marked by blue.

To characterize the progress of myogenesis in our C2C12 clones, we further analyze the canonical signaling pathways enriched in DEGs from day 3 *vs* day 0 independent of genotype. One hundred fourteen significant canonical signaling pathways with absolute z score > 2 are identified, suggesting a dramatic change in cell physiology from day 0 to day 3 as expected. In the six most significant activated canonical pathways at day 3 compared with day 0 (z score > 2), phagosome formation (z = 4.9), wound healing signaling pathway (z = 4.8), CREB signaling in neurons (z = 4.4), and calcium signaling (z = 4.3) have been well described as critical for myogenic fusion (**Figure 23**). The other two activated pathways are fibrosis-related (Pulmonary Fibrosis Idiopathic Signaling Pathway (z = 4.6) and Hepatic Fibrosis Signaling Pathway (z = 4.4)) (**Figure 23**). Much evidence support that fibroblast growth factors (FGFs) and fibroblast growth factor receptors (FGFRs) regulate the myogenic program, particularly at the early stage. Increased FGFs are detected after injury of muscle tissue. However, their role in muscle regeneration remains unclear [261-263].

Toward differentiation, the most inhibited canonical signaling pathways at day 3 compared with day 0 focused on cell cycle and DNA repair, including cell cycle control of chromosomal replication (z = -4.8), kinetochore metaphase signaling pathway (z = -4.2), BER (Base Excision Repair) pathway (z = -3.5), RAN signaling (z = -3), and cyclins and cell cycle regulation (z = -2.8) (**Figure 23**). The downregulation of these signaling at day 3 indicates the exit from cell proliferation status.

Together, the analysis of enriched canonical signaling pathways of day 3 *vs* day 0 supports our hypothesis that both *Trim32* WT and KO initiate differentiation.

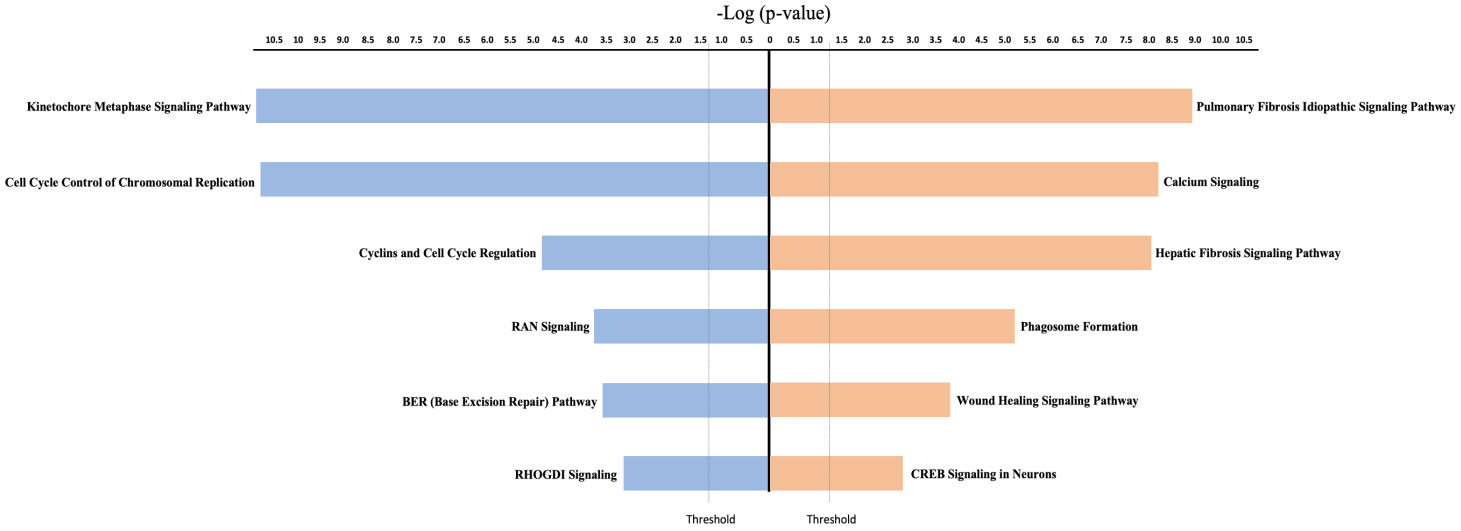

Figure 23 The most active and inhibited canonical signaling pathways of Day 3 vs day 0, ranked by the value of –Log (p-value). Threshold p-value = 0.05. The canonical signaling pathways activated at day 3 is marked by orange, and the canonical signaling pathways inhibited at day 3 is marked by blue.

The validation and further analysis of RNAseq results is still in progress, however, in general, the RNAseq analysis suggest a difference in the onset of the differentiation program in WT and KO C2C12 clones. Therefore, the expression level of some Myogenic Regulatory Factors (MRFs) was extrapolated and presented here. At day 0, the RNA level of *Pax7, Myf5*, and *MyoD* were investigated because their expression is a sign of activated satellite cells. The RNA level of *Pax7* and *Myof5* do not show a significant difference in WT and KO. Only *MyoD* shows a mild down-regulation in KO compared with WT. The similar RNA level of these MRFs at day 0 suggests comparable status of D0 myoblasts in *Trim32* WT and KO clones (**Figure 24**). At day 3, *MyoD* and *Myogenin (MyoG)*, the master regulators of myogenic differentiation; *Myomixer* (*MYMX*) and *Myomaker* (*MYMK*), regulators of myogenic fusion; *Myosin heavy chain* (*MHC*), the marker for myogenic differentiation, are all down-regulated in KO cells (**Figure 24**). These results suggest, at least at the RNA level, that *Trim32* KO C2C12 likely starts the differentiation program with delay (or impairment) compared to WT cells.

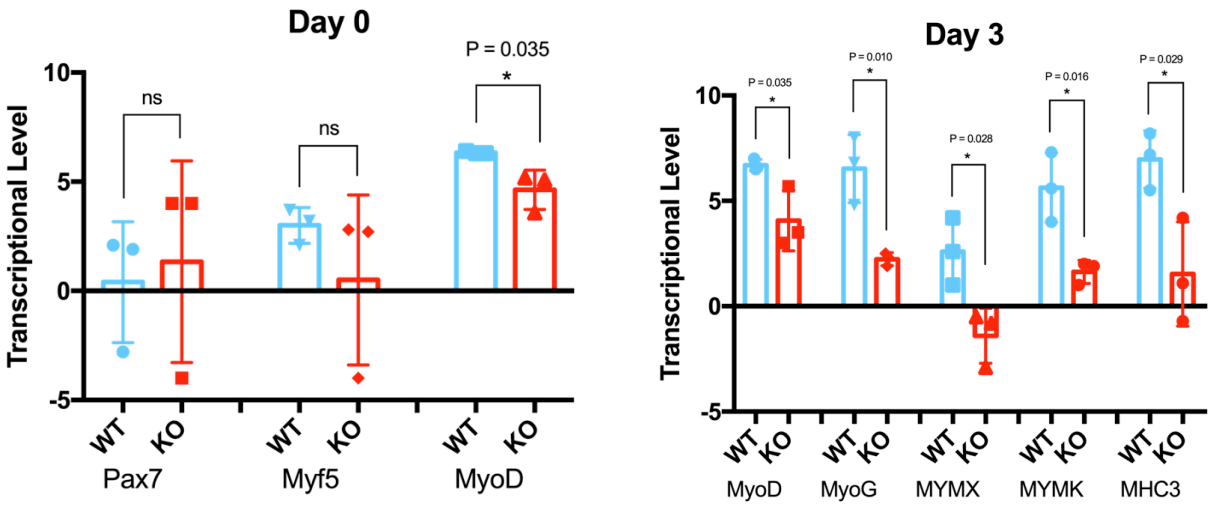

Figure 24 RNA transcriptional level of some myogenic regulatory factors (MRFs) in *Trim32* WT and KO myoblasts (day 0, left graph; day 3, right graph). The Y axis represents the logCPM (logarithm of counts per million reads) after normalization.

3. The knock-out of *Trim32* inhibits the differentiation of C2C12 cells

In parallel to the RNAseq result that indicates impaired differentiation in *Trim32* KO cells, we further evaluated differentiating of *Trim32* WT and KO C2C12 cells in culture. The marker of myogenic differentiation, myosin heavy chain (MHC), was used to follow the differentiation process. MHC is the main protein in muscle contraction (see Introduction); thus, it is only expressed in the differentiating myocytes and myotubes. The parental C2C12 cells, and the 3 WT and 3 KO clones were seeded at the density of 7.5×10^4 cells/mL in growth medium (see Materials and Methods). When the myoblasts reached 85% – 90% confluence, the growth medium (GM) was replaced by the differentiation medium (DM) to induce differentiation (see Materials and Methods). Immunofluorescence and western blot to analyze the expression of MHC at day 0, 3, and 8 of differentiation (**Figure 25**).

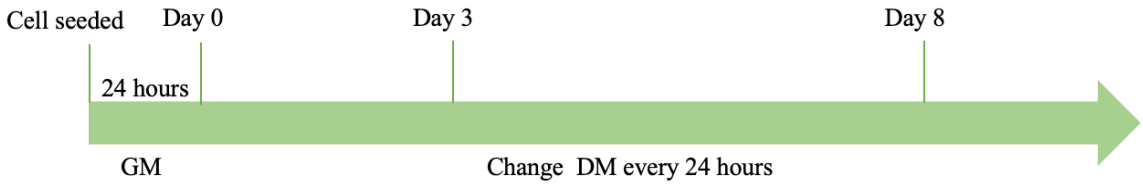

Figure 25 Experimental scheme of C2C12 cells differentiation. Proliferating C2C12 myoblasts are seeded in the growth medium (GM) on the day before day 0. GM is replaced with differentiation medium (DM) at Day 0 to induce myogenic differentiation. Cells are collected at Day 0, Day 3, and Day 8 for analysis.

At day 0, C2C12 myoblasts keep proliferating in the undifferentiated condition. Thus, no MHC can be detected in the immunofluorescence images in parental C2C12, WT, and KO myoblasts (**Figure 26**). C2C12 parental and WT cells initiate the myogenic program as soon as the differentiating condition is applied. Some fusiform myocytes (mono-nucleus) and small myotubes (two or three nuclei) are stained with MHC in immunofluorescence images at day 3. On the contrary, no MHC-positive cells can be detected in the KO cells after differentiating for 3 days (**Figure 26**), indicating that the knock-out of *Trim32* affects C2C12 cell differentiation.

WT and KO clones show a significant difference in myotube formation at day 8 (**Figure 26**). Although myotubes stained with MHC can be detected in both WT and KO cells, they are reduced in the latter. The analysis of the differentiation index confirms more myotubes formation in WT than KO (**Figure 27**). In addition, the few myotubes generated by KO cells display morphologic abnormalities. Both parental C2C12 and WT cells generate long, fusiform myotubes with well-organized nuclei (**Figure 26**). Instead, most myotubes formed by KO cells are shorter, showing a higher ratio of diameter/length (**Figures 26 and 27**). In addition, the nuclei of KO myotubes are distributed in the most hypertrophic part of myotubes (**Figure 26**). The morphologically abnormal KO myotubes are probably the consequence of the disorganization of filament proteins. As mentioned in the introduction, some findings point out that many sarcomere filament proteins, including actin, α-actinin, tropomyosin, dysbindin, and desmin, are substrates of TRIM32 in muscles. These proteins are essential for maintaining muscle fibril structure. The loss of *Trim32* may induce disordered accumulation of these proteins in C2C12 and ultimately results in the observed abnormal myotubes.

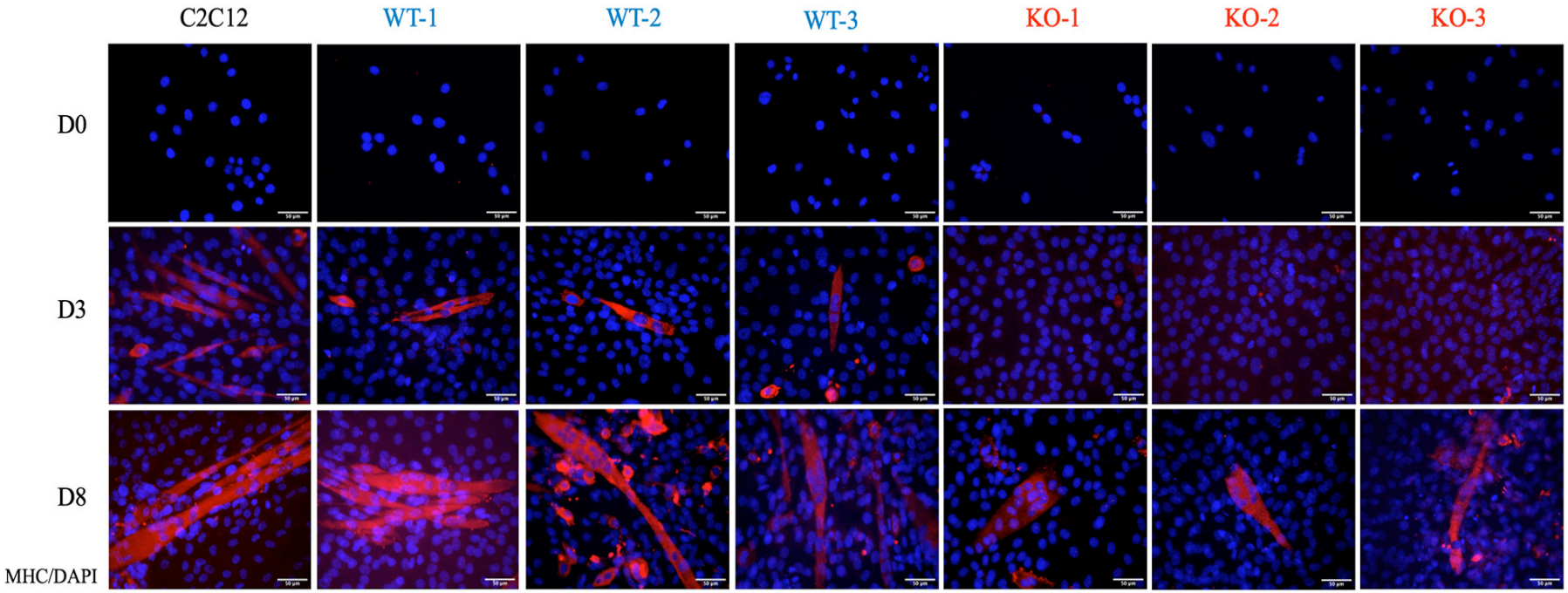

Figure 26 Analysis of myotube formation of *Trim32* KO, WT and C2C12 parental C2C12 cells under maintenance conditions (day 0) as well as 3 and 8 days after the induction of myogenic differentiation. The myotubes are marked through an anti-myosin heavy chain III (red) in immunofluorescence. Nuclei are counterstained with DAPI (blue). Fewer and shorter myotubes can be detected in KO myoblasts. (40x magnification; scale bar = 50 µm)

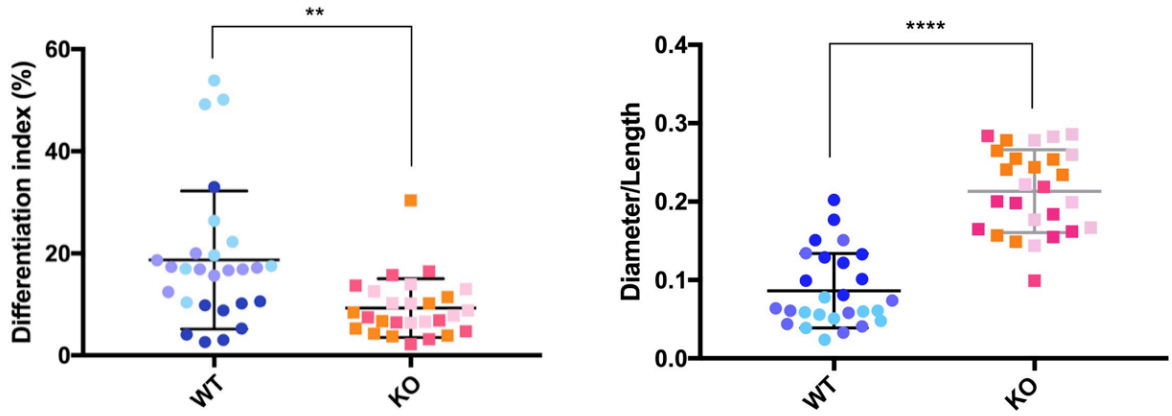

	WT	KO
Mean ± SEM	18,72 ± 2,611	9,281 ± 1,109

	WT	KO
Mean ± SEM	0,086 ± 0,009	0,213 ± 0,014

Figure 27 Scatter dot plot of differentiation index (left) and ratio of diameter/length (right) in *Trim32* KO and WT clones. Differentiation index was measured as the percentage of the nuclei number in MHC+ myotubes relative to the total nuclei number. The measurement of myotube is described in Materials and methods. Tables below the graphs display the mean and SEM (Standard Error of the Mean). Mean ± SEM, n=3, $^{**}p < 0{,}005$, $^{****}p < 0{,}0001$.

Moreover, the change of MHC level during differentiation revealed by western blot also indicates a defect in myogenesis in KO cells. A pretty low level of MHC is detected at day 0 in all clones (**Figure 28**), consistent with the proliferating condition. Although we observed scattered small myotubes formation in WT at day 3 in immunofluorescence images, no difference in MHC is detected in WT and KO cells (**figure 28**), probably due to the low percentage of MHC-positive cells at this point. Consistent with the increased myotubes formation in WT, western blot reveals much higher expression of MHC in WT cells than KO after 8 days of differentiation (**Figure 28**).

The characterization of myotubes and MHC expression prove that inactivation of *Trim32* causes deficient myogenesis of C2C12 cells but does not entirely abolish myotubes formation.

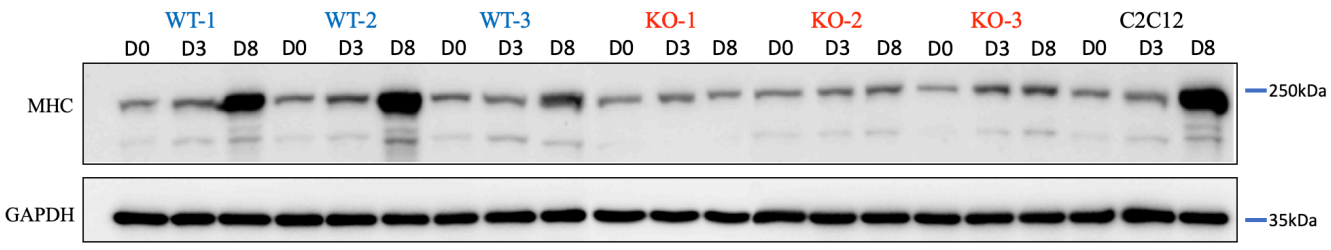

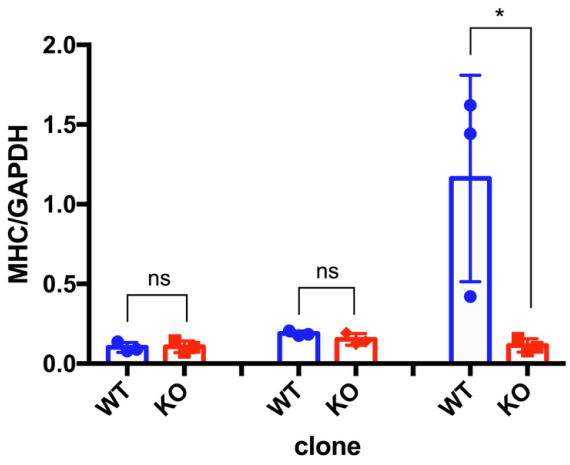

Figure 28 Representative Western Blot analysis of *Trim32* WT, KO, and parental C2C12 protein extracts under maintenance conditions (D0) as well as 3 (D3) and 8 (D8) days after the induction of myogenic differentiation analyzed with anti-MHC antibody. The graph below shows the quantification of MHC. 20 µg of protein extract was loaded, and GAPDH was detected as loading control (mean ± SEM; n=3; Unpaired T test; **P* < 0,05).

4. The knock-out of *Trim32* does not affect MyoD protein level

MyoD, also known as myoblast determination protein 1, heterodimerizes with bHLH E-proteins, recognizing and regulating myogenic bHLH target gene transcription. MyoD binding occurs before differentiation, which indicates that it plays an early myogenic regulation in myogenesis. Genetic deletion of *MyoD* in human myoblasts completely abolished the myogenesis potential, although MyoD null mice appeared normal and fertile and did not show any overt muscle phenotypes [164]. Probably *in vivo*, Myf5, MRF4, and other MRFs can efficiently compensate the differentiation potentials. Indeed, the MRFs collaborate in partially redundant transcriptional networks to regulate myoblast cell fate *in vivo*, but this effect is not always observed in cultured cells. In the myogenic process, MyoD starts to be expressed when the satellite cells are stimulated, and reaches a pick at the beginning of myocyte differentiation. Then, its expression gradually decreases with the maturation of myotubes. To investigate whether TRIM32 can affect master MRFs in the myogenic process, we analyzed MyoD protein expression.

Trim32 WT and KO proliferating cells show high expression of MyoD (Day 0), then it decreases with differentiation (**Figure 29**). However, no significant difference can be detected when comparing the MyoD level in WT and KO cells (**Figure 29**).

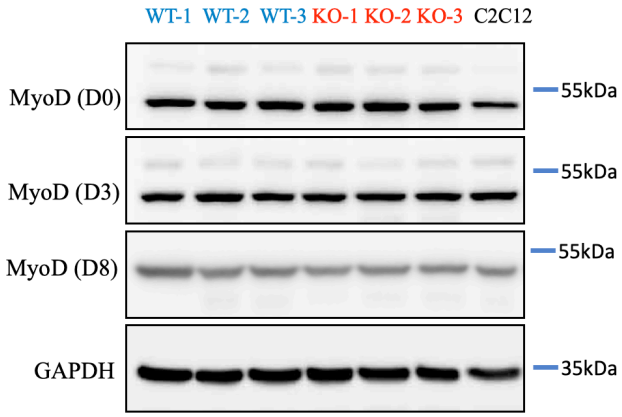

Figure 29 Representative Western Blot analysis of *Trim32* WT, KO, and parental C2C12 cells under maintenance conditions (D0) as well as 3 (D3) and 8 (D8) days after the induction of myogenic differentiation using anti-MyoD antibody. 20 µg of protein extract was loaded, and GAPDH was detected as loading control.

Immunofluorescence experiments also show the same percentage of MyoD-positive cells and localization of MyoD in both WT and KO cells at different time points (Day 0, 3, and 8) (**Figure 30**). At day 0, MyoD is detected also in the cytoplasm in all the genotypes and then by day 3 is only detected in the nucleus. To exclude the possible false positive caused by the antibody, we confirmed the result with two different commercial MyoD antibodies. The slight downregulation of MyoD transcript observed in *Trim32* KO clones (see above) is not present at the protein level. To accurately validate the difference at the RNA level, q-RT-PCR is further needed. Nevertheless, judging from the protein analysis, the defective differentiation in *Trim32* KO C2C12 clones is not caused by malfunction of MyoD.

As a critical regulator in myogenesis, the abundance of MyoD is a marker for muscle regeneration potential. A low level of MyoD is usually observed in aged skeletal muscle and muscle diseases. Unexpectedly, a similar MyoD level is detected in *Trim32* KO and WT cells, suggesting the limited effect of TRIM32 in the early stage of myogenesis, which is consistent with the low level of expression of TRIM32 in proliferating myoblasts reported in some work of literature. Since the deficient myogenesis in *Trim32* KO C2C12 cells is not due to MyoD, we further investigated its downstream signaling.

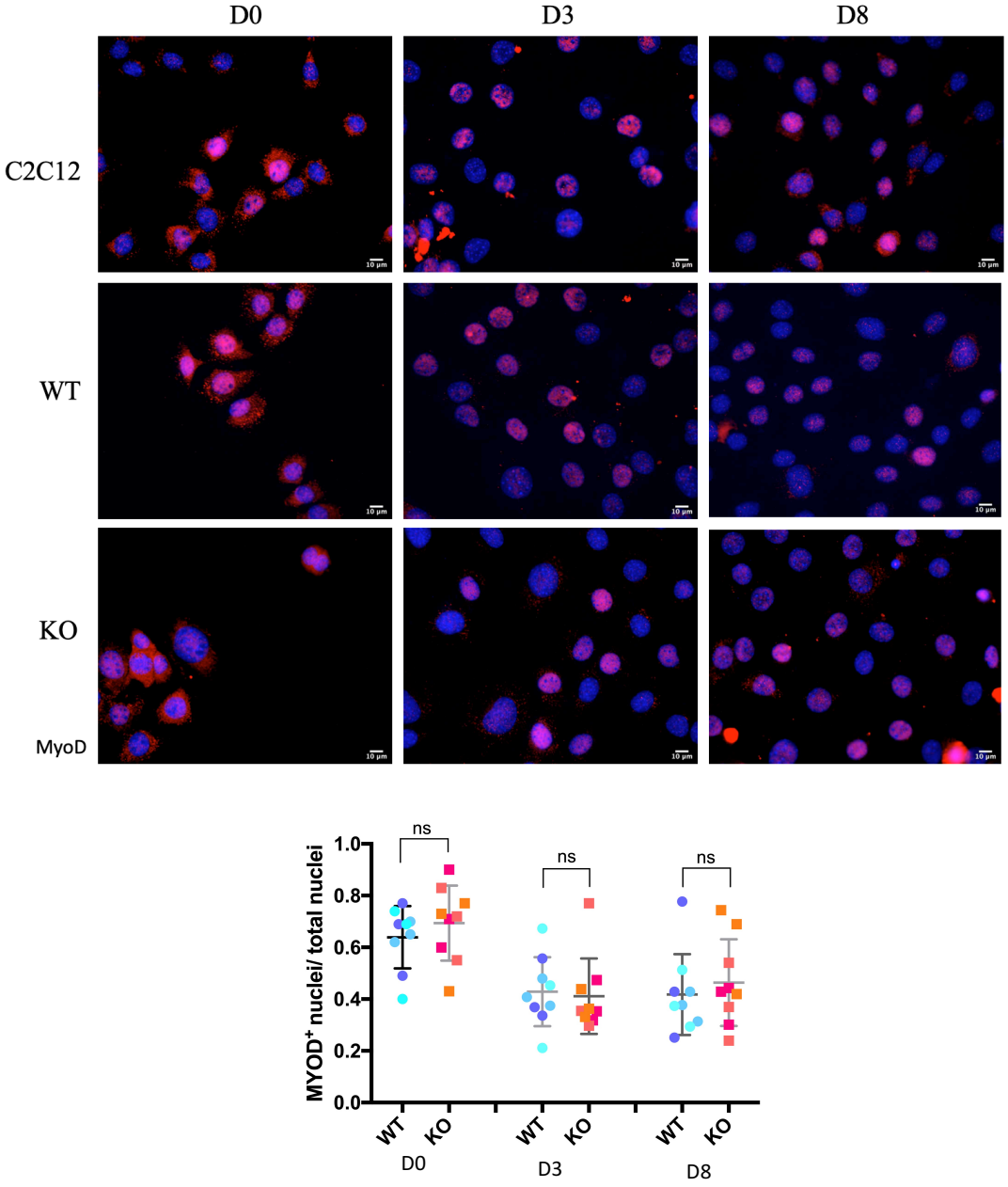

Figure 30 Analysis of MyoD cellular distribution under maintenance conditions (D0) as well as 3 and 8 days after the induction of myogenic differentiation in representative WT and KO clones, and in parental C2C12 cells. Nuclei were counterstained with DAPI (blue). (63x magnification; scale bar = 10 µm). The graph shows the percentage of MyoD positive nuclei: no significant difference is detected comparing WT and KO clones. (mean ± SEM; n = 3; unpaired t-test, 63x magnification; scale bar = 10 µm).

5. The knock-out of *Trim32* affects Myogenin protein level during differentiation

Myogenin (MyoG) is a downstream target of MyoD. MyoD synergistically cooperates with other co-activators, such as MEF2C and NFATc2/c3, at the Myogenin promoter to activate its expression. The overexpression of Myogenin in myoblasts can induce differentiation as well, but more than ten times less efficient than MyoD. Increased Myogenin during differentiation suggests its critical role at the advanced stage of differentiation.

We explored Myogenin levels in *Trim32* KO, WT, and C2C12 parental cells. As expected, Myogenin protein is only detected in western blot at day 8 (**Figure 31**) of differentiation but not before (Data not shown). This result is consistent with its role as the master regulator for the terminal differentiation. However, *Trim32* KO shows lower expression of Myogenin than *Trim32* WT and parental C2C12 cells at day 8 (**Figure 31**).

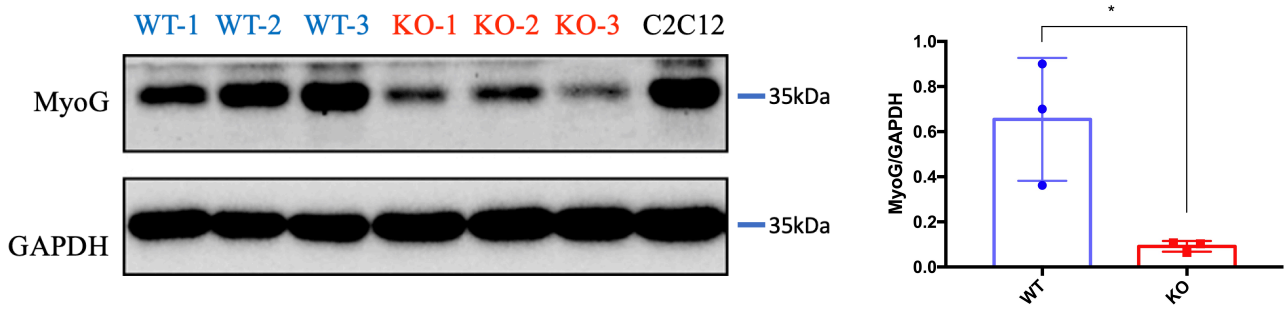

Figure 31 Representative Western Blot analysis of *Trim32* WT, KO, and parental C2C12 cells 8 days after the induction of myogenic differentiation using anti-MyoG antibody. Quantification shows a reduced level of Myogenin in *Trim32* KO C2C12 cells at Day 8. 20 µg of protein extract was loaded and GAPDH was detected as loading control (mean ± SEM; n=3; Unpaired T test, **P*<0,05).

Consistently, immunofluorescence images show an increase of Myogenin during differentiation in *Trim32* KO, WT, and C2C12 parental cells, even though in *Trim32* KO it was much reduced (**Figure 32a**). Notably, in *Trim32* WT and parental C2C12 myotubes at day 8, a relatively high level of Myogenin is present, but almost no Myogenin can be detected in the abnormal myotubes in all the *Trim32* KO clones (**Figure 32b**).

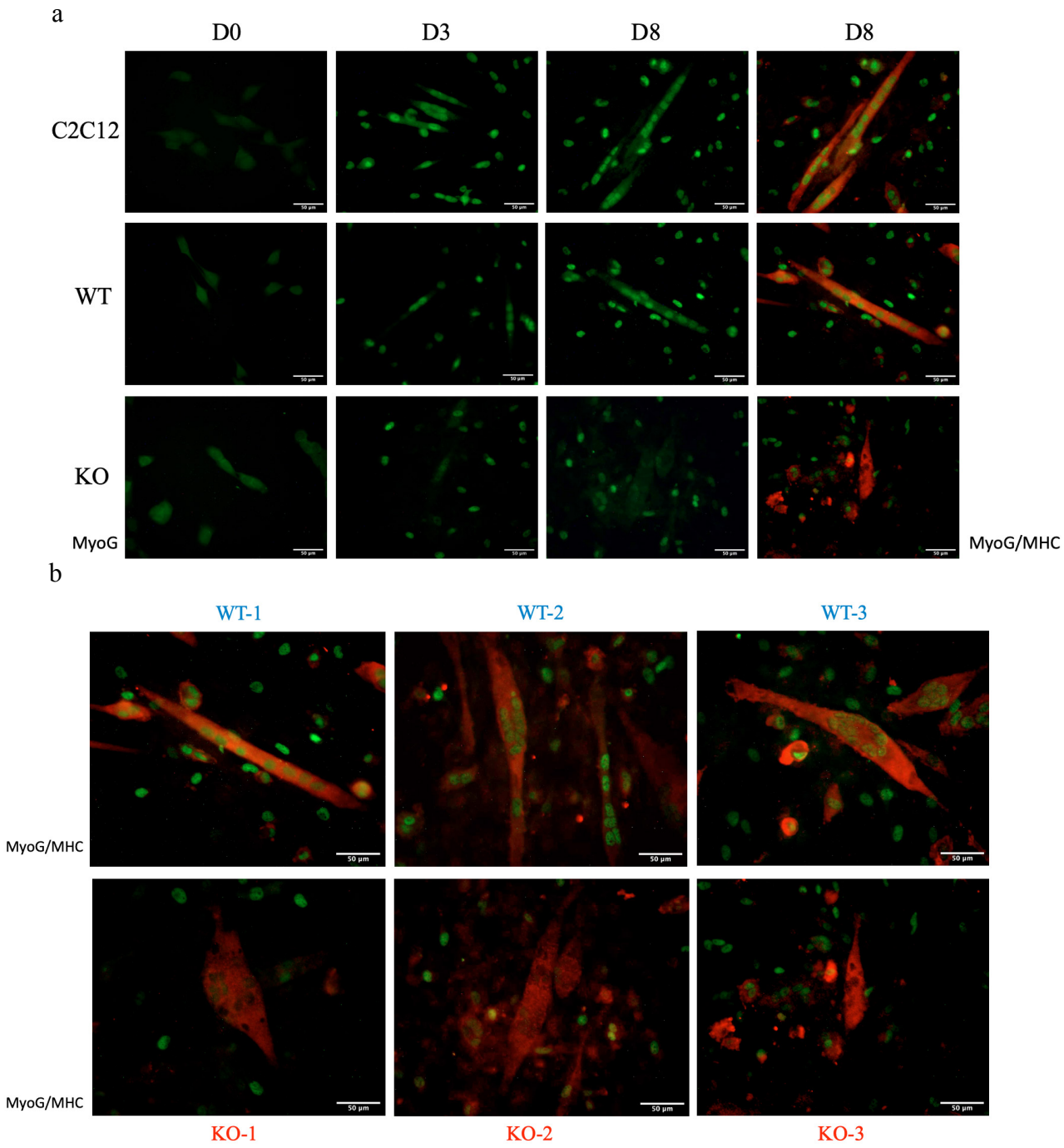

Figure 32 Myogenin immunofluorescence under maintenance conditions (D0) as well as 3 (D3) and 8(D8) days after the induction of myogenic differentiation. Myosin heavy chain III (MHC III) is used as a marker of differentiation. Immunofluorescence shows Myogenin (green) in the nuclei and MHC III (red) in the cytoplasm. a. images of representative *Trim32* KO and WT clones, and C2C12 parental cells taken at day 0, 3, and 8 of differentiation. b. Analysis of Myogenin expression 8 days after the induction of myogenic differentiation in the three *Trim32* KO and WT clones. 40x magnification; scale bar = 50 µm.

The low level of Myogenin in *Trim32* KO cells highlights that TRIM32 eventually affects the advanced stage of differentiation. Myogenin work as a surrogate of MyoD to continually sustain muscle fusion that boosts the sizes of myotubes at the later stage when MyoD expression declines. Therefore, the low level of Myogenin expression, particularly in *Trim32* KO myotubes, blocks the nascent myotubes hypertrophy and maturation, resulting in small Myotubes. Unlike the complete loss of ability to differentiate in *MyoD* KO myoblasts, the knock-out of *Myogenin* in human myoblasts displayed relatively moderate defects in the myogenic process, such as a low differentiation index and low fusion index. Further, the Myogenin-null mice keep a limiting ability to generate a few differentiated myofibers [172,264,265]. According to these findings, the fewer and abnormal *Trim32* KO myotubes might be the result of the decreased Myogenin observed.

Based on the MyoD and Myogenin analysis in the *Trim32* KO cells, TRIM32 does not affect myogenic specification but regulates myogenic differentiation. Previous research revealed that although MyoD controls Myogenin expression, many other molecules are involved in this process. In this scenario, TRIM32 likely reduces Myogenin through pathways downstream or parallel to MyoD.

6. The knock-out of *Trim32* increases c-Myc level

We then sought to demonstrate how TRIM32 affects Myogenin in differentiation. Previous research has shown that the c-Myc can antagonize MyoD and thus impede the activation of Myogenin expression. [242,243] c-Myc is a proto-oncogene that regulates cell proliferation in many cell lines, including C2C12 myoblasts. A sustained expression of c-Myc in C2C12 myoblasts halts differentiation and myotubes formation. Indeed, we observed reduced c-Myc levels in C2C12 myoblasts within 36 hours of differentiation (**Figure 33**).

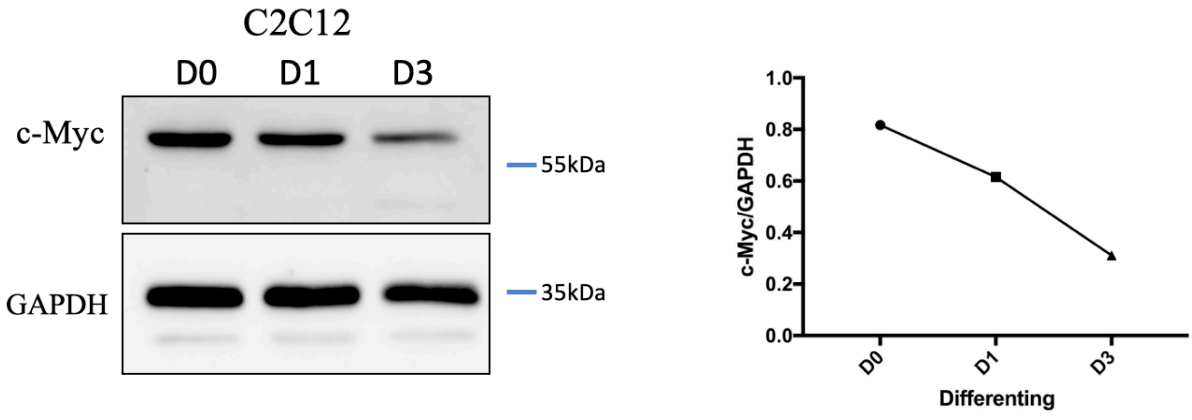

Figure 33 Western Blot analysis of c-Myc level in parental C2C12 cells under maintenance conditions (D0) as well as 1 (D3) day and 3 (D8) days of differentiating. Quantification of c-Myc level shows gradually reduced level upon differentiation. 20 µg of protein extract was loaded and GAPDH was detected as loading control.

On the other hand, TRIM32 was reported to regulate c-Myc levels in both neural progenitor cells and myoblasts, probably through ubiquitination and targeting c-Myc to degradation although these data are still unclear. Therefore, we asked whether the knock-out of *Trim32* increases c-Myc level in C2C12 cells. We analyzed c-Myc level in *Trim32* KO, WT, and C2C12 parental cells during differentiation by western blot. Unlike similar c-Myc levels detected at day 0 and day 8 in KO and WT cells, a slight but statistically significant higher level of c-Myc is observed at day 3 in KO clones compared with WT (**Figure 34**).

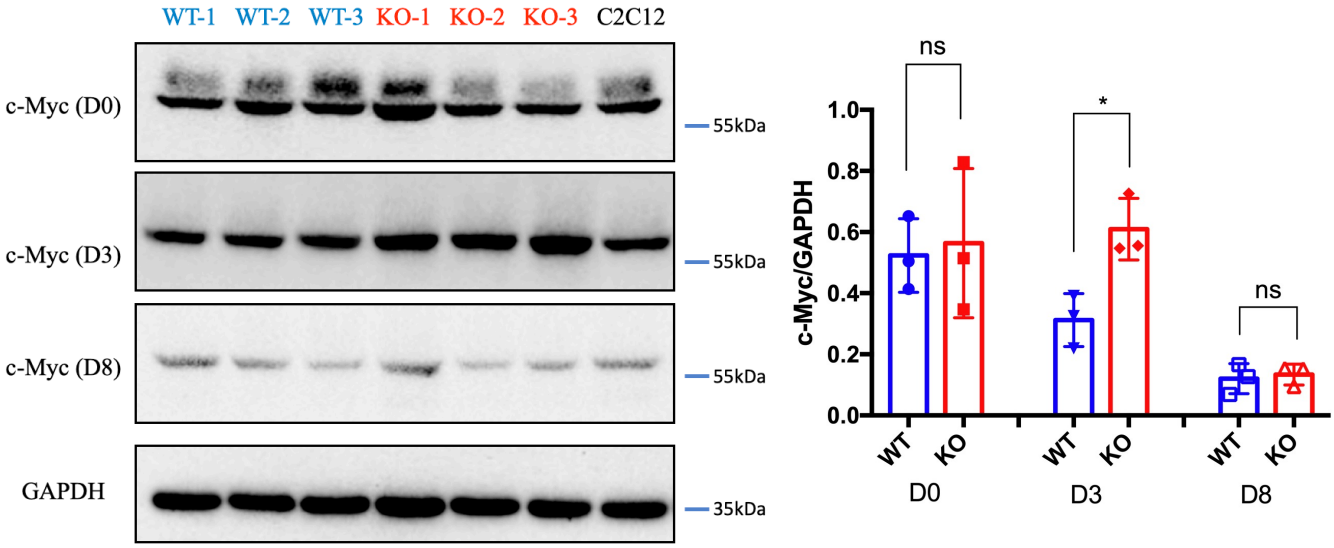

Figure 34 Representative Western Blot analysis of c-Myc in *Trim32* KO and WT C2C12 cells at different time points of differentiating (D0, D3, and D8). Quantification shows a higher level of c-Myc in KO cells compared with WT at Day 3. 20 µg of protein extract was loaded and GAPDH was detected as loading control. (mean ± SEM; n=3; Unpaired T test, **P*<0,05).

In order to further support that the above-described regulation of c-Myc at day 3 of differentiation is regulated by TRIM32, we overexpressed full-length TRIM32 and a truncated TRIM32 lacking RING domain, therefore catalytically inactive, in Hela cells by transfecting GFP-TRIM32 and GFP-ΔRING-TRIM32 plasmids (**Figure 35**). The empty vector is transfected as a control showing no effect on the endogenous c-Myc level. In line with previous reports, overexpression of TRIM32 downregulates endogenous c-Myc level in a dose-dependent manner. Most importantly, the overexpression of TRIM32 lacking the RING domain does not affect endogenous c-Myc level compared with control,

suggesting that the E3 ligase activity of TRIM32 is necessary for regulating endogenous c-Myc level in Hela cells (**Figure 35**).

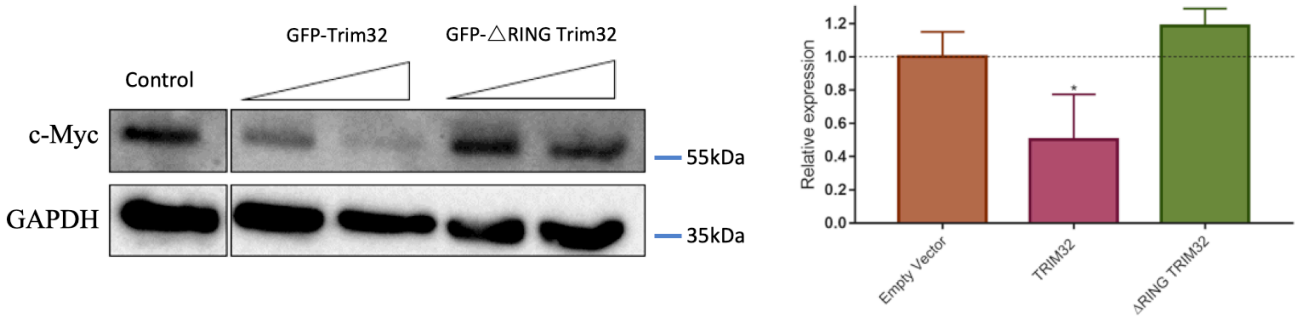

Figure 35 HeLa cells were transfected with 2.5µg or 5µg of GFP-TRIM32 or GFP-ΔRING TRIM32 plasmids. Control was transfected with 2.5µg of empty vector. Representative Western Blot assay of the endogenous c-Myc levels and GAPDH control. Quantification of at least three assays for each condition (n=3) using densitometry analysis with the Image Lab software. For relative protein, expression results are shown as the ratio between c-Myc and GAPDH. Statistical analysis was performed by a student's t-test $*P < 0{,}05$.

Given our data and that c-Myc has been described as a possible substrate of TRIM32, we first examined the role of proteasome in c-Myc degradation in C2C12 cells. MG132 is a proteasome inhibitor and when applying it to parental C2C12 and WT cells at day 3 of differentiation, a significant accumulation of c-Myc is detected (**Figure 36a**). In these exposures c-Myc is not even detectable at 0 hour (vehicle treatment) (**Figure 36a**). This result indicated that c-Myc is degraded through proteasome system in C2C12 and WT cells at day 3 of differentiation.

Subsequently, the combination treatment of cycloheximide (protein synthesis inhibitor) and MG132 was further assayed. As we expect, the treatment of cycloheximide and MG132 does not show different effects in *Trim32* WT and KO cells at day 0 and day 8 (**Figure 36b**).

At day 3, as a protein synthesis inhibitor, cycloheximide efficiently inhibits c-Myc protein levels in WT but not in KO clones, indicating higher stability of the c-Myc protein in KO clones (**Figure 36b, lanes 1 and 5**). The downregulation of c-Myc level in WT clones can be partially rescued by MG132 in the WT clone (**Figure 36b, lanes 1 and 3**).

Interestingly, the treatment of MG132 alone can significantly increase c-Myc level compared with vehicle treatment (**Figure 36b, lanes 6 and 8**) in the KO clone at day 3, indicating a proteasome-

dependent degradation of c-Myc also in KO clones. However, when we treated the KO clones with MG132 upon cycloheximide at day 3, MG132 failed to increase the c-Myc level (**Figure 39b, lanes 5 and 7**), suggesting that proteasome does not involve in c-Myc degradation in this condition. These two conflicting results lead the mechanism of c-Myc turnover in *Trim32* KO cells more elusive.

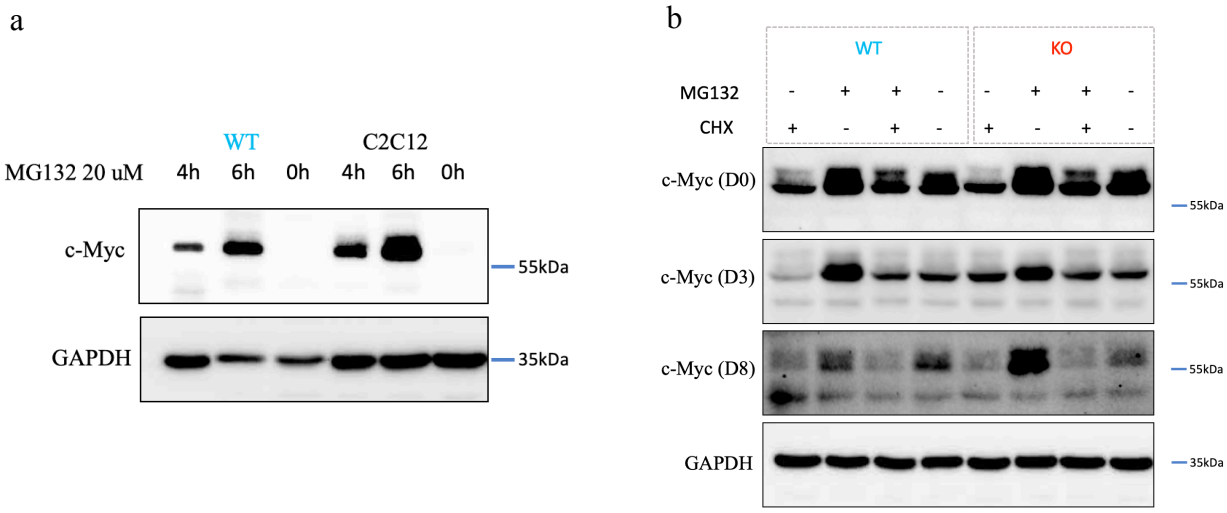

Figure 36 Representative Western Blot analysis of c-Myc level in *Trim32* WT, KO and parental C2C12 cells. a. At day 3 of differentiation, myoblasts are treated with proteasome inhibitor MG132 (20 uM in DM) for 0, 4 and 6 hours. b. Under maintenance condition (day 0), and day 3, day 8 of differentiation, cells are treated with cycloheximide (CHX, protein synthesis inhibitor, 50 ug/mL), MG132 (20 uM), and the combination of CHX and MG132 in GM (day 0) and DM (day 3 and day8). 20 µg of protein extract was loaded and GAPDH was detected as loading control.

The investigation of the mechanism that TRIM32 regulates c-Myc is still in progress. Apart from the high possibility of mediating c-Myc degradation, we cannot exclude that TRIM32 might also regulate c-Myc production through an unknown mechanism. It will be interesting to investigate more in-depth the molecular mechanisms of TRIM32-mediated c-Myc regulation and whether the phosphorylation of c-Myc is a prerequisite for its ubiquitination.

To date, two E3 ligase enzymes have been well characterized to mediate c-Myc ubiquitination [266]. The F-box protein Skp2 targets c-Myc for ubiquitination by binding to the MB2 domain of c-Myc, inducing c-Myc degradation. Interestingly, Skp2 also serves as a transcriptional coactivator for c-Myc, enhancing c-Myc transactivation for target genes. Skp2 is a two-face ligase that increases the degradation of c-Myc, but the other side of the coin is improving the activity of c-Myc. A similar

mode of action has also been found in many Ub ligases [267]. Whether TRIM32 can function as a regulator of c-Myc expression or activity requires further investigation.

The other F-box protein, Fbw7, is proved to mediate c-Myc ubiquitination and degradation dependent on the phosphorylation of Thr-58 and Ser-62 in the MB1 domain. This pattern of degradation induced by Fbw7 is very important because mutations in Thr-58 and Ser-62 are frequently found in tumors [268]. Phosphorylation of Ser-62 is mediated by the Ras–ERK pathway and is a pre-requirement for phosphorylation of Thr-58, mediated by glycogen synthase kinase 3 (GSK3). GSK3 is a well-known substrate of AKT. It has been heavily studied that phosphorylation by AKT inhibits GSK3 activity via the formation of an auto-inhibitory pseudosubstrate sequence [269].

The network analysis based on DEGs from RNAseq of *Trim32* WT and KO clones at day 3 reveals a network of molecules regulated by AKT. AKT, also known as protein kinase B, is activated by phosphorylation mediated by PI3K. TRIM32 has been reported to reduce PI3K-Akt-FoxO signaling in muscle atrophy by promoting plakoglobin-PI3K dissociation. TRIM32 may promote GSK3 phosphorylating c-Myc by regulating PI3K-AKT-GSK3 axis. To determine TRIM32's effect on AKT activity, we are analyzing the phosphorylation of AKT at Thr-308 and Ser-473 residues and the phosphorylation of GSK3 in *Trim32* WT and KO cells (work in progress).

7. The knock-out of *Trim32* affects C2C12 proliferation

c-Myc activates a diverse group of genes involved in various cellular physiological pathways, and many of them strongly correlate with cell proliferation. Indeed, the analysis of RNAseq reveals the activation of cell cycle-related signaling pathways in *Trim32* KO cells at Day 3, suggesting an impairment in properly exiting cell cycle of *Trim32* KO cells at day 3. In order to check cell proliferation, we examined Phospho-histone H3 Ser10 (pHH3) by immunofluorescence under maintenance conditions (Day 0) and 3 days after induction of differentiation. pHH3 is a protein phosphorylated during chromatin condensation in mitosis, and thus the level of pHH3 can be used to assess mitotic activity. At day 0, the statistical analysis shows the same percentage of pHH3 positive myoblasts in *Trim32* KO and WT C2C12 cells (**Figure 37**), indicating the same mitotic rate under maintenance conditions. The induction of differentiation slows down proliferation in both *Trim32* KO WT C2C12 cells because the percentage of pHH3 myoblasts decreases from day 0 to day 3 (2.8 % *vs* 0.2 % in *Trim32* WT; 2.2 % *vs* 0.4% in *Trim32* KO). However, at day 3, a significantly higher percentage of pHH3 positive myoblasts in *Trim32* KO than WT is observed (**Figure 37**), indicating a higher proliferation rate in *Trim32* KO cells.

These data in *Trim32* KO myoblasts indicates that KO cells are less efficient in withdrawing from the cell cycle and initiating differentiation. On the other hand, the higher proliferation of *Trim32* KO at day 3 is likely related to the high stability or synthesis of c-Myc.

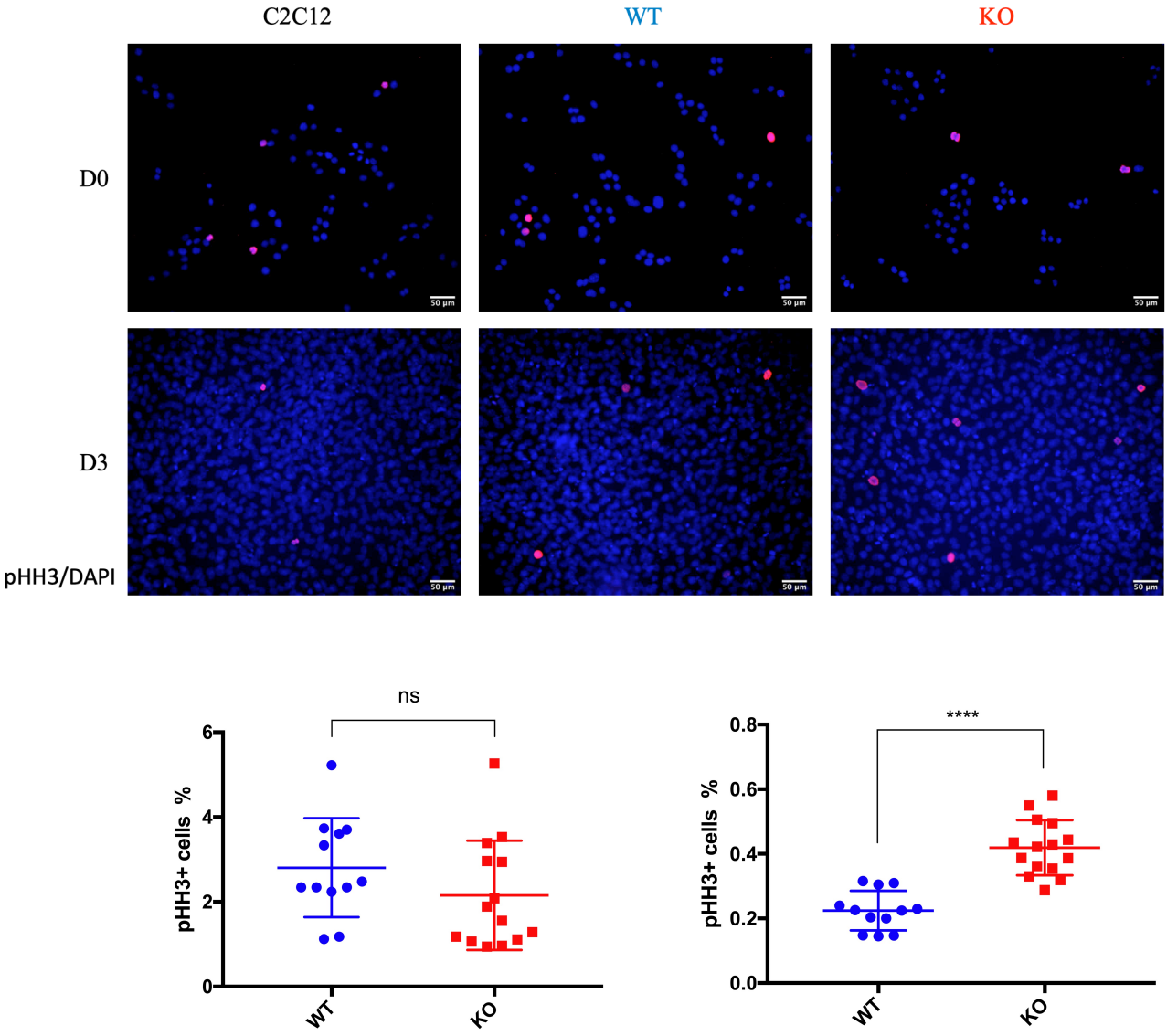

Figure 37 Analysis of C2C12 mitotic rate under maintenance conditions (D0) and 3 days (D3) after the induction of myogenic differentiation using Phospho-histone H3 (red) as a marker of cells in S-phase. Nuclei were counterstained with DAPI (blue). Quantification of pHH3 myoblasts revealed a progressive decrease in the percentage of proliferating myoblasts at Day 3. No significant difference in the percentage of Phh3 positive cells in *Trim32* WT and KO clones can be detected at Day 0. A higher percentage of proliferating myoblasts in *Trim32* KO compared with WT is observed at D3. (mean ± SEM; unpaired t-test, ****P<0,0001, n = 3, 20x magnification, Scale bar, 50 µm).

Although *Trim32*-dificient C2C12 cells show a comparable level of MyoD with the WT clones, the significant downregulated Myogenin results in the impaired terminal differentiation, which is determined by the lower MHC level and abnormal myotubes generation. The activation of MyoD is the key step of myogenic lineage and the start of myogenic program. However, MyoD is not necessary for the muscle development. The MyoD gene targeted mice express Myogenin, and are able to generate muscle tissue. This could benefit from the overlapping function of MyoD and Myf5 *in vivo* as we discussed in the introduction. As a downstream target of MyoD and Myf5, Myogenin is necessary for muscle development and regeneration, controlling the terminal differentiation of myoblasts. The knock-out of Myogenin suppresses muscle development and prevents muscle regeneration *in vivo.* Therefore, the decreased Myogenin caused by the knock-out of *Trim32* strongly suggests an impaired muscle regeneration in LGMDR8 patients.

Based on our results, TRIM32 shows a limited effect to the first stage of muscle regeneration. In the proliferating condition, *Trim32* KO and WT clones are more homogeneous, including same proliferating rate, same MyoD expression, and comparable transcriptome pattern. However, with the myogenesis progresses, TRIM32 KO clones show an impaired differentiation, represented as insufficient Myogenin and higher mitotic activity. These data indicate the critical role of TRIM32 in the second stage of muscle regeneration. We observed a sharply decreased c-Myc in C2C12 from proliferating to differentiating, and likely TRIM32 contributes to this process. At the beginning of second stage of muscle regeneration, the normal myoblasts exit from cell-cycle, and continue myogenic differentiation with Myogenin upregulation, whereas in the pathologic TRIM32-deficient muscle, the accumulation of c-Myc prevent myoblasts from appropriate cell-cycle withdrawal, thus these cells are unable to express Myogenin, and eventually failed to form new myofibers. Another possible explanation is that the ability of MyoD to activate Myogenin expression is countered by c-Myc, a funding that is supported by a literature report describing that ectopically expressed c-Myc inhibits Myogenin bypassing MyoD [243].

CONCLUSIONS

Mutations in *TRIM32* are the genetic cause of LGMDR8 disease, but the underlying pathogenic mechanism is still unknown. The early studies were focused on the role of TRIM32 in muscle atrophy. However, the low expression of TRIM32 during muscle atrophy *in vivo* indicates a minimal effect of TRIM32 in this process. In recent years, increasing evidence highlighted TRIM32 functions predominantly in muscle regeneration. Different mutations and full-deletion of *TRIM32* have been discovered in LGMDR8 patients. Most of the missense mutations cluster in the NHL domain, which could disturb TRIM32 self-association and substrate binding. The *TRIM32* NHL domain mutants could significantly impact the ability to form homo-oligomers, and thus they may be degraded rapidly in cytoplasm. We speculate that in patients either carrying full-deletion of *TRIM32* or a short truncated TRIM32, the function of TRIM32 is abolished. For patients carrying the other mutations in *TRIM32*, because of inability of self-associate of these variants, can be highly unstable *in vivo*. In this scenario, TRIM32 mutated proteins probably low or no activity *in vivo*.

In this project, we generated *Trim32* knock-out and wild-type immortalized mouse myoblast C2C12 cells. Using these C2C12 clones as a research model, we further explored the role of TRIM32 in the myogenic program and the possible molecular mechanism underlying LGMDR8. Some published works point to an increase of TRIM32 during myogenic differentiation (data not shown). However, we clearly observed a stable level in C2C12 parental and *Trim32* WT cells in our experiments. The loss function of TRIM32 in KO cells results in a deficiency but not in a completely abolished myogenic program, based on the characterization of myotubes formation and myosin heavy chain expression. This result indicates the critical role of TRIM32 in myoblast differentiation.

The RNA of myogenic regulatory factors (MRFs) in *Trim32* KO cells started to show a significantly decreased level compared with WT at day 3 of differentiation, indicating the impairment of differentiation. Of the main MRFs, MyoD, a master regulator in the early stage of myogenesis, does not show any difference in *Trim32* KO and WT. On the other hand, we found a significant decrease of Myogenin in *Trim32* KO cells, particularly in *Trim32* KO myotubes, compared with WT cells at day 8 of differentiation. Myogenin expression is regulated by MyoD and mainly functions in the late stage of differentiation. Other works of literature point out that the loss function of Myogenin causes the formation of small myofibril, which is consistent with the result obtained in our experiments. It has been reported that the over-expression of Myogenin can also affect metabolic enzymes *in vivo*, with levels of oxidative enzymes increased and glycolytic enzymes decreased. The change from anaerobic respiration to aerobic metabolism may indicate the switch from type II myofibril to type I

myofibril. [270] Whether this switch exists in *Trim32* KO myotubes can be further analyzed by detecting myosin heavy chain 7 (a representative MHC for type 1 myofibril). The decrease of Myogenin in KO cells can be caused by the downregulation of its synthesis or increased degradation, and this will be determined in future experiments.

In addition, we found that c-Myc, which has been reported to inhibit MyoD transactivation of Myogenin, is slightly but statically increased in *Trim32* KO cells at day 3 compared with WT clones. Interestingly, this difference in c-Myc level is not detected at day 0 and day 8. Therefore, we hypothesis that TRIM32 might regulate c-Myc level at the beginning of myogenic differentiation when c-Myc needs to be degraded to allow the onset of differentiation. Our results indicate that TRIM32 regulates c-Myc proteasome-dependent degradation. The exogenously overexpressed TRIM32 in Hela cells can reduce the endogenous c-Myc level in a dose-dependent manner. Two possible pathways are envisaged: 1. TRIM32 mediates ubiquitination of c-Myc directly and targets degradation. Our preliminary Co-IP did not show a direct interaction of TRIM32 and c-Myc although this may occur transiently. 2. TRIM32 regulates c-Myc level through other signaling pathways. It will be interesting to investigate how TRIM32 controls c-Myc level and which condition is changed between day 0 (no effect on c-Myc) and day 3 when the difference in c-Myc level is observed. In this scenario, we speculate that TRIM32 may affect c-Myc phosphorylation by regulating GS3K activity, with the phosphorylation of c-Myc may be a pre-requirement for its degradation as it is reported for the c-Myc E3 ligase Fbw7. More investigation is needed to clarify the connection between TRIM32 and c-Myc.

Although Skp2 and Fbw7 are assessed E3 ligase of c-Myc, we don't know the connection between these enzymes and TRIM32, and whether an overlapping effect on c-Myc exists or if they work in different phases or different cell types. This point is critical because Skp2 is mainly expressed in S phase, and Fbw7 is expressed throughout the cell cycle. Likely, the two E3 ligases induce c-Myc degradation predominantly in the highly proliferating cells, such as tumors and proliferating myoblasts. However, C2C12 is an immortalized cell line that not only proliferates but also differentiates in the proper condition. Based on our result, we can suggest that TRIM32 is another E3 ligase of c-Myc mainly functioning in differentiating C2C12 cells.

c-Myc is a well-described proto-oncogene that promotes cell proliferation. We found a higher Phospho-histone H3 level in *Trim32* KO cells compared with WT at day 3, indicating higher rate of proliferation, which could be due to the higher level of c-Myc in KO cells. This result suggests high

mitotic index and possible a block of cell transition to differentiation in *Trim32* KO cells. The downstream targets of c-Myc, such as CDK4 and CCND2, need to be assessed to confirm this hypothesis. Besides, the c-Myc function loss and gain experiments can further help us to understand the role of c-Myc in the proliferation and differentiation of C2C12 myoblasts. However, so far, we failed to exogenously overexpress c-Myc at day 3 of differentiation. As c-Myc usually is active as part of a heterodimeric complex with its partner protein, MAX, we also try to inhibit c-Myc activity in *Trim32* KO cells by treating with 10058-F4, a small molecule blocking c-Myc and MAX association [271]. But the myogenic process is subtly regulated, and the window and expression level of each molecule working in this process, including c-Myc, is tightly controlled. Improper order and over or insufficient expression can damage or even abolish the myogenic process. Therefore, we must first explore the optimal administration time and dose of the treatment.

The results presented in this thesis work open to further research on two aspects. One is to investigate further the molecular mechanism of TRIM32 regulating c-Myc in myogenic program along two working hypotheses: 1) c-Myc is a substrate of TRIM32. TRIM32 can induce c-myc degradation in a ubiquitin-dependent way; 2) TRIM32 regulate c-Myc degradation through other pathways, for example AKT-GSK3β-c-Myc pathways. On the other hand, to dissect in depth the effect of TRIM32-c-Myc axis on myogenic program, particularly testing whether *Trim32* KO clones can regain myogenic ability by either re-introducing TRIM32 or suppressing c-Myc. In the long-term, it will be interesting to translate our cell system findings (for example TRIM32-c-Myc) in LGMDR8 animal model, which will provide more support for the further therapy development.

In summary, we demonstrate the impaired but not collapsed myogenic program in *Trim32* knock-out C2C12 myoblasts, highlighting possible stages during differentiation when TRIM32 can be relevant. These data are an important basis for future work to address the pathogenesis of LGMDR8.

ACKNOWLEDGEMENTS

This work has received funding from the European Union's Horizon 2020 research and Innovation Program under the Marie Sklodowska-Curie grant agreement 813599.

REFERENCES

1. WALTON, J.N.; NATTRASS, F.J. ON THE CLASSIFICATION, NATURAL HISTORY AND TREATMENT OF THE MYOPATHIES. *Brain* **1954**, *77*, 169-231.
2. Iyadurai, S.J.; Kissel, J.T. The Limb-Girdle Muscular Dystrophies and the Dystrophinopathies. *Continuum (Minneapolis, Minn.)* **2016**, *22*, 1954-1977.
3. Angelini, C. LGMD. Identification, description and classification. *Acta myologica : myopathies and cardiomyopathies : official journal of the Mediterranean Society of Myology* **2020**, *39*, 207-217.
4. Georganopoulou, D.G.; Moisiadis, V.G.; Malik, F.A.; Mohajer, A.; Dashevsky, T.M.; Wuu, S.T.; Hu, C.K. A Journey with LGMD: From Protein Abnormalities to Patient Impact. *The protein journal* **2021**, *40*, 466-488.
5. Nigro, V.; Savarese, M. Genetic basis of limb-girdle muscular dystrophies: the 2014 update. *Acta myologica : myopathies and cardiomyopathies : official journal of the Mediterranean Society of Myology* **2014**, *33*, 1-12.
6. Straub, V.; Murphy, A.; Udd, B. 229th ENMC international workshop: Limb girdle muscular dystrophies - Nomenclature and reformed classification Naarden, the Netherlands, 17-19 March 2017. *Neuromuscular disorders : NMD* **2018**, *28*, 702-710.
7. Weiler, T.; Greenberg, C.R.; Nylen, E.; Morgan, K.; Fujiwara, T.M.; Crumley, M.J.; Zelinski, T.; Halliday, W.; Nickel, B.; Triggs-Raine, B.; et al. Limb girdle muscular dystrophy in Manitoba Hutterites does not map to any of the known LGMD loci. *American journal of medical genetics* **1997**, *72*, 363-368.
8. Frosk, P.; Weiler, T.; Nylen, E.; Sudha, T.; Greenberg, C.R.; Morgan, K.; Fujiwara, T.M.; Wrogemann, K. Limb-girdle muscular dystrophy type 2H associated with mutation in TRIM32, a putative E3-ubiquitin-ligase gene. *American journal of human genetics* **2002**, *70*, 663-672.
9. Weiler, T.; Greenberg, C.R.; Zelinski, T.; Nylen, E.; Coghlan, G.; Crumley, M.J.; Fujiwara, T.M.; Morgan, K.; Wrogemann, K. A gene for autosomal recessive limb-girdle muscular dystrophy in Manitoba Hutterites maps to chromosome region 9q31-q33: evidence for another limb-girdle muscular dystrophy locus. *American journal of human genetics* **1998**, *63*, 140-147.
10. Shieh, P.B.; Kudryashova, E.; Spencer, M.J. Limb-girdle muscular dystrophy 2H and the role of TRIM32. *Handbook of clinical neurology* **2011**, *101*, 125-133.
11. Mathews, K.D.; Moore, S.A. Limb-girdle muscular dystrophy. *Current neurology and neuroscience reports* **2003**, *3*, 78-85.
12. Wei, X.J.; Miao, J.; Kang, Z.X.; Gao, Y.L.; Wang, Z.Y.; Yu, X.F. A novel homozygous exon2 deletion of TRIM32 gene in a Chinese patient with sarcotubular myopathy: A case report and literature review. *Bosnian journal of basic medical sciences* **2021**, *21*, 495-500.
13. Johnson, K.; De Ridder, W.; Töpf, A.; Bertoli, M.; Phillips, L.; De Jonghe, P.; Baets, J.; Deconinck, T.; Rakocevic Stojanovic, V.; Perić, S.; et al. Extending the clinical and mutational spectrum of TRIM32-related myopathies in a non-Hutterite population. *Journal of neurology, neurosurgery, and psychiatry* **2019**, *90*, 490-493.
14. Ten Dam, L.; de Visser, M.; Ginjaar, I.B.; van Duyvenvoorde, H.A.; van Koningsbruggen, S.; van der Kooi, A.J. Elucidation of the Genetic Cause in Dutch Limb Girdle Muscular Dystrophy Families: A 27-Year's Journey. *Journal of neuromuscular diseases* **2021**, *8*, 261-272.
15. Nigro, V.; Aurino, S.; Piluso, G. Limb girdle muscular dystrophies: update on genetic diagnosis and therapeutic approaches. *Current opinion in neurology* **2011**, *24*, 429-436.
16. Krahn, M.; Borges, A.; Navarro, C.; Schuit, R.; Stojkovic, T.; Torrente, Y.; Wein, N.; Pécheux, C.; Lévy, N. Identification of different genomic deletions and one duplication in the dysferlin

gene using multiplex ligation-dependent probe amplification and genomic quantitative PCR. *Genetic testing and molecular biomarkers* **2009**, *13*, 439-442.
17. Papić, L.; Fischer, D.; Trajanoski, S.; Höftberger, R.; Fischer, C.; Ströbel, T.; Schmidt, W.M.; Bittner, R.E.; Schabhüttl, M.; Gruber, K.; et al. SNP-array based whole genome homozygosity mapping: a quick and powerful tool to achieve an accurate diagnosis in LGMD2 patients. *European journal of medical genetics* **2011**, *54*, 214-219.
18. Boyden, S.E.; Salih, M.A.; Duncan, A.R.; White, A.J.; Estrella, E.A.; Burgess, S.L.; Seidahmed, M.Z.; Al-Jarallah, A.S.; Alkhalidi, H.M.; Al-Maneea, W.M.; et al. Efficient identification of novel mutations in patients with limb girdle muscular dystrophy. *Neurogenetics* **2010**, *11*, 449-455.
19. Bockhorst, J.; Wicklund, M. Limb Girdle Muscular Dystrophies. *Neurologic clinics* **2020**, *38*, 493-504.
20. Forsting, J.; Rohm, M.; Froeling, M.; Güttsches, A.K.; Südkamp, N.; Roos, A.; Vorgerd, M.; Schlaffke, L.; Rehmann, R. Quantitative muscle MRI captures early muscle degeneration in calpainopathy. *Scientific reports* **2022**, *12*, 19676.
21. Nalini, A.; Polavarapu, K.; Sunitha, B.; Kulkarni, S.; Gayathri, N.; Srinivas Bharath, M.M.; Modi, S.; Preethish-Kumar, V. A prospective study on the immunophenotypic characterization of limb girdle muscular dystrophies 2 in India. *Neurology India* **2015**, *63*, 548-560.
22. Narayanaswami, P.; Weiss, M.; Selcen, D.; David, W.; Raynor, E.; Carter, G.; Wicklund, M.; Barohn, R.J.; Ensrud, E.; Griggs, R.C.; et al. Evidence-based guideline summary: diagnosis and treatment of limb-girdle and distal dystrophies: report of the guideline development subcommittee of the American Academy of Neurology and the practice issues review panel of the American Association of Neuromuscular & Electrodiagnostic Medicine. *Neurology* **2014**, *83*, 1453-1463.
23. Liewluck, T.; Tracy, J.A.; Sorenson, E.J.; Engel, A.G. Scapuloperoneal muscular dystrophy phenotype due to TRIM32-sarcotubular myopathy in South Dakota Hutterite. *Neuromuscular disorders : NMD* **2013**, *23*, 133-138.
24. Kumarasinghe, L.; Xiong, L.; Garcia-Gimeno, M.A.; Lazzari, E.; Sanz, P.; Meroni, G. TRIM32 and Malin in Neurological and Neuromuscular Rare Diseases. *Cells* **2021**, *10*.
25. Schoser, B.G.; Frosk, P.; Engel, A.G.; Klutzny, U.; Lochmüller, H.; Wrogemann, K. Commonality of TRIM32 mutation in causing sarcotubular myopathy and LGMD2H. *Annals of neurology* **2005**, *57*, 591-595.
26. Saccone, V.; Palmieri, M.; Passamano, L.; Piluso, G.; Meroni, G.; Politano, L.; Nigro, V. Mutations that impair interaction properties of TRIM32 associated with limb-girdle muscular dystrophy 2H. *Human mutation* **2008**, *29*, 240-247.
27. Chiang, A.P.; Beck, J.S.; Yen, H.J.; Tayeh, M.K.; Scheetz, T.E.; Swiderski, R.E.; Nishimura, D.Y.; Braun, T.A.; Kim, K.Y.; Huang, J.; et al. Homozygosity mapping with SNP arrays identifies TRIM32, an E3 ubiquitin ligase, as a Bardet-Biedl syndrome gene (BBS11). *Proceedings of the National Academy of Sciences of the United States of America* **2006**, *103*, 6287-6292.
28. Fridell, R.A.; Harding, L.S.; Bogerd, H.P.; Cullen, B.R. Identification of a novel human zinc finger protein that specifically interacts with the activation domain of lentiviral Tat proteins. *Virology* **1995**, *209*, 347-357.
29. Metzger, M.B.; Pruneda, J.N.; Klevit, R.E.; Weissman, A.M. RING-type E3 ligases: master manipulators of E2 ubiquitin-conjugating enzymes and ubiquitination. *Biochimica et biophysica acta* **2014**, *1843*, 47-60.
30. Hatakeyama, S. TRIM Family Proteins: Roles in Autophagy, Immunity, and Carcinogenesis. *Trends in biochemical sciences* **2017**, *42*, 297-311.
31. Meroni, G. TRIM E3 Ubiquitin Ligases in Rare Genetic Disorders. *Advances in experimental medicine and biology* **2020**, *1233*, 311-325.

32. Lazzari, E.; Meroni, G. TRIM32 ubiquitin E3 ligase, one enzyme for several pathologies: From muscular dystrophy to tumours. *The international journal of biochemistry & cell biology* **2016**, *79*, 469-477.
33. Borden, K.L.; Freemont, P.S. The RING finger domain: a recent example of a sequence-structure family. *Current opinion in structural biology* **1996**, *6*, 395-401.
34. Budhidarmo, R.; Nakatani, Y.; Day, C.L. RINGs hold the key to ubiquitin transfer. *Trends in biochemical sciences* **2012**, *37*, 58-65.
35. Lazzari, E.; El-Halawany, M.S.; De March, M.; Valentino, F.; Cantatore, F.; Migliore, C.; Onesti, S.; Meroni, G. Analysis of the Zn-Binding Domains of TRIM32, the E3 Ubiquitin Ligase Mutated in Limb Girdle Muscular Dystrophy 2H. *Cells* **2019**, *8*.
36. Koliopoulos, M.G.; Esposito, D.; Christodoulou, E.; Taylor, I.A.; Rittinger, K. Functional role of TRIM E3 ligase oligomerization and regulation of catalytic activity. *The EMBO journal* **2016**, *35*, 1204-1218.
37. Tocchini, C.; Ciosk, R. TRIM-NHL proteins in development and disease. *Seminars in cell & developmental biology* **2015**, *47-48*, 52-59.
38. Liu, J.; Zhang, C.; Wang, X.L.; Ly, P.; Belyi, V.; Xu-Monette, Z.Y.; Young, K.H.; Hu, W.; Feng, Z. E3 ubiquitin ligase TRIM32 negatively regulates tumor suppressor p53 to promote tumorigenesis. *Cell death and differentiation* **2014**, *21*, 1792-1804.
39. Borg, K.; Stucka, R.; Locke, M.; Melin, E.; Ahlberg, G.; Klutzny, U.; Hagen, M.; Huebner, A.; Lochmüller, H.; Wrogemann, K.; et al. Intragenic deletion of TRIM32 in compound heterozygotes with sarcotubular myopathy/LGMD2H. *Human mutation* **2009**, *30*, E831-844.
40. Servián-Morilla, E.; Cabrera-Serrano, M.; Rivas-Infante, E.; Carvajal, A.; Lamont, P.J.; Pelayo-Negro, A.L.; Ravenscroft, G.; Junckerstorff, R.; Dyke, J.M.; Fletcher, S.; et al. Altered myogenesis and premature senescence underlie human TRIM32-related myopathy. *Acta neuropathologica communications* **2019**, *7*, 30.
41. Kudryashova, E.; Kramerova, I.; Spencer, M.J. Satellite cell senescence underlies myopathy in a mouse model of limb-girdle muscular dystrophy 2H. *The Journal of clinical investigation* **2012**, *122*, 1764-1776.
42. Kudryashova, E.; Struyk, A.; Mokhonova, E.; Cannon, S.C.; Spencer, M.J. The common missense mutation D489N in TRIM32 causing limb girdle muscular dystrophy 2H leads to loss of the mutated protein in knock-in mice resulting in a Trim32-null phenotype. *Human molecular genetics* **2011**, *20*, 3925-3932.
43. Overå, K.S.; Garcia-Garcia, J.; Bhujabal, Z.; Jain, A.; Øvervatn, A.; Larsen, K.B.; Deretic, V.; Johansen, T.; Lamark, T.; Sjøttem, E. TRIM32, but not its muscular dystrophy-associated mutant, positively regulates and is targeted to autophagic degradation by p62/SQSTM1. *Journal of cell science* **2019**, *132*.
44. Hershko, A.; Ciechanover, A. The ubiquitin system. *Annual review of biochemistry* **1998**, *67*, 425-479.
45. Grabbe, C.; Husnjak, K.; Dikic, I. The spatial and temporal organization of ubiquitin networks. *Nature reviews. Molecular cell biology* **2011**, *12*, 295-307.
46. Schwartz, A.L.; Ciechanover, A. Targeting proteins for destruction by the ubiquitin system: implications for human pathobiology. *Annual review of pharmacology and toxicology* **2009**, *49*, 73-96.
47. Goldstein, G.; Scheid, M.; Hammerling, U.; Schlesinger, D.H.; Niall, H.D.; Boyse, E.A. Isolation of a polypeptide that has lymphocyte-differentiating properties and is probably represented universally in living cells. *Proceedings of the National Academy of Sciences of the United States of America* **1975**, *72*, 11-15.
48. Pickart, C.M.; Eddins, M.J. Ubiquitin: structures, functions, mechanisms. *Biochimica et biophysica acta* **2004**, *1695*, 55-72.
49. Komander, D.; Rape, M. The ubiquitin code. *Annual review of biochemistry* **2012**, *81*, 203-229.

50. Husnjak, K.; Dikic, I. Ubiquitin-binding proteins: decoders of ubiquitin-mediated cellular functions. *Annual review of biochemistry* **2012**, *81*, 291-322.
51. Khaminets, A.; Behl, C.; Dikic, I. Ubiquitin-Dependent And Independent Signals In Selective Autophagy. *Trends in cell biology* **2016**, *26*, 6-16.
52. Betschinger, J.; Eisenhaber, F.; Knoblich, J.A. Phosphorylation-induced autoinhibition regulates the cytoskeletal protein Lethal (2) giant larvae. *Current biology : CB* **2005**, *15*, 276-282.
53. Fallon, L.; Bélanger, C.M.; Corera, A.T.; Kontogiannea, M.; Regan-Klapisz, E.; Moreau, F.; Voortman, J.; Haber, M.; Rouleau, G.; Thorarinsdottir, T.; et al. A regulated interaction with the UIM protein Eps15 implicates parkin in EGF receptor trafficking and PI(3)K-Akt signalling. *Nature cell biology* **2006**, *8*, 834-842.
54. Ye, Y.; Rape, M. Building ubiquitin chains: E2 enzymes at work. *Nature reviews. Molecular cell biology* **2009**, *10*, 755-764.
55. Akutsu, M.; Dikic, I.; Bremm, A. Ubiquitin chain diversity at a glance. *Journal of cell science* **2016**, *129*, 875-880.
56. Chen, Z.J. Ubiquitination in signaling to and activation of IKK. *Immunological reviews* **2012**, *246*, 95-106.
57. Harper, J.W.; Schulman, B.A. Structural complexity in ubiquitin recognition. *Cell* **2006**, *124*, 1133-1136.
58. Lecker, S.H.; Goldberg, A.L.; Mitch, W.E. Protein degradation by the ubiquitin-proteasome pathway in normal and disease states. *Journal of the American Society of Nephrology : JASN* **2006**, *17*, 1807-1819.
59. Kravtsova-Ivantsiv, Y.; Ciechanover, A. Non-canonical ubiquitin-based signals for proteasomal degradation. *Journal of cell science* **2012**, *125*, 539-548.
60. Rock, K.L.; Gramm, C.; Rothstein, L.; Clark, K.; Stein, R.; Dick, L.; Hwang, D.; Goldberg, A.L. Inhibitors of the proteasome block the degradation of most cell proteins and the generation of peptides presented on MHC class I molecules. *Cell* **1994**, *78*, 761-771.
61. Glickman, M.H.; Ciechanover, A. The ubiquitin-proteasome proteolytic pathway: destruction for the sake of construction. *Physiological reviews* **2002**, *82*, 373-428.
62. Pickart, C.M. Back to the future with ubiquitin. *Cell* **2004**, *116*, 181-190.
63. Khalil, R. Ubiquitin-Proteasome Pathway and Muscle Atrophy. *Advances in experimental medicine and biology* **2018**, *1088*, 235-248.
64. Schiaffino, S.; Dyar, K.A.; Ciciliot, S.; Blaauw, B.; Sandri, M. Mechanisms regulating skeletal muscle growth and atrophy. *The FEBS journal* **2013**, *280*, 4294-4314.
65. Bilodeau, P.A.; Coyne, E.S.; Wing, S.S. The ubiquitin proteasome system in atrophying skeletal muscle: roles and regulation. *American journal of physiology. Cell physiology* **2016**, *311*, C392-403.
66. Baehr, L.M.; West, D.W.D.; Marshall, A.G.; Marcotte, G.R.; Baar, K.; Bodine, S.C. Muscle-specific and age-related changes in protein synthesis and protein degradation in response to hindlimb unloading in rats. *Journal of applied physiology (Bethesda, Md. : 1985)* **2017**, *122*, 1336-1350.
67. Banerjee, R.; He, J.; Spaniel, C.; Quintana, M.T.; Wang, Z.; Bain, J.; Newgard, C.B.; Muehlbauer, M.J.; Willis, M.S. Non-targeted metabolomics analysis of cardiac Muscle Ring Finger-1 (MuRF1), MuRF2, and MuRF3 in vivo reveals novel and redundant metabolic changes. *Metabolomics : Official journal of the Metabolomic Society* **2015**, *11*, 312-322.
68. Yang, W.L.; Wang, J.; Chan, C.H.; Lee, S.W.; Campos, A.D.; Lamothe, B.; Hur, L.; Grabiner, B.C.; Lin, X.; Darnay, B.G.; et al. The E3 ligase TRAF6 regulates Akt ubiquitination and activation. *Science (New York, N.Y.)* **2009**, *325*, 1134-1138.
69. Yang, W.L.; Wu, C.Y.; Wu, J.; Lin, H.K. Regulation of Akt signaling activation by ubiquitination. *Cell cycle (Georgetown, Tex.)* **2010**, *9*, 487-497.

70. Yang, W.L.; Zhang, X.; Lin, H.K. Emerging role of Lys-63 ubiquitination in protein kinase and phosphatase activation and cancer development. *Oncogene* **2010**, *29*, 4493-4503.
71. Hayden, M.S.; Ghosh, S. Shared principles in NF-kappaB signaling. *Cell* **2008**, *132*, 344-362.
72. Sobhian, B.; Shao, G.; Lilli, D.R.; Culhane, A.C.; Moreau, L.A.; Xia, B.; Livingston, D.M.; Greenberg, R.A. RAP80 targets BRCA1 to specific ubiquitin structures at DNA damage sites. *Science (New York, N.Y.)* **2007**, *316*, 1198-1202.
73. Jiang, Q.; Foglizzo, M.; Morozov, Y.I.; Yang, X.; Datta, A.; Tian, L.; Thada, V.; Li, W.; Zeqiraj, E.; Greenberg, R.A. Autologous K63 deubiquitylation within the BRCA1-A complex licenses DNA damage recognition. *The Journal of cell biology* **2022**, *221*.
74. Lee, I.; Schindelin, H. Structural insights into E1-catalyzed ubiquitin activation and transfer to conjugating enzymes. *Cell* **2008**, *134*, 268-278.
75. Schulman, B.A.; Harper, J.W. Ubiquitin-like protein activation by E1 enzymes: the apex for downstream signalling pathways. *Nature reviews. Molecular cell biology* **2009**, *10*, 319-331.
76. Tokgöz, Z.; Bohnsack, R.N.; Haas, A.L. Pleiotropic effects of ATP.Mg2+ binding in the catalytic cycle of ubiquitin-activating enzyme. *The Journal of biological chemistry* **2006**, *281*, 14729-14737.
77. van Wijk, S.J.; Timmers, H.T. The family of ubiquitin-conjugating enzymes (E2s): deciding between life and death of proteins. *FASEB journal : official publication of the Federation of American Societies for Experimental Biology* **2010**, *24*, 981-993.
78. Liu, W.; Tang, X.; Qi, X.; Fu, X.; Ghimire, S.; Ma, R.; Li, S.; Zhang, N.; Si, H. The Ubiquitin Conjugating Enzyme: An Important Ubiquitin Transfer Platform in Ubiquitin-Proteasome System. *International journal of molecular sciences* **2020**, *21*.
79. Vittal, V.; Stewart, M.D.; Brzovic, P.S.; Klevit, R.E. Regulating the Regulators: Recent Revelations in the Control of E3 Ubiquitin Ligases. *The Journal of biological chemistry* **2015**, *290*, 21244-21251.
80. Toma-Fukai, S.; Shimizu, T. Structural Diversity of Ubiquitin E3 Ligase. *Molecules (Basel, Switzerland)* **2021**, *26*.
81. Rotin, D.; Kumar, S. Physiological functions of the HECT family of ubiquitin ligases. *Nature reviews. Molecular cell biology* **2009**, *10*, 398-409.
82. Mathieu, N.A.; Levin, R.H.; Spratt, D.E. Exploring the Roles of HERC2 and the NEDD4L HECT E3 Ubiquitin Ligase Subfamily in p53 Signaling and the DNA Damage Response. *Frontiers in oncology* **2021**, *11*, 659049.
83. Broix, L.; Jagline, H.; Ivanova, E.; Schmucker, S.; Drouot, N.; Clayton-Smith, J.; Pagnamenta, A.T.; Metcalfe, K.A.; Isidor, B.; Louvier, U.W.; et al. Mutations in the HECT domain of NEDD4L lead to AKT-mTOR pathway deregulation and cause periventricular nodular heterotopia. *Nature genetics* **2016**, *48*, 1349-1358.
84. Novellasdemunt, L.; Kucharska, A.; Jamieson, C.; Prange-Barczynska, M.; Baulies, A.; Antas, P.; van der Vaart, J.; Gehart, H.; Maurice, M.M.; Li, V.S. NEDD4 and NEDD4L regulate Wnt signalling and intestinal stem cell priming by degrading LGR5 receptor. *The EMBO journal* **2020**, *39*, e102771.
85. Infante, P.; Lospinoso Severini, L.; Bernardi, F.; Bufalieri, F.; Di Marcotullio, L. Targeting Hedgehog Signalling through the Ubiquitylation Process: The Multiple Roles of the HECT-E3 Ligase Itch. *Cells* **2019**, *8*.
86. Smit, J.J.; Sixma, T.K. RBR E3-ligases at work. *EMBO reports* **2014**, *15*, 142-154.
87. Vander Kooi, C.W.; Ohi, M.D.; Rosenberg, J.A.; Oldham, M.L.; Newcomer, M.E.; Gould, K.L.; Chazin, W.J. The Prp19 U-box crystal structure suggests a common dimeric architecture for a class of oligomeric E3 ubiquitin ligases. *Biochemistry* **2006**, *45*, 121-130.
88. Aravind, L.; Koonin, E.V. The U box is a modified RING finger - a common domain in ubiquitination. *Current biology : CB* **2000**, *10*, R132-134.
89. Deshaies, R.J.; Joazeiro, C.A.P. RING Domain E3 Ubiquitin Ligases. *Annual review of biochemistry* **2009**, *78*, 399-434.

90. Fiorentini, F.; Esposito, D.; Rittinger, K. Does it take two to tango? RING domain self-association and activity in TRIM E3 ubiquitin ligases. *Biochemical Society Transactions* **2020**, *48*, 2615-2624.
91. Wilkinson, K.D. Regulation of ubiquitin-dependent processes by deubiquitinating enzymes. *FASEB journal : official publication of the Federation of American Societies for Experimental Biology* **1997**, *11*, 1245-1256.
92. Reyes-Turcu, F.E.; Ventii, K.H.; Wilkinson, K.D. Regulation and cellular roles of ubiquitin-specific deubiquitinating enzymes. *Annual review of biochemistry* **2009**, *78*, 363-397.
93. Amerik, A.Y.; Hochstrasser, M. Mechanism and function of deubiquitinating enzymes. *Biochimica et biophysica acta* **2004**, *1695*, 189-207.
94. Luo, Q.; Wu, X.; Nan, Y.; Chang, W.; Zhao, P.; Zhang, Y.; Su, D.; Liu, Z. TRIM32/USP11 Balances ARID1A Stability and the Oncogenic/Tumor-Suppressive Status of Squamous Cell Carcinoma. *Cell Reports* **2020**, *30*, 98-111.e115.
95. Goldbraikh, D.; Neufeld, D.; Eid-Mutlak, Y.; Lasry, I.; Gilda, J.E.; Parnis, A.; Cohen, S. USP1 deubiquitinates Akt to inhibit PI3K-Akt-FoxO signaling in muscle during prolonged starvation. *EMBO reports* **2020**, *21*, e48791.
96. Nicklas, S.; Hillje, A.L.; Okawa, S.; Rudolph, I.M.; Collmann, F.M.; van Wuellen, T.; Del Sol, A.; Schwamborn, J.C. A complex of the ubiquitin ligase TRIM32 and the deubiquitinase USP7 balances the level of c-Myc ubiquitination and thereby determines neural stem cell fate specification. *Cell death and differentiation* **2019**, *26*, 728-740.
97. Janssen, I.; Heymsfield, S.B.; Wang, Z.M.; Ross, R. Skeletal muscle mass and distribution in 468 men and women aged 18-88 yr. *Journal of applied physiology (Bethesda, Md. : 1985)* **2000**, *89*, 81-88.
98. Shadrin, I.Y.; Khodabukus, A.; Bursac, N. Striated muscle function, regeneration, and repair. *Cellular and Molecular Life Sciences* **2016**, *73*, 4175-4202.
99. Hanson, J.; Huxley, H.E. Structural basis of the cross-striations in muscle. *Nature* **1953**, *172*, 530-532.
100. Huxley, H.E. Electron microscope studies of the organisation of the filaments in striated muscle. *Biochimica et biophysica acta* **1953**, *12*, 387-394.
101. Schiaffino, S.; Reggiani, C. Fiber types in mammalian skeletal muscles. *Physiological reviews* **2011**, *91*, 1447-1531.
102. Bagher, P.; Segal, S.S. Regulation of blood flow in the microcirculation: role of conducted vasodilation. *Acta physiologica (Oxford, England)* **2011**, *202*, 271-284.
103. Frontera, W.R.; Ochala, J. Skeletal muscle: a brief review of structure and function. *Calcified tissue international* **2015**, *96*, 183-195.
104. Segal, S.S. Integration of blood flow control to skeletal muscle: key role of feed arteries. *Acta physiologica Scandinavica* **2000**, *168*, 511-518.
105. Hikida, R.S. Aging changes in satellite cells and their functions. *Current aging science* **2011**, *4*, 279-297.
106. Stone, W.L.; Leavitt, L.; Varacallo, M. Physiology, Growth Factor. In *StatPearls*; StatPearls Publishing

107. Tolkatchev, D.; Smith, G.E.; Kostyukova, A.S. Chapter Eight - Role of intrinsic disorder in muscle sarcomeres. In *Progress in Molecular Biology and Translational Science*, Uversky, V.N., Ed.; Academic Press: 2019; Volume 166, pp. 311-340.
108. Mansfield, P.J.; Neumann, D.A. Chapter 3 - Structure and Function of Skeletal Muscle. In *Essentials of Kinesiology for the Physical Therapist Assistant (Third Edition)*, Mansfield, P.J., Neumann, D.A., Eds.; Mosby: St. Louis (MO), 2019; pp. 34-49.
109. Young, P.; Ferguson, C.; Bañuelos, S.; Gautel, M. Molecular structure of the sarcomeric Z-disk: two types of titin interactions lead to an asymmetrical sorting of alpha-actinin. *The EMBO journal* **1998**, *17*, 1614-1624.

110. Trinick, J. Titin and nebulin: protein rulers in muscle? *Trends in biochemical sciences* **1994**, *19*, 405-409.
111. Wang, K.; McClure, J.; Tu, A. Titin: major myofibrillar components of striated muscle. *Proceedings of the National Academy of Sciences of the United States of America* **1979**, *76*, 3698-3702.
112. Agarkova, I.; Perriard, J.C. The M-band: an elastic web that crosslinks thick filaments in the center of the sarcomere. *Trends in cell biology* **2005**, *15*, 477-485.
113. Koubassova, N.A.; Tsaturyan, A.K. Molecular mechanism of actin-myosin motor in muscle. *Biochemistry. Biokhimiia* **2011**, *76*, 1484-1506.
114. Ehler, E.; Gautel, M. The sarcomere and sarcomerogenesis. *Advances in experimental medicine and biology* **2008**, *642*, 1-14.
115. Avila, G.; de la Rosa, J.A.; Monsalvo-Villegas, A.; Montiel-Jaen, M.G. Ca(2+) Channels Mediate Bidirectional Signaling between Sarcolemma and Sarcoplasmic Reticulum in Muscle Cells. *Cells* **2019**, *9*.
116. Webb, R.C. Smooth muscle contraction and relaxation. *Advances in physiology education* **2003**, *27*, 201-206.
117. Somlyo, A.P.; Somlyo, A.V. The sarcoplasmic reticulum: then and now. *Novartis Foundation symposium* **2002**, *246*, 258-268; discussion 268-271, 272-256.
118. Gollapudi, S.K.; Michael, J.J.; Chandra, M. Striated Muscle Dynamics. In *Reference Module in Biomedical Sciences*; Elsevier: 2014.
119. Pardo, J.V.; Siliciano, J.D.; Craig, S.W. A vinculin-containing cortical lattice in skeletal muscle: transverse lattice elements ("costameres") mark sites of attachment between myofibrils and sarcolemma. *Proceedings of the National Academy of Sciences of the United States of America* **1983**, *80*, 1008-1012.
120. Bloch, R.J.; Capetanaki, Y.; O'Neill, A.; Reed, P.; Williams, M.W.; Resneck, W.G.; Porter, N.C.; Ursitti, J.A. Costameres: repeating structures at the sarcolemma of skeletal muscle. *Clinical orthopaedics and related research* **2002**, S203-210.
121. Jaka, O.; Casas-Fraile, L.; López de Munain, A.; Sáenz, A. Costamere proteins and their involvement in myopathic processes. *Expert Reviews in Molecular Medicine* **2015**, *17*, e12.
122. Sparrow, J.C.; Schöck, F. The initial steps of myofibril assembly: integrins pave the way. *Nature reviews. Molecular cell biology* **2009**, *10*, 293-298.
123. Estrella, N.L.; Naya, F.J. Transcriptional networks regulating the costamere, sarcomere, and other cytoskeletal structures in striated muscle. *Cellular and molecular life sciences : CMLS* **2014**, *71*, 1641-1656.
124. Campbell, K.P. Three muscular dystrophies: loss of cytoskeleton-extracellular matrix linkage. *Cell* **1995**, *80*, 675-679.
125. Anastasi, G.; Cutroneo, G.; Rizzo, G.; Arco, A.; Santoro, G.; Bramanti, P.; Vitetta, A.G.; Pisani, A.; Trimarchi, F.; Favaloro, A. Sarcoglycan and integrin localization in normal human skeletal muscle: a confocal laser scanning microscope study. *European journal of histochemistry : EJH* **2004**, *48*, 245-252.
126. Matsumura, K.; Campbell, K.P. Dystrophin-glycoprotein complex: its role in the molecular pathogenesis of muscular dystrophies. *Muscle & nerve* **1994**, *17*, 2-15.
127. Song, W.K.; Wang, W.; Foster, R.F.; Bielser, D.A.; Kaufman, S.J. H36-alpha 7 is a novel integrin alpha chain that is developmentally regulated during skeletal myogenesis. *The Journal of cell biology* **1992**, *117*, 643-657.
128. Song, W.K.; Wang, W.; Sato, H.; Bielser, D.A.; Kaufman, S.J. Expression of alpha 7 integrin cytoplasmic domains during skeletal muscle development: alternate forms, conformational change, and homologies with serine/threonine kinases and tyrosine phosphatases. *Journal of cell science* **1993**, *106 (Pt 4)*, 1139-1152.
129. Fujita, H.; Nedachi, T.; Kanzaki, M. Accelerated de novo sarcomere assembly by electric pulse stimulation in C2C12 myotubes. *Experimental cell research* **2007**, *313*, 1853-1865.

130. Black, B.L.; Olson, E.N. Transcriptional control of muscle development by myocyte enhancer factor-2 (MEF2) proteins. *Annual review of cell and developmental biology* **1998**, *14*, 167-196.
131. Koenig, M.; Hoffman, E.P.; Bertelson, C.J.; Monaco, A.P.; Feener, C.; Kunkel, L.M. Complete cloning of the Duchenne muscular dystrophy (DMD) cDNA and preliminary genomic organization of the DMD gene in normal and affected individuals. *Cell* **1987**, *50*, 509-517.
132. Monaco, A.P.; Neve, R.L.; Colletti-Feener, C.; Bertelson, C.J.; Kurnit, D.M.; Kunkel, L.M. Isolation of candidate cDNAs for portions of the Duchenne muscular dystrophy gene. *Nature* **1986**, *323*, 646-650.
133. Hoffman, E.P.; Knudson, C.M.; Campbell, K.P.; Kunkel, L.M. Subcellular fractionation of dystrophin to the triads of skeletal muscle. *Nature* **1987**, *330*, 754-758.
134. Crosbie, R.H.; Heighway, J.; Venzke, D.P.; Lee, J.C.; Campbell, K.P. Sarcospan, the 25-kDa transmembrane component of the dystrophin-glycoprotein complex. *The Journal of biological chemistry* **1997**, *272*, 31221-31224.
135. Barresi, R.; Campbell, K.P. Dystroglycan: from biosynthesis to pathogenesis of human disease. *Journal of cell science* **2006**, *119*, 199-207.
136. Hynes, R.O. Integrins: versatility, modulation, and signaling in cell adhesion. *Cell* **1992**, *69*, 11-25.
137. Lu, M.H.; DiLullo, C.; Schultheiss, T.; Holtzer, S.; Murray, J.M.; Choi, J.; Fischman, D.A.; Holtzer, H. The vinculin/sarcomeric-alpha-actinin/alpha-actin nexus in cultured cardiac myocytes. *The Journal of cell biology* **1992**, *117*, 1007-1022.
138. Schwartz, M.A.; Schaller, M.D.; Ginsberg, M.H. Integrins: emerging paradigms of signal transduction. *Annual review of cell and developmental biology* **1995**, *11*, 549-599.
139. Peng, X.; Nelson, E.S.; Maiers, J.L.; DeMali, K.A. New insights into vinculin function and regulation. *International review of cell and molecular biology* **2011**, *287*, 191-231.
140. Legate, K.R.; Montañez, E.; Kudlacek, O.; Fässler, R. ILK, PINCH and parvin: the tIPP of integrin signalling. *Nature reviews. Molecular cell biology* **2006**, *7*, 20-31.
141. Serrano, A.L.; Mann, C.J.; Vidal, B.; Ardite, E.; Perdiguero, E.; Muñoz-Cánoves, P. Chapter seven - Cellular and Molecular Mechanisms Regulating Fibrosis in Skeletal Muscle Repair and Disease. In *Current Topics in Developmental Biology*, Pavlath, G.k., Ed.; Academic Press: 2011; Volume 96, pp. 167-201.
142. Kablar, B.; Asakura, A.; Krastel, K.; Ying, C.; May, L.L.; Goldhamer, D.J.; Rudnicki, M.A. MyoD and Myf-5 define the specification of musculature of distinct embryonic origin. *Biochemistry and cell biology = Biochimie et biologie cellulaire* **1998**, *76*, 1079-1091.
143. Hutcheson, D.A.; Zhao, J.; Merrell, A.; Haldar, M.; Kardon, G. Embryonic and fetal limb myogenic cells are derived from developmentally distinct progenitors and have different requirements for beta-catenin. *Genes & development* **2009**, *23*, 997-1013.
144. Campion, D.R.; Richardson, R.L.; Reagan, J.O.; Kraeling, R.R. Changes in the satellite cell population during postnatal growth of pig skeletal muscle. *Journal of animal science* **1981**, *52*, 1014-1018.
145. Gamble, H.J.; Fenton, J.; Allsopp, G. Electron microscope observations on human fetal striated muscle. *Journal of anatomy* **1978**, *126*, 567-589.
146. Schultz, E.; Gibson, M.C.; Champion, T. Satellite cells are mitotically quiescent in mature mouse muscle: an EM and radioautographic study. *The Journal of experimental zoology* **1978**, *206*, 451-456.
147. Snow, M.H. A quantitative ultrastructural analysis of satellite cells in denervated fast and slow muscles of the mouse. *The Anatomical record* **1983**, *207*, 593-604.
148. Duan, D.; Goemans, N.; Takeda, S.; Mercuri, E.; Aartsma-Rus, A. Duchenne muscular dystrophy. *Nature reviews. Disease primers* **2021**, *7*, 13.

149. Chargé, S.B.; Rudnicki, M.A. Cellular and molecular regulation of muscle regeneration. *Physiological reviews* **2004**, *84*, 209-238.
150. Hubank, M.; Schatz, D.G. Identifying differences in mRNA expression by representational difference analysis of cDNA. *Nucleic acids research* **1994**, *22*, 5640-5648.
151. Seale, P.; Sabourin, L.A.; Girgis-Gabardo, A.; Mansouri, A.; Gruss, P.; Rudnicki, M.A. Pax7 is required for the specification of myogenic satellite cells. *Cell* **2000**, *102*, 777-786.
152. Cornelison, D.D.; Wold, B.J. Single-cell analysis of regulatory gene expression in quiescent and activated mouse skeletal muscle satellite cells. *Developmental biology* **1997**, *191*, 270-283.
153. Schultz, E.; Jaryszak, D.L.; Gibson, M.C.; Albright, D.J. Absence of exogenous satellite cell contribution to regeneration of frozen skeletal muscle. *Journal of muscle research and cell motility* **1986**, *7*, 361-367.
154. Gnocchi, V.F.; White, R.B.; Ono, Y.; Ellis, J.A.; Zammit, P.S. Further characterisation of the molecular signature of quiescent and activated mouse muscle satellite cells. *PloS one* **2009**, *4*, e5205.
155. Fielding, R.A.; Manfredi, T.J.; Ding, W.; Fiatarone, M.A.; Evans, W.J.; Cannon, J.G. Acute phase response in exercise. III. Neutrophil and IL-1 beta accumulation in skeletal muscle. *The American journal of physiology* **1993**, *265*, R166-172.
156. Vetrone, S.A.; Montecino-Rodriguez, E.; Kudryashova, E.; Kramerova, I.; Hoffman, E.P.; Liu, S.D.; Miceli, M.C.; Spencer, M.J. Osteopontin promotes fibrosis in dystrophic mouse muscle by modulating immune cell subsets and intramuscular TGF-beta. *The Journal of clinical investigation* **2009**, *119*, 1583-1594.
157. Chen, S.E.; Gerken, E.; Zhang, Y.; Zhan, M.; Mohan, R.K.; Li, A.S.; Reid, M.B.; Li, Y.P. Role of TNF-{alpha} signaling in regeneration of cardiotoxin-injured muscle. *American journal of physiology. Cell physiology* **2005**, *289*, C1179-1187.
158. Li, Y.P. TNF-alpha is a mitogen in skeletal muscle. *American journal of physiology. Cell physiology* **2003**, *285*, C370-376.
159. Guttridge, D.C.; Albanese, C.; Reuther, J.Y.; Pestell, R.G.; Baldwin, A.S., Jr. NF-kappaB controls cell growth and differentiation through transcriptional regulation of cyclin D1. *Molecular and cellular biology* **1999**, *19*, 5785-5799.
160. Horsley, V.; Jansen, K.M.; Mills, S.T.; Pavlath, G.K. IL-4 acts as a myoblast recruitment factor during mammalian muscle growth. *Cell* **2003**, *113*, 483-494.
161. Cooper, R.N.; Tajbakhsh, S.; Mouly, V.; Cossu, G.; Buckingham, M.; Butler-Browne, G.S. In vivo satellite cell activation via Myf5 and MyoD in regenerating mouse skeletal muscle. *Journal of cell science* **1999**, *112 (Pt 17)*, 2895-2901.
162. Cornelison, D.D.; Filla, M.S.; Stanley, H.M.; Rapraeger, A.C.; Olwin, B.B. Syndecan-3 and syndecan-4 specifically mark skeletal muscle satellite cells and are implicated in satellite cell maintenance and muscle regeneration. *Developmental biology* **2001**, *239*, 79-94.
163. Cornelison, D.D.; Olwin, B.B.; Rudnicki, M.A.; Wold, B.J. MyoD(-/-) satellite cells in single-fiber culture are differentiation defective and MRF4 deficient. *Developmental biology* **2000**, *224*, 122-137.
164. Megeney, L.A.; Kablar, B.; Garrett, K.; Anderson, J.E.; Rudnicki, M.A. MyoD is required for myogenic stem cell function in adult skeletal muscle. *Genes & development* **1996**, *10*, 1173-1183.
165. Maley, M.A.; Fan, Y.; Beilharz, M.W.; Grounds, M.D. Intrinsic differences in MyoD and myogenin expression between primary cultures of SJL/J and BALB/C skeletal muscle. *Experimental cell research* **1994**, *211*, 99-107.
166. Smith, C.K., 2nd; Janney, M.J.; Allen, R.E. Temporal expression of myogenic regulatory genes during activation, proliferation, and differentiation of rat skeletal muscle satellite cells. *Journal of cellular physiology* **1994**, *159*, 379-385.

167. Yablonka-Reuveni, Z.; Rivera, A.J. Temporal expression of regulatory and structural muscle proteins during myogenesis of satellite cells on isolated adult rat fibers. *Developmental biology* **1994**, *164*, 588-603.
168. Ganassi, M.; Badodi, S.; Ortuste Quiroga, H.P.; Zammit, P.S.; Hinits, Y.; Hughes, S.M. Myogenin promotes myocyte fusion to balance fibre number and size. *Nature Communications* **2018**, *9*, 4232.
169. Schmidt, M.; Schüler, S.C.; Hüttner, S.S.; von Eyss, B.; von Maltzahn, J. Adult stem cells at work: regenerating skeletal muscle. *Cellular and molecular life sciences : CMLS* **2019**, *76*, 2559-2570.
170. Bär, A.; Pette, D. Three fast myosin heavy chains in adult rat skeletal muscle. *FEBS Letters* **1988**, *235*, 153-155.
171. Schiaffino, S.; Gorza, L.; Sartore, S.; Saggin, L.; Ausoni, S.; Vianello, M.; Gundersen, K.; LØmo, T. Three myosin heavy chain isoforms in type 2 skeletal muscle fibres. *Journal of Muscle Research & Cell Motility* **1989**, *10*, 197-205.
172. Hasty, P.; Bradley, A.; Morris, J.H.; Edmondson, D.G.; Venuti, J.M.; Olson, E.N.; Klein, W.H. Muscle deficiency and neonatal death in mice with a targeted mutation in the myogenin gene. *Nature* **1993**, *364*, 501-506.
173. Moretti, I.; Ciciliot, S.; Dyar, K.A.; Abraham, R.; Murgia, M.; Agatea, L.; Akimoto, T.; Bicciato, S.; Forcato, M.; Pierre, P.; et al. MRF4 negatively regulates adult skeletal muscle growth by repressing MEF2 activity. *Nat Commun* **2016**, *7*, 12397.
174. Mak, K.L.; To, R.Q.; Kong, Y.; Konieczny, S.F. The MRF4 activation domain is required to induce muscle-specific gene expression. *Molecular and cellular biology* **1992**, *12*, 4334-4346.
175. Lazure, F.; Blackburn, D.M.; Corchado, A.H.; Sahinyan, K.; Karam, N.; Sharanek, A.; Nguyen, D.; Lepper, C.; Najafabadi, H.S.; Perkins, T.J.; et al. Myf6/MRF4 is a myogenic niche regulator required for the maintenance of the muscle stem cell pool. *EMBO reports* **2020**, *21*, e49499.
176. Vélez, E.J.; Lutfi, E.; Azizi, S.; Montserrat, N.; Riera-Codina, M.; Capilla, E.; Navarro, I.; Gutiérrez, J. Contribution of in vitro myocytes studies to understanding fish muscle physiology. *Comparative biochemistry and physiology. Part B, Biochemistry & molecular biology* **2016**, *199*, 67-73.
177. Lehka, L.; Rędowicz, M.J. Mechanisms regulating myoblast fusion: A multilevel interplay. *Seminars in cell & developmental biology* **2020**, *104*, 81-92.
178. Horsley, V.; Pavlath, G.K. Forming a multinucleated cell: molecules that regulate myoblast fusion. *Cells, tissues, organs* **2004**, *176*, 67-78.
179. Hindi, S.M.; Tajrishi, M.M.; Kumar, A. Signaling mechanisms in mammalian myoblast fusion. *Science signaling* **2013**, *6*, re2.
180. Abmayr, S.M.; Balagopalan, L.; Galletta, B.J.; Hong, S.J. Cell and molecular biology of myoblast fusion. *International review of cytology* **2003**, *225*, 33-89.
181. Zhang, H.; Wen, J.; Bigot, A.; Chen, J.; Shang, R.; Mouly, V.; Bi, P. Human myotube formation is determined by MyoD-Myomixer/Myomaker axis. *Science advances* **2020**, *6*.
182. Zhao, T.T.; Jin, F.; Li, J.G.; Xu, Y.Y.; Dong, H.T.; Liu, Q.; Xing, P.; Zhu, G.L.; Xu, H.; Yin, S.C.; et al. TRIM32 promotes proliferation and confers chemoresistance to breast cancer cells through activation of the NF-κB pathway. *Journal of Cancer* **2018**, *9*, 1349-1356.
183. Wang, J.; Fang, Y.; Liu, T. TRIM32 Promotes the Growth of Gastric Cancer Cells through Enhancing AKT Activity and Glucose Transportation. *BioMed Research International* **2020**, *2020*, 4027627.
184. Wang, C.; Xu, J.; Fu, H.; Zhang, Y.; Zhang, X.; Yang, D.; Zhu, Z.; Wei, Z.; Hu, Z.; Yan, R.; et al. TRIM32 promotes cell proliferation and invasion by activating β-catenin signalling in gastric cancer. *Journal of cellular and molecular medicine* **2018**, *22*, 5020-5028.

185. Fu, B.; Wang, L.; Ding, H.; Schwamborn, J.C.; Li, S.; Dorf, M.E. TRIM32 Senses and Restricts Influenza A Virus by Ubiquitination of PB1 Polymerase. *PLoS pathogens* **2015**, *11*, e1004960.
186. Zhang, J.; Hu, M.M.; Wang, Y.Y.; Shu, H.B. TRIM32 protein modulates type I interferon induction and cellular antiviral response by targeting MITA/STING protein for K63-linked ubiquitination. *The Journal of biological chemistry* **2012**, *287*, 28646-28655.
187. Loedige, I.; Filipowicz, W. TRIM-NHL proteins take on miRNA regulation. *Cell* **2009**, *136*, 818-820.
188. Bodine, S.C.; Baehr, L.M. Skeletal muscle atrophy and the E3 ubiquitin ligases MuRF1 and MAFbx/atrogin-1. *American journal of physiology. Endocrinology and metabolism* **2014**, *307*, E469-484.
189. Foletta, V.C.; White, L.J.; Larsen, A.E.; Léger, B.; Russell, A.P. The role and regulation of MAFbx/atrogin-1 and MuRF1 in skeletal muscle atrophy. *Pflugers Archiv : European journal of physiology* **2011**, *461*, 325-335.
190. Castillero, E.; Alamdari, N.; Lecker, S.H.; Hasselgren, P.O. Suppression of atrogin-1 and MuRF1 prevents dexamethasone-induced atrophy of cultured myotubes. *Metabolism: clinical and experimental* **2013**, *62*, 1495-1502.
191. Kudryashova, E.; Kudryashov, D.; Kramerova, I.; Spencer, M.J. Trim32 is a ubiquitin ligase mutated in limb girdle muscular dystrophy type 2H that binds to skeletal muscle myosin and ubiquitinates actin. *Journal of molecular biology* **2005**, *354*, 413-424.
192. Cohen, S.; Zhai, B.; Gygi, S.P.; Goldberg, A.L. Ubiquitylation by Trim32 causes coupled loss of desmin, Z-bands, and thin filaments in muscle atrophy. *The Journal of cell biology* **2012**, *198*, 575-589.
193. Bawa, S.; Gameros, S.; Baumann, K.; Brooks, D.S.; Kollhoff, J.A.; Zolkiewski, M.; Re Cecconi, A.D.; Panini, N.; Russo, M.; Piccirillo, R.; et al. Costameric integrin and sarcoglycan protein levels are altered in a Drosophila model for Limb-girdle muscular dystrophy type 2H. *Molecular biology of the cell* **2021**, *32*, 260-273.
194. Di Rienzo, M.; Piacentini, M.; Fimia, G.M. A TRIM32-AMBRA1-ULK1 complex initiates the autophagy response in atrophic muscle cells. *Autophagy* **2019**, *15*, 1674-1676.
195. Di Rienzo, M.; Antonioli, M.; Fusco, C.; Liu, Y.; Mari, M.; Orhon, I.; Refolo, G.; Germani, F.; Corazzari, M.; Romagnoli, A.; et al. Autophagy induction in atrophic muscle cells requires ULK1 activation by TRIM32 through unanchored K63-linked polyubiquitin chains. *Science advances* **2019**, *5*, eaau8857.
196. Russell, R.C.; Tian, Y.; Yuan, H.; Park, H.W.; Chang, Y.Y.; Kim, J.; Kim, H.; Neufeld, T.P.; Dillin, A.; Guan, K.L. ULK1 induces autophagy by phosphorylating Beclin-1 and activating VPS34 lipid kinase. *Nature cell biology* **2013**, *15*, 741-750.
197. Cohen, S.; Lee, D.; Zhai, B.; Gygi, S.P.; Goldberg, A.L. Trim32 reduces PI3K-Akt-FoxO signaling in muscle atrophy by promoting plakoglobin-PI3K dissociation. *The Journal of cell biology* **2014**, *204*, 747-758.
198. Chen, L.; Huang, J.; Ji, Y.; Zhang, X.; Wang, P.; Deng, K.; Jiang, X.; Ma, G.; Li, H. Tripartite motif 32 prevents pathological cardiac hypertrophy. *Clinical science (London, England : 1979)* **2016**, *130*, 813-828.
199. Nicklas, S.; Otto, A.; Wu, X.; Miller, P.; Stelzer, S.; Wen, Y.; Kuang, S.; Wrogemann, K.; Patel, K.; Ding, H.; et al. TRIM32 regulates skeletal muscle stem cell differentiation and is necessary for normal adult muscle regeneration. *PloS one* **2012**, *7*, e30445.
200. Kudryashova, E.; Wu, J.; Havton, L.A.; Spencer, M.J. Deficiency of the E3 ubiquitin ligase TRIM32 in mice leads to a myopathy with a neurogenic component. *Human molecular genetics* **2009**, *18*, 1353-1367.
201. Kudryashova, E.; Struyk, A.; Mokhonova, E.; Cannon, S.C.; Spencer, M.J. The common missense mutation D489N in TRIM32 causing limb girdle muscular dystrophy 2H leads to

loss of the mutated protein in knock-in mice resulting in a Trim32-null phenotype. *Human molecular genetics* **2011**, *20*, 3925-3932.
202. Bawa, S.; Brooks, D.S.; Neville, K.E.; Tipping, M.; Sagar, M.A.; Kollhoff, J.A.; Chawla, G.; Geisbrecht, B.V.; Tennessen, J.M.; Eliceiri, K.W.; et al. Drosophila TRIM32 cooperates with glycolytic enzymes to promote cell growth. *eLife* **2020**, *9*.
203. Yu, C.; Hao, X.; Zhang, S.; Hu, W.; Li, J.; Sun, J.; Zheng, M. Characterization of the prognostic values of the NDRG family in gastric cancer. *Therapeutic advances in gastroenterology* **2019**, *12*, 1756284819858507.
204. Chen, B.; Nelson, D.M.; Sadovsky, Y. N-myc down-regulated gene 1 modulates the response of term human trophoblasts to hypoxic injury. *The Journal of biological chemistry* **2006**, *281*, 2764-2772.
205. Yin, X.; Yu, H.; He, X.K.; Yan, S.X. Prognostic and biological role of the N-Myc downstream-regulated gene family in hepatocellular carcinoma. *World journal of clinical cases* **2022**, *10*, 2072-2086.
206. Anderson, K.J.; Russell, A.P.; Foletta, V.C. NDRG2 promotes myoblast proliferation and caspase 3/7 activities during differentiation, and attenuates hydrogen peroxide - But not palmitate-induced toxicity. *FEBS open bio* **2015**, *5*, 668-681.
207. Foletta, V.C.; Prior, M.J.; Stupka, N.; Carey, K.; Segal, D.H.; Jones, S.; Swinton, C.; Martin, S.; Cameron-Smith, D.; Walder, K.R. NDRG2, a novel regulator of myoblast proliferation, is regulated by anabolic and catabolic factors. *The Journal of physiology* **2009**, *587*, 1619-1634.
208. Mir, B.A.; Islam, R.; Kalanon, M.; Russell, A.P.; Foletta, V.C. MicroRNA suppression of stress-responsive NDRG2 during dexamethasone treatment in skeletal muscle cells. *BMC molecular and cell biology* **2019**, *20*, 12.
209. Foletta, V.C.; Brown, E.L.; Cho, Y.; Snow, R.J.; Kralli, A.; Russell, A.P. Ndrg2 is a PGC-1α/ERRα target gene that controls protein synthesis and expression of contractile-type genes in C2C12 myotubes. *Biochimica et biophysica acta* **2013**, *1833*, 3112-3123.
210. Mokhonova, E.I.; Avliyakulov, N.K.; Kramerova, I.; Kudryashova, E.; Haykinson, M.J.; Spencer, M.J. The E3 ubiquitin ligase TRIM32 regulates myoblast proliferation by controlling turnover of NDRG2. *Human molecular genetics* **2015**, *24*, 2873-2883.
211. Zhang, Z.F.; Zhang, J.; Hui, Y.N.; Zheng, M.H.; Liu, X.P.; Kador, P.F.; Wang, Y.S.; Yao, L.B.; Zhou, J. Up-regulation of NDRG2 in senescent lens epithelial cells contributes to age-related cataract in human. *PloS one* **2011**, *6*, e26102.
212. Jackson, P.K. A new RING for SUMO: wrestling transcriptional responses into nuclear bodies with PIAS family E3 SUMO ligases. *Genes & development* **2001**, *15*, 3053-3058.
213. Bischof, O.; Schwamborn, K.; Martin, N.; Werner, A.; Sustmann, C.; Grosschedl, R.; Dejean, A. RETRACTED: The E3 SUMO Ligase PIASy Is a Regulator of Cellular Senescence and Apoptosis. *Molecular Cell* **2006**, *22*, 783-794.
214. Geiss-Friedlander, R.; Melchior, F. Concepts in sumoylation: a decade on. *Nature Reviews Molecular Cell Biology* **2007**, *8*, 947-956.
215. Yang, Y.; He, Y.; Wang, X.; Liang, Z.; He, G.; Zhang, P.; Zhu, H.; Xu, N.; Liang, S. Protein SUMOylation modification and its associations with disease. *Open biology* **2017**, *7*.
216. Albor, A.; El-Hizawi, S.; Horn, E.J.; Laederich, M.; Frosk, P.; Wrogemann, K.; Kulesz-Martin, M. The interaction of Piasy with Trim32, an E3-ubiquitin ligase mutated in limb-girdle muscular dystrophy type 2H, promotes Piasy degradation and regulates UVB-induced keratinocyte apoptosis through NFkappaB. *The Journal of biological chemistry* **2006**, *281*, 25850-25866.
217. Horn, E.J.; Albor, A.; Liu, Y.; El-Hizawi, S.; Vanderbeek, G.E.; Babcock, M.; Bowden, G.T.; Hennings, H.; Lozano, G.; Weinberg, W.C.; et al. RING protein Trim32 associated with skin carcinogenesis has anti-apoptotic and E3-ubiquitin ligase properties. *Carcinogenesis* **2004**, *25*, 157-167.

218. Mokhonova, E.I.; Avliyakulov, N.K.; Kramerova, I.; Kudryashova, E.; Haykinson, M.J.; Spencer, M.J. The E3 ubiquitin ligase TRIM32 regulates myoblast proliferation by controlling turnover of NDRG2. *Human molecular genetics* **2015**, *24*, 2873-2883.
219. Schwamborn, J.C.; Berezikov, E.; Knoblich, J.A. The TRIM-NHL protein TRIM32 activates microRNAs and prevents self-renewal in mouse neural progenitors. *Cell* **2009**, *136*, 913-925.
220. Zhu, Q.; Couillard-Després, S.; Julien, J.P. Delayed maturation of regenerating myelinated axons in mice lacking neurofilaments. *Experimental neurology* **1997**, *148*, 299-316.
221. Elder, G.A.; Friedrich, V.L., Jr.; Bosco, P.; Kang, C.; Gourov, A.; Tu, P.H.; Lee, V.M.; Lazzarini, R.A. Absence of the mid-sized neurofilament subunit decreases axonal calibers, levels of light neurofilament (NF-L), and neurofilament content. *The Journal of cell biology* **1998**, *141*, 727-739.
222. Lu, L.; Katsaros, D.; de la Longrais, I.A.; Sochirca, O.; Yu, H. Hypermethylation of let-7a-3 in epithelial ovarian cancer is associated with low insulin-like growth factor-II expression and favorable prognosis. *Cancer research* **2007**, *67*, 10117-10122.
223. He, X.Y.; Chen, J.X.; Zhang, Z.; Li, C.L.; Peng, Q.L.; Peng, H.M. The let-7a microRNA protects from growth of lung carcinoma by suppression of k-Ras and c-Myc in nude mice. *Journal of cancer research and clinical oncology* **2010**, *136*, 1023-1028.
224. Johnson, S.M.; Grosshans, H.; Shingara, J.; Byrom, M.; Jarvis, R.; Cheng, A.; Labourier, E.; Reinert, K.L.; Brown, D.; Slack, F.J. RAS is regulated by the let-7 microRNA family. *Cell* **2005**, *120*, 635-647.
225. Song, J.; Cho, K.J.; Oh, Y.; Lee, J.E. Let7a involves in neural stem cell differentiation relating with TLX level. *Biochemical and Biophysical Research Communications* **2015**, *462*, 396-401.
226. Hillje, A.L.; Worlitzer, M.M.; Palm, T.; Schwamborn, J.C. Neural stem cells maintain their stemness through protein kinase C ζ-mediated inhibition of TRIM32. *Stem cells (Dayton, Ohio)* **2011**, *29*, 1437-1447.
227. Wang, Z.; Yoo, Y.J.; De La Torre, R.; Topham, C.; Hanifin, J.; Simpson, E.; Messing, R.O.; Kulesz-Martin, M.; Liu, Y. Inverse Correlation of TRIM32 and Protein Kinase C ζ in T Helper Type 2-Biased Inflammation. *The Journal of investigative dermatology* **2021**, *141*, 1297-1307.e1293.
228. Bahnassawy, L.; Perumal, T.M.; Gonzalez-Cano, L.; Hillje, A.L.; Taher, L.; Makalowski, W.; Suzuki, Y.; Fuellen, G.; del Sol, A.; Schwamborn, J.C. TRIM32 modulates pluripotency entry and exit by directly regulating Oct4 stability. *Scientific reports* **2015**, *5*, 13456.
229. Luo, W.; Chen, J.; Li, L.; Ren, X.; Cheng, T.; Lu, S.; Lawal, R.A.; Nie, Q.; Zhang, X.; Hanotte, O. c-Myc inhibits myoblast differentiation and promotes myoblast proliferation and muscle fibre hypertrophy by regulating the expression of its target genes, miRNAs and lincRNAs. *Cell death and differentiation* **2019**, *26*, 426-442.
230. Kato, G.J.; Lee, W.M.; Chen, L.L.; Dang, C.V. Max: functional domains and interaction with c-Myc. *Genes & development* **1992**, *6*, 81-92.
231. Walhout, A.J.; Gubbels, J.M.; Bernards, R.; van der Vliet, P.C.; Timmers, H.T. c-Myc/Max heterodimers bind cooperatively to the E-box sequences located in the first intron of the rat ornithine decarboxylase (ODC) gene. *Nucleic acids research* **1997**, *25*, 1493-1501.
232. Ala, M. Target c-Myc to treat pancreatic cancer. *Cancer biology & therapy* **2022**, *23*, 34-50.
233. Pelengaris, S.; Khan, M.; Evan, G. c-MYC: more than just a matter of life and death. *Nature reviews. Cancer* **2002**, *2*, 764-776.
234. Yada, M.; Hatakeyama, S.; Kamura, T.; Nishiyama, M.; Tsunematsu, R.; Imaki, H.; Ishida, N.; Okumura, F.; Nakayama, K.; Nakayama, K.I. Phosphorylation-dependent degradation of c-Myc is mediated by the F-box protein Fbw7. *The EMBO journal* **2004**, *23*, 2116-2125.
235. Amati, B. Myc degradation: dancing with ubiquitin ligases. *Proceedings of the National Academy of Sciences of the United States of America* **2004**, *101*, 8843-8844.
236. Sammak, S.; Hamdani, N.; Gorrec, F.; Allen, M.D.; Freund, S.M.V.; Bycroft, M.; Zinzalla, G. Crystal Structures and Nuclear Magnetic Resonance Studies of the Apo Form of the c-

MYC:MAX bHLHZip Complex Reveal a Helical Basic Region in the Absence of DNA. *Biochemistry* **2019**, *58*, 3144-3154.
237. Melnik, S.; Werth, N.; Boeuf, S.; Hahn, E.M.; Gotterbarm, T.; Anton, M.; Richter, W. Impact of c-MYC expression on proliferation, differentiation, and risk of neoplastic transformation of human mesenchymal stromal cells. *Stem cell research & therapy* **2019**, *10*, 73.
238. Wilson, A.; Murphy, M.J.; Oskarsson, T.; Kaloulis, K.; Bettess, M.D.; Oser, G.M.; Pasche, A.C.; Knabenhans, C.; Macdonald, H.R.; Trumpp, A. c-Myc controls the balance between hematopoietic stem cell self-renewal and differentiation. *Genes & development* **2004**, *18*, 2747-2763.
239. Pelengaris, S.; Khan, M. The many faces of c-MYC. *Archives of Biochemistry and Biophysics* **2003**, *416*, 129-136.
240. Seyer, P.; Grandemange, S.; Busson, M.; Carazo, A.; Gamaléri, F.; Pessemesse, L.; Casas, F.; Cabello, G.; Wrutniak-Cabello, C. Mitochondrial activity regulates myoblast differentiation by control of c-Myc expression. *Journal of cellular physiology* **2006**, *207*, 75-86.
241. Luo, W.; Chen, J.; Li, L.; Ren, X.; Cheng, T.; Lu, S.; Lawal, R.A.; Nie, Q.; Zhang, X.; Hanotte, O. c-Myc inhibits myoblast differentiation and promotes myoblast proliferation and muscle fibre hypertrophy by regulating the expression of its target genes, miRNAs and lincRNAs. *Cell Death & Differentiation* **2019**, *26*, 426-442.
242. La Rocca, S.A.; Crouch, D.H.; Gillespie, D.A. c-Myc inhibits myogenic differentiation and myoD expression by a mechanism which can be dissociated from cell transformation. *Oncogene* **1994**, *9*, 3499-3508.
243. Miner, J.H.; Wold, B.J. c-myc inhibition of MyoD and myogenin-initiated myogenic differentiation. *Molecular and cellular biology* **1991**, *11*, 2842-2851.
244. Russo, S.; Tomatis, D.; Collo, G.; Tarone, G.; Tatò, F. Myogenic conversion of NIH3T3 cells by exogenous MyoD family members: dissociation of terminal differentiation from myotube formation. *Journal of cell science* **1998**, *111 (Pt 6)*, 691-700.
245. Anderson, S.; Poudel, K.R.; Roh-Johnson, M.; Brabletz, T.; Yu, M.; Borenstein-Auerbach, N.; Grady, W.N.; Bai, J.; Moens, C.B.; Eisenman, R.N.; et al. MYC-nick promotes cell migration by inducing fascin expression and Cdc42 activation. *Proceedings of the National Academy of Sciences of the United States of America* **2016**, *113*, E5481-5490.
246. Mousavi, K.; Sartorelli, V. Myc-nick: the force behind c-Myc. *Science signaling* **2010**, *3*, pe49.
247. Conacci-Sorrell, M.; Ngouenet, C.; Eisenman, R.N. Myc-nick: a cytoplasmic cleavage product of Myc that promotes alpha-tubulin acetylation and cell differentiation. *Cell* **2010**, *142*, 480-493.
248. Dobin, A.; Gingeras, T.R. Mapping RNA-seq Reads with STAR. *Current protocols in bioinformatics* **2015**, *51*, 11.14.11-11.14.19.
249. Love, M.I.; Huber, W.; Anders, S. Moderated estimation of fold change and dispersion for RNA-seq data with DESeq2. *Genome biology* **2014**, *15*, 550.
250. Zhu, A.; Ibrahim, J.G.; Love, M.I. Heavy-tailed prior distributions for sequence count data: removing the noise and preserving large differences. *Bioinformatics* **2018**, *35*, 2084-2092.
251. Stewart, R.; Flechner, L.; Montminy, M.; Berdeaux, R. CREB is activated by muscle injury and promotes muscle regeneration. *PloS one* **2011**, *6*, e24714.
252. Lin, Y.H.; Chou, L.Y.; Chou, H.C.; Chen, C.H.; Kang, L.; Cheng, T.L.; Wang, C.Z. The Essential Role of Stathmin in Myoblast C2C12 for Vertical Vibration-Induced Myotube Formation. *Biomolecules* **2021**, *11*.
253. Winter, B.; Braun, T.; Arnold, H.H. cAMP-dependent protein kinase represses myogenic differentiation and the activity of the muscle-specific helix-loop-helix transcription factors Myf-5 and MyoD. *The Journal of biological chemistry* **1993**, *268*, 9869-9878.

254. Constantin, B.; Cognard, C.; Raymond, G. Myoblast fusion requires cytosolic calcium elevation but not activation of voltage-dependent calcium channels. *Cell calcium* **1996**, *19*, 365-374.
255. Sinha, S.; Elbaz-Alon, Y.; Avinoam, O. Ca(2+) as a coordinator of skeletal muscle differentiation, fusion and contraction. *The FEBS journal* **2022**, *289*, 6531-6542.
256. Quach, N.L.; Biressi, S.; Reichardt, L.F.; Keller, C.; Rando, T.A. Focal adhesion kinase signaling regulates the expression of caveolin 3 and beta1 integrin, genes essential for normal myoblast fusion. *Molecular biology of the cell* **2009**, *20*, 3422-3435.
257. Rudnicki, M.A.; Williams, B.O. Wnt signaling in bone and muscle. *Bone* **2015**, *80*, 60-66.
258. Eming, S.A.; Martin, P.; Tomic-Canic, M. Wound repair and regeneration: mechanisms, signaling, and translation. *Science translational medicine* **2014**, *6*, 265sr266.
259. Sokol, J.; Biringer, K.; Skerenova, M.; Hasko, M.; Bartosova, L.; Stasko, J.; Danko, J.; Kubisz, P. Platelet aggregation abnormalities in patients with fetal losses: the GP6 gene polymorphism. *Fertility and Sterility* **2012**, *98*, 1170-1174.
260. Wei, L.; Zhou, W.; Croissant, J.D.; Johansen, F.E.; Prywes, R.; Balasubramanyam, A.; Schwartz, R.J. RhoA signaling via serum response factor plays an obligatory role in myogenic differentiation. *The Journal of biological chemistry* **1998**, *273*, 30287-30294.
261. Scata, K.A.; Bernard, D.W.; Fox, J.; Swain, J.L. FGF receptor availability regulates skeletal myogenesis. *Experimental cell research* **1999**, *250*, 10-21.
262. Florini, J.R.; Ewton, D.Z.; Magri, K.A. Hormones, growth factors, and myogenic differentiation. *Annual review of physiology* **1991**, *53*, 201-216.
263. Jeong, J.; Choi, K.H.; Kim, S.H.; Lee, D.K.; Oh, J.N.; Lee, M.; Choe, G.C.; Lee, C.K. Combination of cell signaling molecules can facilitate MYOD1-mediated myogenic transdifferentiation of pig fibroblasts. *Journal of animal science and biotechnology* **2021**, *12*, 64.
264. Nabeshima, Y.; Hanaoka, K.; Hayasaka, M.; Esumi, E.; Li, S.; Nonaka, I.; Nabeshima, Y. Myogenin gene disruption results in perinatal lethality because of severe muscle defect. *Nature* **1993**, *364*, 532-535.
265. Venuti, J.M.; Morris, J.H.; Vivian, J.L.; Olson, E.N.; Klein, W.H. Myogenin is required for late but not early aspects of myogenesis during mouse development. *The Journal of cell biology* **1995**, *128*, 563-576.
266. Farrell, A.S.; Sears, R.C. MYC degradation. *Cold Spring Harbor perspectives in medicine* **2014**, *4*.
267. Kim, S.Y.; Herbst, A.; Tworkowski, K.A.; Salghetti, S.E.; Tansey, W.P. Skp2 regulates Myc protein stability and activity. *Mol Cell* **2003**, *11*, 1177-1188.
268. Bahram, F.; von der Lehr, N.; Cetinkaya, C.; Larsson, L.-G. c-Myc hot spot mutations in lymphomas result in inefficient ubiquitination and decreased proteasome-mediated turnover. *Blood* **2000**, *95*, 2104-2110.
269. Hermida, M.A.; Dinesh Kumar, J.; Leslie, N.R. GSK3 and its interactions with the PI3K/AKT/mTOR signalling network. *Advances in biological regulation* **2017**, *65*, 5-15.
270. Hughes, S.M.; Chi, M.M.; Lowry, O.H.; Gundersen, K. Myogenin induces a shift of enzyme activity from glycolytic to oxidative metabolism in muscles of transgenic mice. *The Journal of cell biology* **1999**, *145*, 633-642.
271. Ghaffarnia, R.; Nasrollahzadeh, A.; Bashash, D.; Nasrollahzadeh, N.; Mousavi, S.A.; Ghaffari, S.H. Inhibition of c-Myc using 10058-F4 induces anti-tumor effects in ovarian cancer cells via regulation of FOXO target genes. *European Journal of Pharmacology* **2021**, *908*, 174345.